Advances on the pyroresistive behaviour of conductive polymer composite

A thesis submitted in partial fulfilment of the requirements of the

Degree of Doctor of Philosophy

By

Eric Kwame Anokye Asare

School of Engineering and Materials Science

Queen Mary University of London

Mile End Road, London E1 4NS

I, **ERIC KWAME ANOKYE ASARE**, confirm that the research included within this thesis is my own work or that where it has been carried out in collaboration with, or supported by others, that this is duly acknowledged below and my contribution indicated. Previously published material is also acknowledged below.

I attest that I have exercised reasonable care to ensure that the work is original, and does not to the best of my knowledge break any UK law, infringe any third party's copyright or other Intellectual Property Right, or contain any confidential material.

I accept that the College has the right to use plagiarism detection software to check the electronic version of the thesis.

I confirm that this thesis has not been previously submitted for the award of a degree by this or any other university.

Signature:

Date: 29/01/2016

Details of collaboration and publications:

Asare, E., et al., *Effect of particle size and shape on positive temperature coefficient (PTC) of conductive polymer composites (CPC) — a model study.* Materials & Design, 2016. **97**: p. 459-463.

Asare, E., et al., *Effect of mixed fillers on positive temperature coefficient of conductive polymer composites.* Nanocomposites, 2016. **2**(2): p. 58-64.

Dedication

This thesis is dedicated to my lovely life partner Samantha Josephine Boateng-Tuady. Her constant support and encouragement sustained me throughout the PhD journey. I am extremely grateful for your patience and for providing an ear when I needed to rant and moan about PhD and life in general.

Acknowledgement

I would like to thank my supervisor, Dr Emiliano Bilotti, for his guidance and advices throughout the PhD. He kept me motivated and his advices has significantly improved my research and reporting skills and I will be forever grateful to him for the opportunity and all his help during my PhD.

I am indebted to Dr. Wei Tu who trained me in most of the polymer processing machines and also improved my laboratory skills. I am also grateful for the long discussions I had with him about my results and all his help in resolving experimental issues and explaining some of the observations from my experiments.

I want to express my sincere gratitude to Mr Russell Bailey for all his help in imaging my samples and for always giving me his time even at his busiest.

My colleagues from the polymer group and room 372 are all acknowledged especially Dr Pelin Yilmaz, Dr Nimra Jalali, Alex Wibawa, Halimat-Shaddiya Yewande Raji and Yi Lui for making my days lovely and delightful especially Halimat and Pelin.

Finally my deepest gratitude goes to my family, especially my parents Mr Emmanuel Asare and Mrs Elizabeth Manu for all their encouragement and love. My friends Maro Eruteya, Tunde Eyite, Kristel Chambers and Adewale Lamina are also appreciated for being there for me and providing an escape from PhD life.

Abstract

The positive temperature coefficient (PTC) effect in conductive polymer composites (CPC) are still poorly understood with the thermal expansion of the polymer matrix accepted as the main cause. This thesis aims to study a model system able to explain the effect of the filler size and shape on the PTC behaviour of CPCs. Silver coated glass spheres and flakes are used as conductive fillers due to the ease in controlling uniform size and shape. In a controlled system it was demonstrated that the PTC intensity increases with increasing filler size and with decreasing filler content, both for conductive fillers.

Combinations of different conductive fillers were investigated to explore the possibility to obtain both low percolation thresholds and high PTC intensities. Model systems in which at least one of the two conductive fillers is of relatively homogenous size and shape were used to facilitate unravelling some of the complicated relationships between (mixed) conductive fillers and the PTC effect. The PTC intensity of mixed fillers composites were dominated by the filler with the lowest PTC intensity, even at very low volume fractions. The PTC intensity was not only influenced by the conductive particle size but also by its size distribution.

The effect of difference in linear coefficient of thermal expansion (CTE) of conductive fillers and polymer matrix based on a change in filler core on PTC behaviour was investigated. Damage to the particles due to the poor adhesion between the silver coating and the PMMA bead lead to the composite behaving like mixed filler composite.

Hybrid polymers filled with silver coated glass flakes was also examined in order to enhance the PTC intensity. The PTC intensity of the composite increased with increasing PPE content but the negative temperature coefficient (NTC) effect was observed in all the composites.

Table of Contents

List of figures

List of Tables

Chapter 1. Introduction

1.1 Background to CPCs and the PTC effect

With the increase of functionality and 'smartness' of electronic consumer products, there is an urgent need for technological progress in fields like wearable electronics, flexible displays and sensors, which require new materials and devices able to respond, possibly autonomously, to a number of stimuli. Conductive polymer composites (CPC) promise to address some of the above challenges, as they have already demonstrated capability in sensing strain [1], liquids and gases [2, 3], damage [4-6] and even degradation [7]. CPCs can also show interesting pyroresistive behaviours with large positive temperature coefficient (PTC) effects, as demonstrated since the 1970s [8], which have found application in self-regulated heaters and over-current protectors [9-11].

Polymers are usually noted as electrically insulating materials and one of the ways to enhance their electrical properties is the introduction of conductive particles into the polymers. The material formed when conductive particles such as carbon black, carbon nanotubes and silver are dispersed in a polymer matrix is known as conductive polymer composites (CPC) [12-18]. The polymer matrix can range from thermosets such as epoxy to elastomers and thermoplastics with high density polyethylene (HDPE) been one of the most used thermoplastic [15-17, 19-25].

Some CPC exhibit an interesting property when the material is heated known as the positive temperature coefficient (PTC) or positive temperature coefficient of

resistance (PTCR) effect although in the thesis it will be referred to as PTC. The PTC effect is the sharp increase in resistivity of the CPC material in a small temperature region.

The PTC effect is still not well understood although many researchers have dedicated attention to this effect. Many research papers have used different conductive particles and polymers but a systematic study of the effects of the particle or the matrix on the PTC effect still lacking. The aim of this thesis is to study systematically the contribution of the filler shape and size on the PTC effect and how that knowledge can be utilised in the design of CPC with optimal pyro-resistive behaviour.

1.2 Applications using PTC effect

The technology for self regulated heaters and overcurrent protectors was provided by Raychem which owns majority of the patents on PTC devices (fig. 1.1).

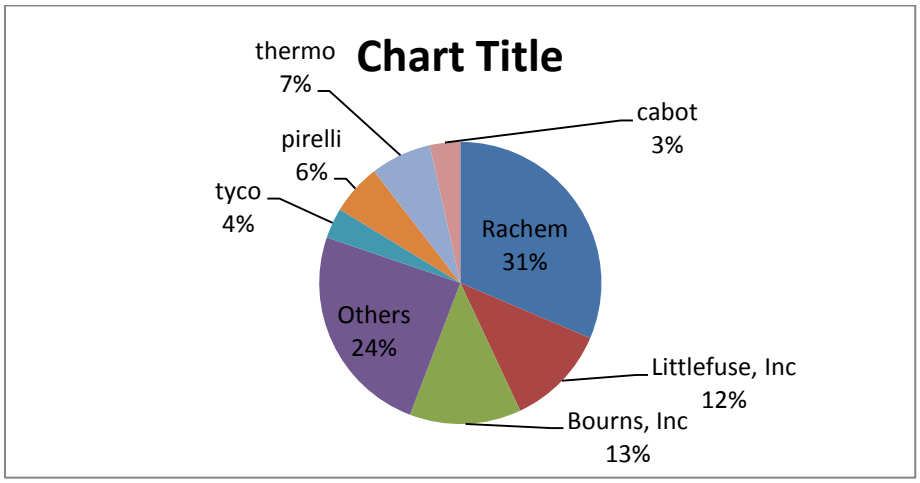

Figure 1.1 Number of patents published from 1977 to 2008.

1.2.1 Self regulated heaters

The first self regulated heater was made by Raychem engineers in 1974 and this revolutionalized the trace heating market. What made this invention revolutionary at the time was the ability of the material to control power outputs based on the temperature changes of the pipes. Not only did the material allow power control, it also made it easier to design with, install and maintain by making it feasible to cut to length on the field.

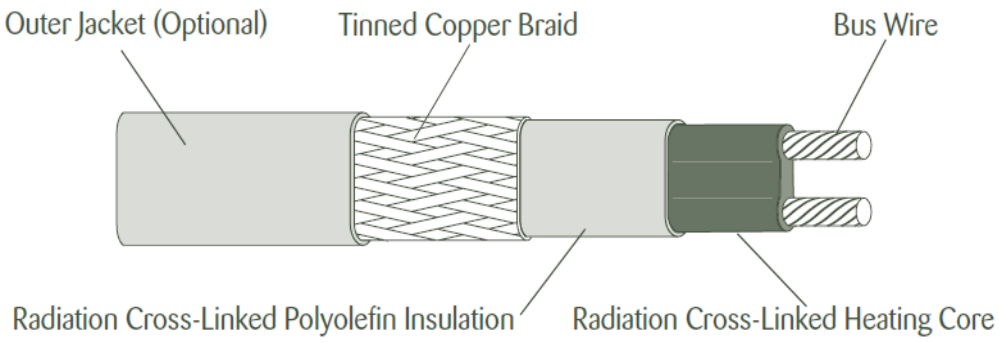

Figure 1.2 Self regulated heat trace cable [26].

These devices are made up of a semi conductive polymer composite (usually cross-linked HDPE and CB) extruded between two parallel bus conductors. The semi conductive polymer composite acts as the heating core. This core is then covered by an insulating polymer jacket. An additional jacket can be used to provide mechanical or corrosion protection for the device (fig. 1.2).

The devices work by changing their power output with change in temperature. At high temperatures, the heat output generated by the self regulated heaters is reduced. This is caused by a disruption in the electrical pathways within the heating core. The conductive paths formed by the conductive filler get broken due

to expansion of the polymer matrix. This reduces the number of effective conductive paths leading to a reduction in heat output. As the temperature reduces, the polymer matrix contracts and this reduces the distance between the conductive fillers therefore helping in the reformation of conductive pathways. This results in an increase in heat output. At low temperatures, the polymer matrix contracts even more leading to an increase in conductive paths. The increase in conductive paths increases the heat output of the device.

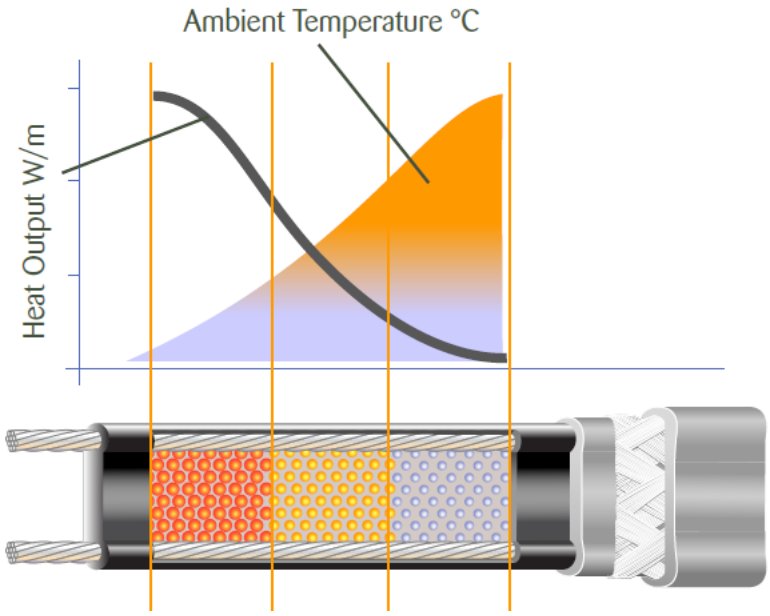

Figure 1.3 Schematic of how the self regulating of heat trace cable work [26].

The smart nature of these devices have lead to their use in a vast range of industries such as the pharmaceuticals, food and beverage, marine, oil and gas, building and construction, mining and power for applications such as;

- Heating and insulating of containers
- De-icing of building roof and gutter
- Melting of surface snow
- Process temperature maintenance

- Underfloor heating

Figure 1.4 Application of self regulated trace heating cable [27].

1.2.2 Over-current circuit protection

Conductive polymer composites with PTC effects are used in circuit protection as current limiter. They protect devices such as the telematics/infotainment system and heating, ventilation and cooling (HVAC) motor in a car by changing their resistance from low to high in response to an overcurrent [28]. An over-current condition occurs when the current passing through a circuit exceeds the “normal” or intended current of that circuit. This high current or excess current generates excess heat which has the potential to cause damage to the equipment. Overcurrent condition can be caused by excessive load and power line overvoltages such as power surges and crosses.

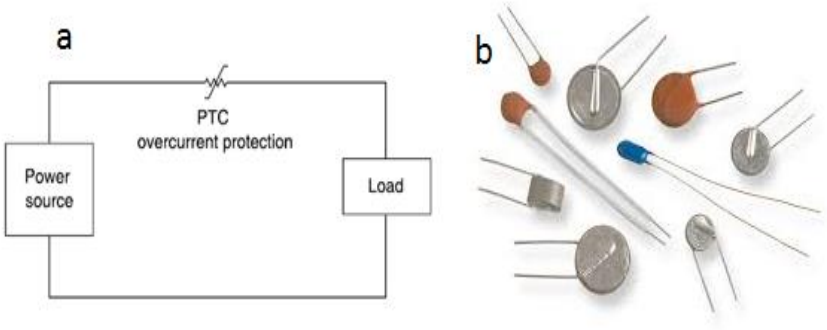

Figure 1.5 a) Schematic of a PTC over-current protector circuit. b) Overcurrent protector [29].

In normal operation conditions (no overcurrent), the resistance of the device is much lower that the circuit. An increase in current causes the device to heat up by I^2R heating. When the temperature of the device reaches the "trip" temperature, its resistance increases and this reduces the amount of current in the circuit therefore allowing the equipment to operate normally. Unlike fuses, the PTC effect is reversible therefore replacement of the device is not needed since the removal of the excess current drops the resistance of the device back to below that of the circuit. This helps to reduce the cost of services and repairs.

Overcurrent circuit protectors are made from conductive polymer composites and in the "tripped" state the conductive networks are broken by the volumetric expansion in the polymer matrix. This increases the resistance of the device therefore helping reduce the amount of current passing through it. When the excess current is removed, the polymer contracts allowing the conductive networks to reform. This reduces the resistance of the device.

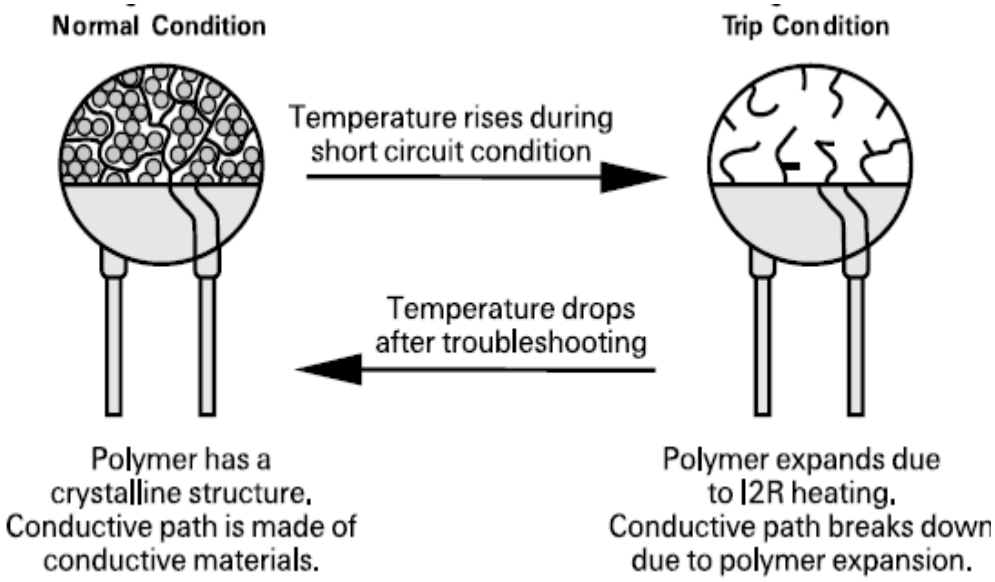

Figure 1.6 How an overcurrent protector works [30].

1.3 Structure of the thesis

This thesis is focused on the effect of conductive filler shape, size and size distribution on the PTC effect of CPC using high density polyethylene (HDPE) as the polymer matrix and silver coated glass (AgS) particles as the conductive fillers. The effect of mixed conductive filler, mismatch in coefficient of thermal expansion (CTE) between conductive particles and the polymer matrix and addition of a second polymer to AgS/HDPE composite on the PTC behaviour is also explored.

Chapter 2 is an overview of conductive polymer composites (CPC) and explores the electrical properties of these materials. A brief description of applications employing CPCs is also discussed. Chapter 2 also reviews the PTC effect associated with CPC and deals mainly with the contributions of the polymer matrix and conductive particles towards the PTC effect.

Description of the materials and experimental procedures used in this research is covered in chapter 3.

Chapter 4 covers the experimental study on the effect of filler size and shape on the PTC effect. Three different sizes of silver coated glass spheres and flakes are employed as conductive particles with high density polyethylene as the polymer matrix in this study. The electrical resistivity of these particles on HDPE polymer matrix is investigated along with the effect of different sized fillers on PTC intensity of HDPE based composites.

Knowledge gained from the size and shape study in chapter 4 is transferred in chapter 5 to examine the effect of hybrid fillers on the PTC effect of high density polyethylene (HDPE).

Two mixed fillers systems are investigated. In one system, silver coated glass flakes (AgF) of different lateral dimension (5 μm and 100 μm) are dispersed in HDPE polymer matrix while CNT is used as the minority filler, in combination with a model conductive spherical filler (AgS) in HDPE for the other system.

Silver coated glass spheres (AgS) particles and silver coated poly(methyl methacrylate) (PMMA) (AgP) beads are used as conductive fillers in HDPE polymer matrix to investigate the effect of linear thermal coefficient of expansion of conductive filler by changing the filler core on PTC effect in chapter 6. The effect of the change in filler core on electrical behaviour and the PTC intensity are both reported in this chapter.

Chapter 7 is an attempt to enhance properties of CPC prepared in previous chapters, like flexibility and processability.

The main conclusions from the investigation are summarised in chapter 8. This chapter also looks at the possible future works on this topic.

Chapter 2. Conductive polymer composites (CPC)

2.1 Introduction

Conductive polymer composites (CPC) consist of conductive fillers dispersed in an insulating polymers matrix. The conductive fillers used in conductive polymer composites can vary from metals, ceramics to carbon based fillers such as carbon black, CF and CNT [16, 31-34]. Polymers filled with metallic particles presents the benefits of polymer processability while the electrical properties are close to that of the metal [34, 35]. The challenges with metal filled polymer systems are high density and degradation of electrical properties due to oxidation on metal surfaces [35, 36]. Compared to carbon black for instance, the volume fraction of metallic particles needed to make an insulating polymer conductive is high [37] and since metal particles are more expensive than carbon black, the total cost of the composite increases. The filler-filler interaction is the main contributor for the conductivity of the composite although other effects such as the filler matrix interactions also affect the conductivity of the composite.

Conductive polymer composites have been used in many applications such as electromagnetic interference (EMI) shielding and have started to replace metals in some applications due to their unique properties such as corrosion resistance and light weight.

In this chapter, the different theories proposed to explain the conduction mechanism of CPC will be discussed briefly as well as the different factors affecting the conductivity of CPCs.

2.2 Conduction mechanism

The addition of conductive particles into an insulating polymer matrix presents three possibilities, namely:

i. No physical contact between conductive particles,
ii. Close proximity between conductive particles,
iii. Physical contact between conductive particles.

The conductivity of polymer composites can only occur as a result of electron tunnelling (close proximity) or physical contact between the conducting fillers [38]. The conductivity of CPCs is govern by the percolation theory. A typical percolation curve is represented in figure 2.1. Insulating polymers filled with conductive particles experiences three states based on the amount of filler in the polymer (fig. 2.1). At low filler concentrations (region I), the distance between the conductive fillers are too big to allow electron tunnelling so the composite remain insulating due to the conductivity been dominated by the polymer matrix. As the filler concentration increases (region II), the distance between the particles reduces and the fillers form linkages and at a critical filler concentration, electron tunnelling and contact between adjacent fillers spans the entire material. The critical filler concentration needed to form an initial conductive path is called the percolation threshold (Pc). An increase in filler concentration after the percolation threshold (Pc) results in a sharp decrease in resistivity of the composite as the electrical property of the filler starts to dominate the electrical

behaviour of the composite. Further increase in filler concentration (region III) increases the number of contact between fillers due to the reduction of inter-filler distance. This increases the number of conductive pathways within the material resulting in the formation of a three dimensional network [39]. Even though there is an increase in conductive pathways, very little change in the conductance of the composite is observed.

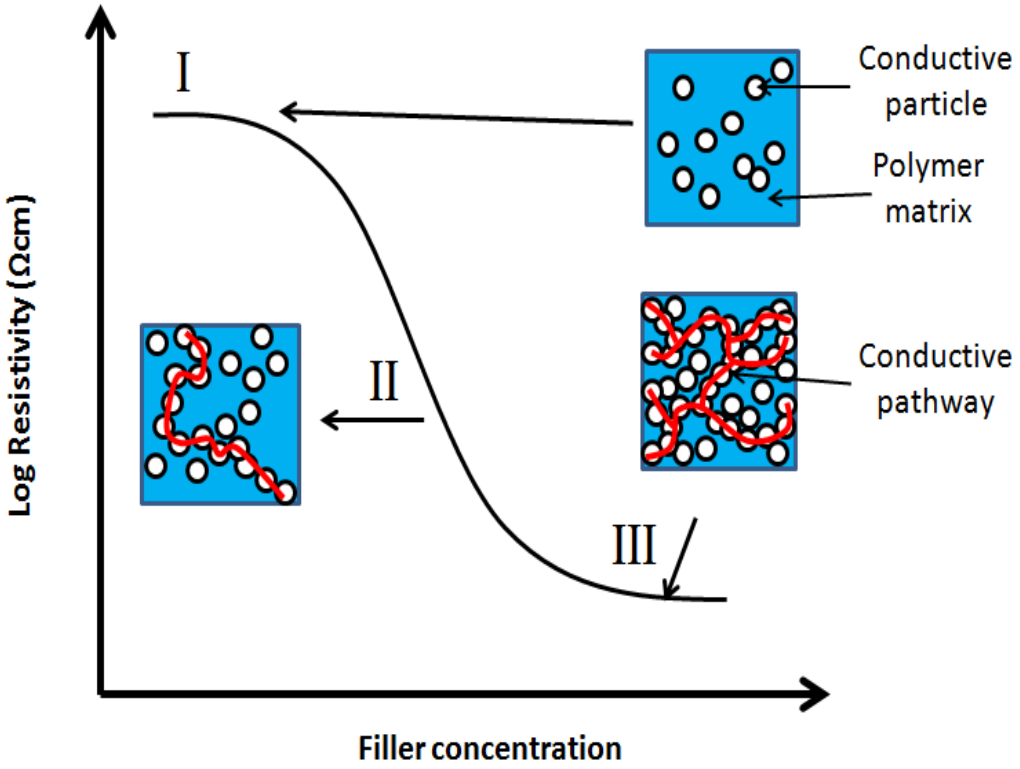

Figure 2.1 percolation behaviour of conductive polymer composite.

2.3 Models proposed to explain the percolation behaviour of CPC

Conductivity of conductive polymer composites is governed by percolation theory which describes the conductivity of the composite close to the transition from

insulator to conductive [36] . The percolation threshold which is the minimum concentration of conductive filler at which the composite moves from insulator to conductive phase is affected by different conditions. The most important properties affecting the percolation threshold are;

- Shape and size of the conductive filler.
- Distribution and dispersion of the conductive filler.
- Interaction between the matrix and conductive filler.
- The processing techniques used in preparation of the composite.

Based on these conditions different electrical percolation models have been proposed to try and explain the conductivity of the composite. Four main models have been developed to try and predict the percolation threshold for conductive polymers namely; Statistical, geometric, thermodynamic and structure oriented [40].

2.3.1 Statistical percolation model

A huge number of papers in the scientific literature have based their percolation threshold on the statistical model [16, 17, 19, 23-25, 41, 42]. The prediction of the percolation threshold is based on the probability of conductive particle being in contact with each other within the composite.

This model for calculating the percolation threshold of conductive composites was made popular by Kirkpatrick [43] and Zallen [44]. Kirkpatrick [43] and Zallen [44] used finite arrays of points connected by bonds to predict the percolation threshold. Using computer stimulations, the fraction of existing bond or points within a cluster can be observed using different statistical laws. The

bonds or points contact each other within the cluster and the percolation threshold is reached when the cluster covers the boundaries of the system. A power law was used to describe the percolation threshold of the form:

$$\sigma = \sigma_0 . (\mathrm{P} - Pc)^t \tag{2.1}$$

where Pc is the critical or percolation threshold and t is the critical exponent which depends on the dimension of the conductive network. Experimental results are usually plotted as log σ against log (P - Pc). The theoretical value for the parameter t is 1.6 - 2 for three dimensional lattices although values as high as 4.6 have been recorded for t in some experiments [45]. For two dimensional lattice the value for t is from 1 to 1.3 [46].

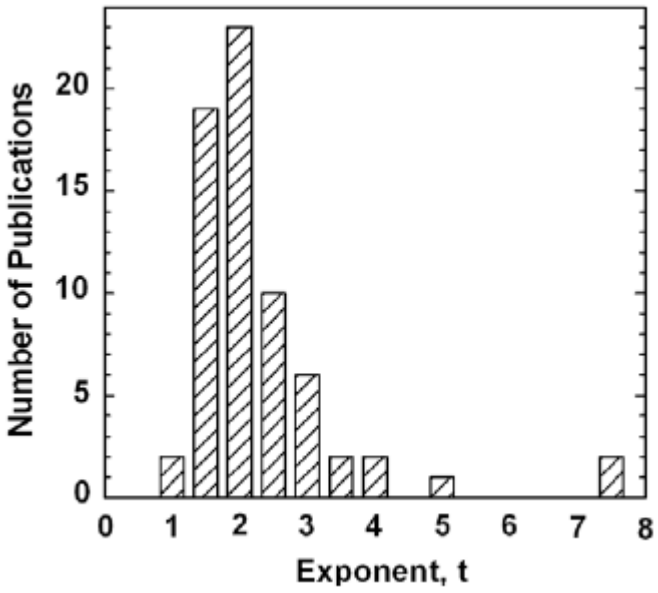

Figure 2.2 Number of publication against reported critical exponent, t [47].

2.3.2 Thermodynamic percolation model

The thermodynamic percolation model relies on the importance of the interaction at the interface or the boundary between the polymer matrix and the individual conductive fillers hence the percolation condition is viewed as a phase separation process [40].

Wessling's model indicated that below the percolation threshold, the conductive particles are arranged in flat agglomerates and distributed randomly in the polymer matrix. Addition of more conductive fillers into the polymer melt causes the spaces of the flat agglomerates to be overfilled. The adsorption layers of some of the conductive fillers are partially destroyed due to the increase in compression stresses. These particles move towards each other until an electrical contact is formed. The continuous migration of conductive fillers towards each other to form electrical contacts leads to the formation of two dimensional conductive network. A three dimensional conductive network is formed by the phase separation of the conductive particles and the polymer matrix caused by the interfacial energies between the conductive filler and the adsorption polymer/polymer boundary [40].

The equation generated by Wessling *et al*.[40] has the general form:

$$V_c = \frac{0.64(1-C)\Phi_0}{\Phi_c}\left[\frac{x}{\left(\gamma_c^{\frac{1}{2}} + \gamma_p^{\frac{1}{2}}\right)^2} + y\right] \tag{2.2}$$

Where V_c is the volume percolation threshold, $\gamma_c \; and \; \gamma_p$ is the surface tension of the conductive filler and polymer matrix respectively, (1 - C) the amorphous part

by volume of the polymer at room temperature. x is a medium value dependant on the molecular weight of the polymer, Φ and Φ_o the volume factor to recognise the appearance of the adsorption layers on each conductive particle.

2.3.3 Geometrical percolation model

Geometrical percolation models deals with the percolation phenomenon observed in sintered mixtures of conductive and insulating powders. The particle diameters of the non sintered powders or the edge length of the sintered particles are the main conditions used in defining the percolation behaviour of the system. This makes this model limited when considering conductive polymer composites.

According to Lux [40], the most prominent geometrical model is the one proposed by Malliaris and Turner [48] but experimentally determined results did not agree with the calculated results using this model. The model proposed by them is based on two equations for the volume percolation threshold. The first equation applies to the volume concentration, V_A, associated with the onset of the formation of conductive network while the second equation deals with the end of the huge jump in conductivity caused by the volume concentration, V_B. The equation took into consideration the arrangement of the conductive fillers on the surface of the insulating ones (θ), diameters of the conductive and insulating powder particles (d and D respectively) and the probability of formation of long bands of conductive particles on the surface of the insulating particles (P_c).

$$V_A = 0.5\, P_C V_B \tag{2.3}$$

$$V_B = 100\left[\frac{1}{1+\left(\frac{\theta D}{4d}\right)}\right] \tag{2.4}$$

2.3.4 Structural oriented percolation model

The conductivity and percolation threshold of a conductive polymer composite differ significantly due to the different processing methods used in preparing the composite. This problem is what caused researchers such as Nielsen to design a model that took into consideration the physical properties of the final composite. The conductivity of the composite according to Nielsen depended mostly on the length to diameter ratio (aspect ratio) of the conductive filler and the coordination number of the filler in the composite. The equation is of the form:

$$\sigma_c = \sigma_p \frac{1+AB\phi}{1+B\psi\phi} \tag{2.5}$$

$$B = \frac{\sigma_f/(\sigma_p - 1)}{\sigma_f/(\sigma_p + A)} \tag{2.6}$$

$$\psi = 1 + \left(\frac{1-P_f}{P_f^2}\right)p_f \tag{2.7}$$

A is a function of the aspect ratio and packing of the conductive fillers, σ_c , σ_p and σ_f are the conductivity of the composite, polymer and conductive filler respectively. P_f represents the coordination number of the conductive filler within the polymer matrix. This equation was used to predict the electrical conductivity as well as the modulus of polymer/metal composites.

McCullough tried this equation on a binary system and found out that it did not agree with the reasons given for the electrical conductivity behaviour of the system. This lead McCullough to develop another equation based on transport equation and adjusted it by adding a chain length factor.

Weber and Kamal considered the aspect ratio, orientation and the dimensions of the conductive filler in designing their models. They came up with two models which tried to describe the conductivity of composite using nickel coated graphite as a conductive filler and polypropylene as matrix. One of the models considered the conductive fillers as "strings" connected at their ends while the other model considered the contact between the conductive fillers (i.e. filler/filler contact) plus the other parameters. The equation developed has the form:

$$\rho_{c,long} = \frac{\pi d^2 \rho_f X}{4\phi_p \ell_c cos^2\theta_a} \tag{2.8}$$

The resistivities of the composite and conductive filler are given by ρ_c and ρ_f, θ_a is the orientation angle and ϕ_p is the percentage of conductive fillers participating in the strings.

2.4 Filler effect on conduction behaviour of CPC

The conduction behaviour of CPC relies heavily on the conductive fillers therefore the properties of the filler is crucial in achieving good CPCs.

2.4.1 Filler size and shape

The size of the conductive fillers is crucial to the conductivity of the composite. An increase in filler size reduces the percolation threshold of the composite and this has been demonstrated by several researchers [49-52]. According to Ota *et al*. [51], the inter-particle distance of randomly dispersed conducting fillers in a polymer matrix decreases with decreasing filler size at the same volume fraction. The decrease in distance between particles makes inter particle contact and electron tunnelling more likely to occur, hence decreasing percolation threshold increasing conductivity. Aggregation of smaller particles in a polymer matrix to form continuous chains is more likely compared to large particles [52, 53]. Smaller fillers have bigger surface areas than their large counterparts and coupled with their ease of aggregating due to the attractive forces (i.e. van der waal force) makes their room temperature resistivity (i.e. percolation threshold) smaller than their large counterparts at the same volume fraction as shown in table 2.1 [52, 53].

Table 2.1 Percolation threshold against particle diameter for carbon black (redrawn from Jing *et al*.) [52].

Specific area (m^2g^{-1})	Particle diameter (nm)	Percolation threshold
86.3	34.8	0.097
45.2	66.4	0.117
20.4	147	0.224

Conductive fillers come in different shapes including spheres, fibres and platelets. The shape of the conductive filler can influence the conductivity of the composite dramatically and this is due to the aspect ratio of the filler. The aspect ratio can be defined as the ratio of the long dimension of conductive filler to the short dimension. For spherical particles, the aspect ratio is one while flakes and fibres

can have aspect ratios in the hundreds. Standard carbon black which are usually modelled as spherical particles (aspect ratio = 1) have high percolation threshold around 10 %wt compared to carbon nanotube with a percolation threshold below 1 %wt as shown in figure 2.3. Mamunya *et al.* [34] using spherical nickel (Ni) particles and dendritic shaped copper (Cu) particles in PVC observed a higher percolation threshold for the spherical particle system compared to the irregular shaped particle system. The way the particles are arranged in the composite (packing density) influences the percolation threshold but the packing density (F value) is determined by the filler shape [34]. The higher the F value for a system, the higher the percolation threshold and in the Ni/PVC system the F value was 0.51 while the F value for the Cu/PVC system was 0.30 [34].

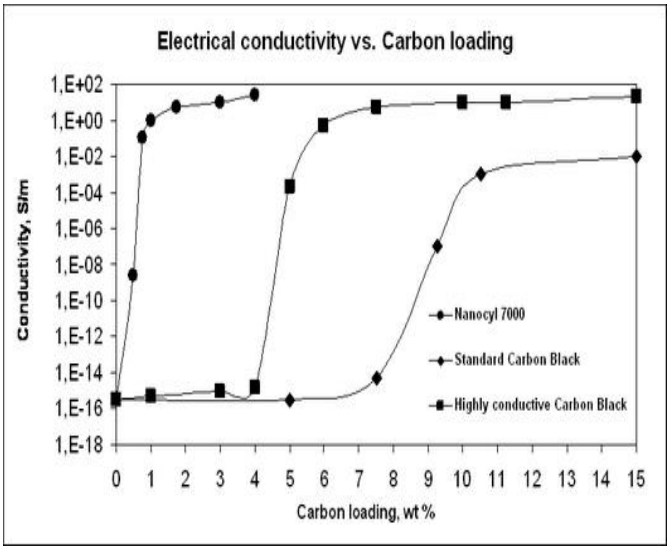

Figure 2.3 Electrical percolation behaviour of carbon black and carbon nanotubes [19].

Bigg and Stutz [54] demonstrated that an increase in aspect ratio of carbon fibres from 10 to 1000 reduces the volume percent of filler needed to reduce the resistivity of the composite to below 100 Ωcm from 10 %Vol. to 1 %Vol. From figure 2.4, it can be seen that as aspect ratio increases the volume fraction of

carbon fibres needed to reduce the resistivity of the composite to below 100 Ωcm decreases.

Although it is generally accepted that an increase in aspect ratio of conductive fillers should lead to a decrease in percolation threshold, some researchers has reported the opposite. For instance Bai and Allaoui [55] demonstrated that an increase in MWNT length results in a decrease in percolation threshold. They argued that an increase in MWNT enhances the possibility of the fillers agglomerating (i.e. increase in entanglement) due to the difficulty in dispersing very high aspect ratio particles and this in turn increases the chance of formation of linkage between the aggregates [55]. Martin *et al.* [56] in their studies involving MWNT dispersed in epoxy found that an increase in filler length resulted in an increase in percolation threshold (fig. 2.5).

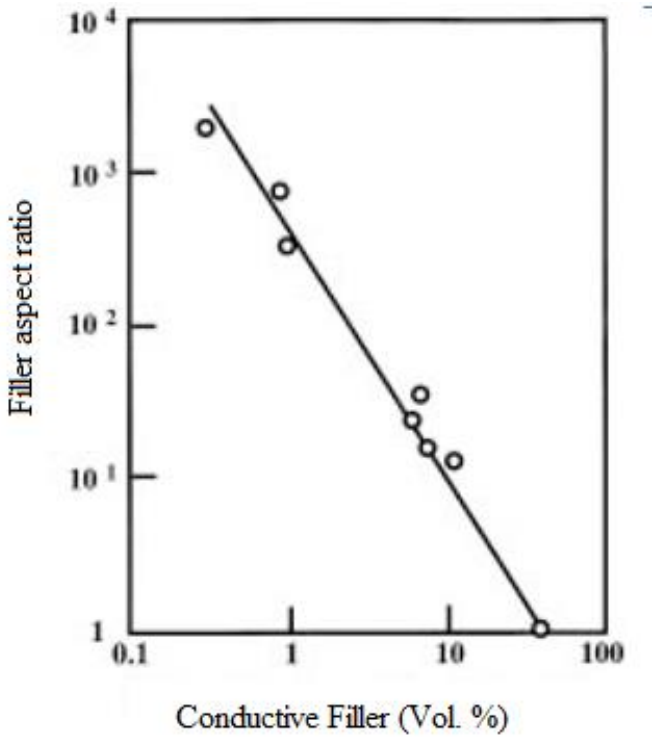

Figure 2.4 Relationship between fibre aspect ratio and volume fraction [54]

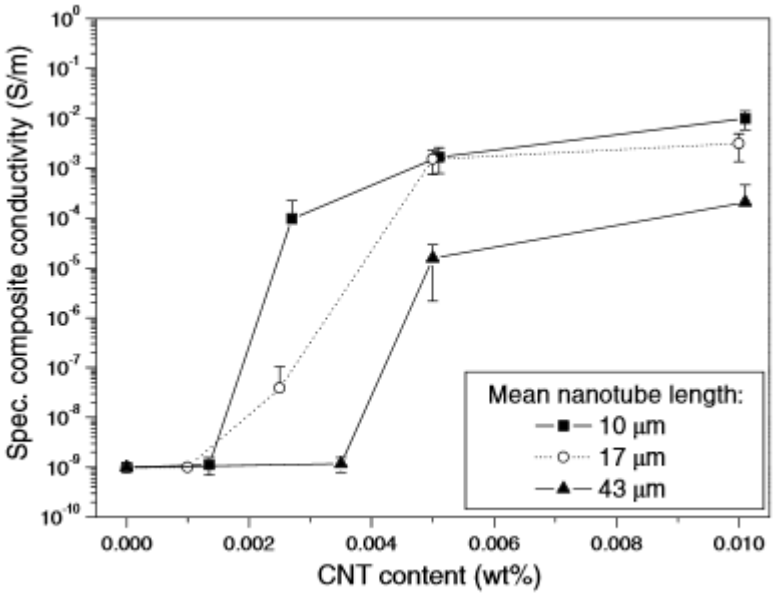

Figure 2.5 Percolation behaviour of MWNT/epoxy system with different sized fillers [56]

2.4.2 Filler type and concentration

The initial conductivity of the filler materials is crucial in determining the conductivity of the final composite. Conductive fillers with high intrinsic conductivity will produce composites with high conductivities. Composites made with conductive fillers such metals will have high conductivity (i.e region III of the percolation curve) compared to composites prepared with carbon based fillers although the percolation threshold of the carbon based fillers will be lower. Mamunya *et al.* [34, 57] in two separate studies demonstrated that poly(vinyl chloride) (PVC) filled with copper (Cu) and MWNT had different percolation threshold. The percolation threshold for the PVC filled MWNT was reported as 0.05 %Vol. with a maximum conductivity of 1×10^{-4} S/cm while the Cu filled PVC had a maximum conductivity of 1×10^{4} S/cm with a percolation threshold of 5 %Vol. Although the amount of filler in the Cu/PVC composite is higher than that of the MWNT/PVC composite (30 %Vol. for Cu/PVC and 0.7 %Vol. for

MWNT/PVC), the maximum conductivities wouldn't change since they were well above the percolation threshold (i.e. region III of figure 2.1). Although the conductivity of the final composite is dependent on the conductivity of the filler, the percolation threshold is more dependent on the filler shape and size.

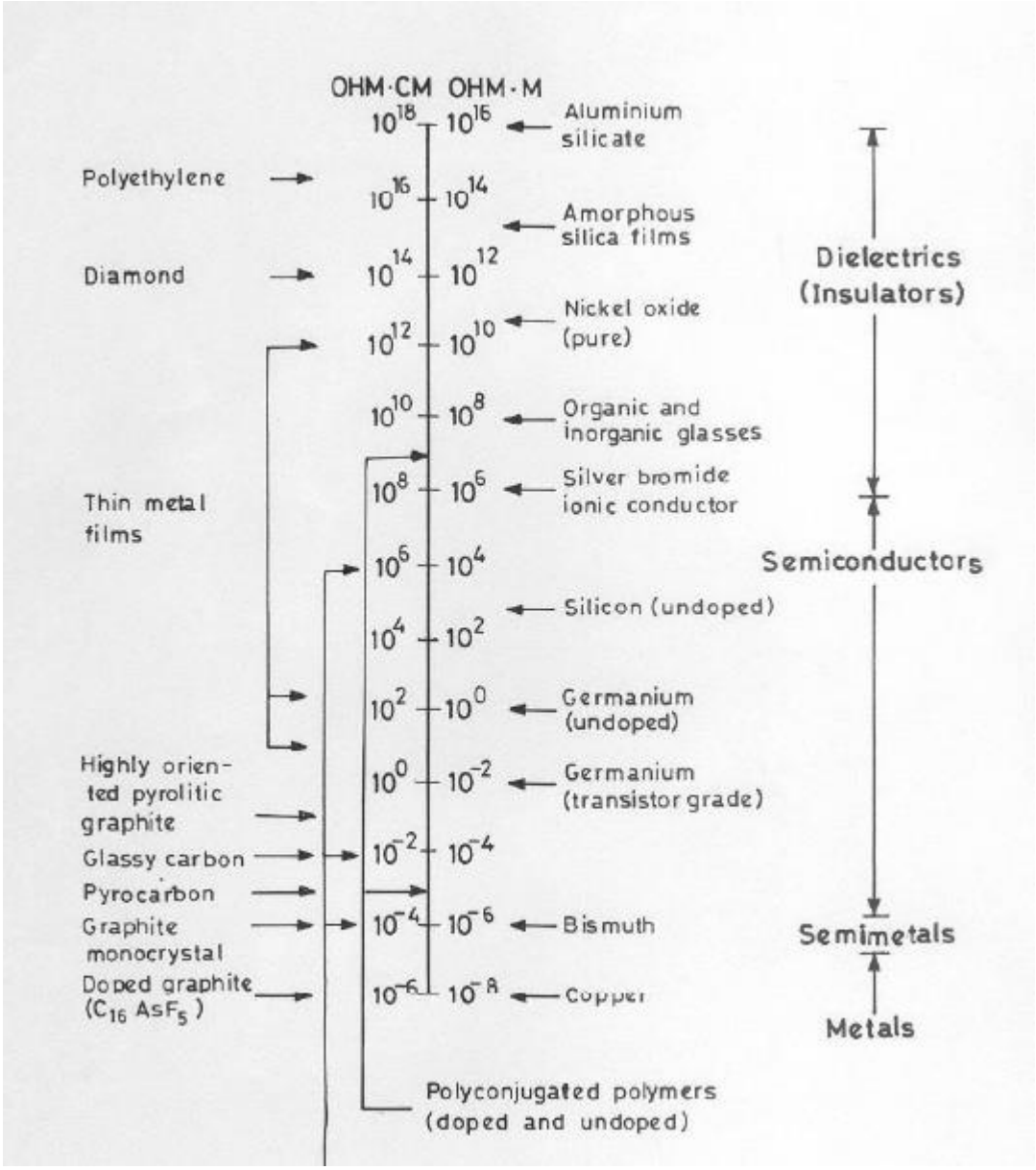

Figure 2.6 Resistivity of different materials [58].

The properties of the conductive filler can be modified by treating the surface of the fillers. Treating the surface of the fillers can result in either a decrease or

increase in percolation threshold and in some cases the percolation threshold remains unchanged (table 2.2). Table 2.2 shows that depending on the type of treatment used, the percolation threshold of the final composite can be reduced. Using low temperatures and reducing the oxidation time for the MWNT will reduce the amount of damage suffered by the fillers and this in turn will reduce the percolation threshold [59].

Table 2.2 Table showing the effect of filler treatment on percolation threshold.

Polymer	Filler	Treatment	Percolation Threshold/ %wt	Ref
Epoxy	MWCNT	no treatment	0.1	[60]
Epoxy	MWCNT	UV/O_3	0.27	[60]
Epoxy	MWCNT	HNO_3, centrifuged, C_3H_6O	0.034	[59]
Epoxy	MWCNT	H_2O_2/NH_4OH, centrifuged, C_3H_6O	0.042	[59]
PC	MWCNT	no treatment	1	[61]
PC	MWCNT	HCl	5	[62]
PCL	MWCNT	no treatment	1.5	[63]
PCL	MWCNT	HNO_3, filtrated	4	[63]
PMMA	SWCNT	no treatment	0.17	[64]
PMMA	SWCNT	$SOCl_2$	0.17	[64]
PP	MWCNT	no treatment	2.62	[65]
PP	MWCNT	HF, HCl	2	[66]

Saeed and Park [63] demonstrated that polycaprolactone (PCL) filled with multiwalled carbon nanotubes (MWNT) modified by nitric acid showed a higher percolation threshold when compared with PCL filled with unmodified MWNT (fig. 2.7). They claimed the increase in percolation threshold might be caused by the destruction of π network during the acid treatment [63].

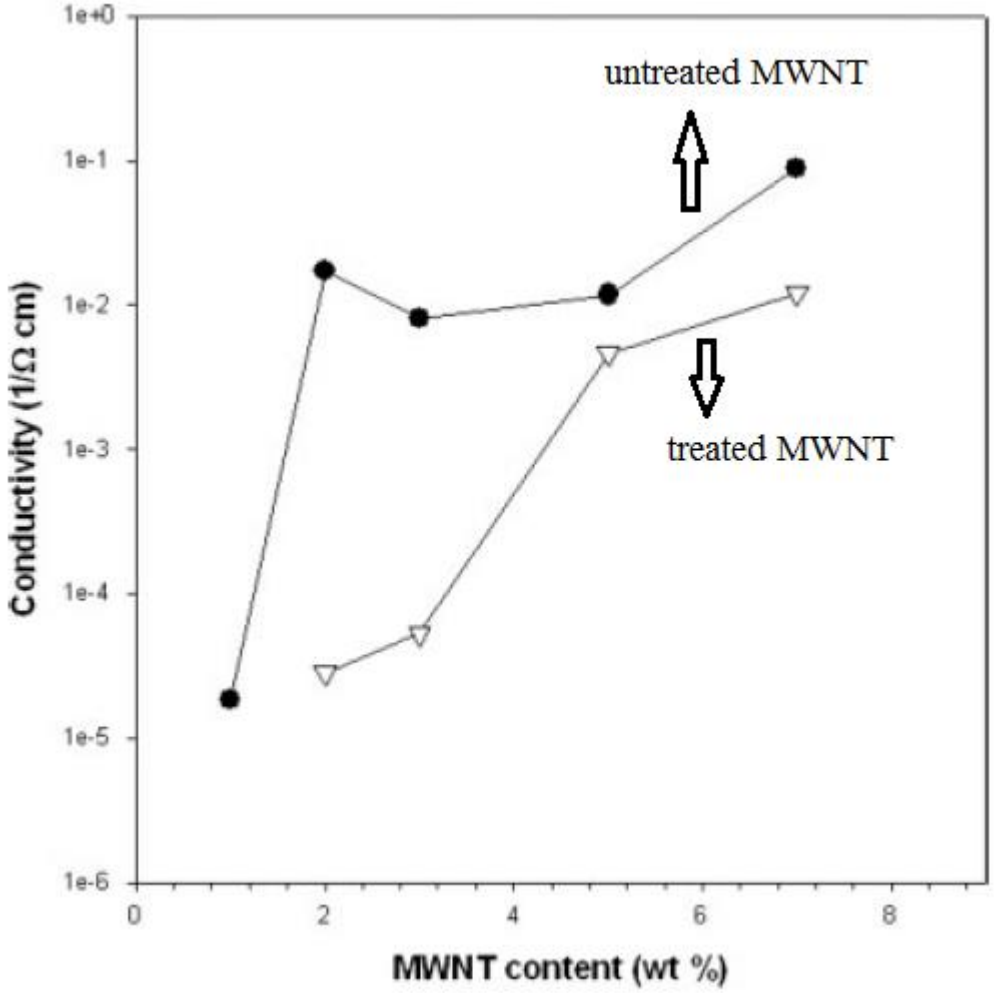

Figure 2.7 Percolation behaviour of PCL filled with treated MWNT and untreated MWNT [63].

Li *et al.* [60] also reported an increase in percolation threshold when they studied epoxy filled with treated MWNT and untreated MWNT. The MWNT treated with UV/O_3 composite showed a percolation threshold of 0.27 wt% compared to 0.1 wt% for the untreated MWNT composite and this was attributed to the entanglement and distribution of the MWNT agglomerates [60]. Dispersion of the surface treated MWNT in the epoxy matrix was improved but the MWNT was damaged, (disentangled) during processing.

Skakalova *et al*. [64], studied the effect on percolation behaviour of singled walled carbon nanotubes (SWNT) modified with thionyl chloride ($SOCl_2$) in polymethylmethacrylate (PMMA). The percolation threshold was similar in both composites but the maximum conductivity achieved was different. SWNT modified with $SOCl_2$ composite showed a higher maximum conductivity value of 100 S/cm while the pristine SWNT composite achieved a value of 17 S/cm. The initial conductivity of the SWNT without surface treatment and the surface treated SWNT were 500 S/cm and 2500 S/cm respectively and this explains the differences in the conductivities of these composites above the percolation threshold.

The amount of conductive filler in the polymer matrix is also important. At low concentrations, the interactions between fillers doesn't span the entire material therefore very little to no change in conductivity is experienced by the composite. As the filler concentration increases, the interactions between the fillers increases therefore formation of conductive pathways become possible. These pathways can span the entire material at the percolation threshold therefore increasing the conductivity of the material. Further increase in filler concentration has less effect on the conductivity of the material as shown in figure 2.1.

2.4.3 Filler distribution

The distribution of the conductive filler into the polymer matrix relies heavily on the processing method used. Conductive fillers can be mixed into a polymer via different routes such as melt extrusion and solution processes [16, 31, 47, 67]. Melt processing techniques such as extrusion and injection moulding are usually employed in industrial production. When injection moulding or extrusion

technique is utilised, high shear forces will occur at the ends (nozzle) and this will lead to filler alignment in the flow direction. This affects the conductivity of the final part when tested in different directions.

Table 2.3 Effect of processing technique on epoxy filled SWCNT composite (table redrawn from Bauhofer and Kovacs) [47].

processing technique	percolation threshold (wt. %)
sonicated	0.1
stirred	0.08
sonicate, heat sheared	0.05
ball milled, heat sheared	0.23
sonicated vacuum pumped	0.074
manually mixed	0.6
calendered, stirred	0.04

The flow of the polymer and the orientation of the mould will determine the orientation of the filler. For brittle fillers, the filler shape and size can be altered when processing techniques such as melt mixing are used. The high shear produced by the screws during mixing can damage the filler therefore influencing the percolation threshold. Villmow *et al.* in an experiment involving PLA and MWCNT argued that an increase in shear stress could cause MWCNT to be shorten. This shortening of the nanotubes reduces the number of physical entanglement between the MWCNT therefore making dispersion easier [68].

Dispersion and distribution of conductive fillers in a polymer matrix can be schematised in four cases (fig 2.8) but one case promotes conductivity. The use of dispersion and distribution in scientific literature can be confusing at times therefore a definition of these terms is needed. For the purpose of this thesis, distribution describes the homogeneity of the particles throughout the matrix while the dispersion is the even distribution of the particles in the matrix [69].

The two states where conductivity might not be possible involve good distribution and good dispersion as well as bad distribution and bad dispersion of conductive fillers in the polymer matrix (fig. 2.8c and 2.8d). The distance between adjacent particles exceed the tunnelling gap therefore conductivity become impossible in these situations.

Figure 2.8a involve fillers been well distributed in the polymer matrix but the dispersion of these fillers is bad. The inter particle distance is too much for tunnelling to occur hence the composite doesn't conduct. The fillers can be well dispersed in the polymer matrix but have bad distribution and the composite will conduct (fig. 2.8b). Although the distribution of the particles are bad, the gap between particles are small enough to allow electron tunnelling or even physical contact between the particles therefore conductivity is possible.

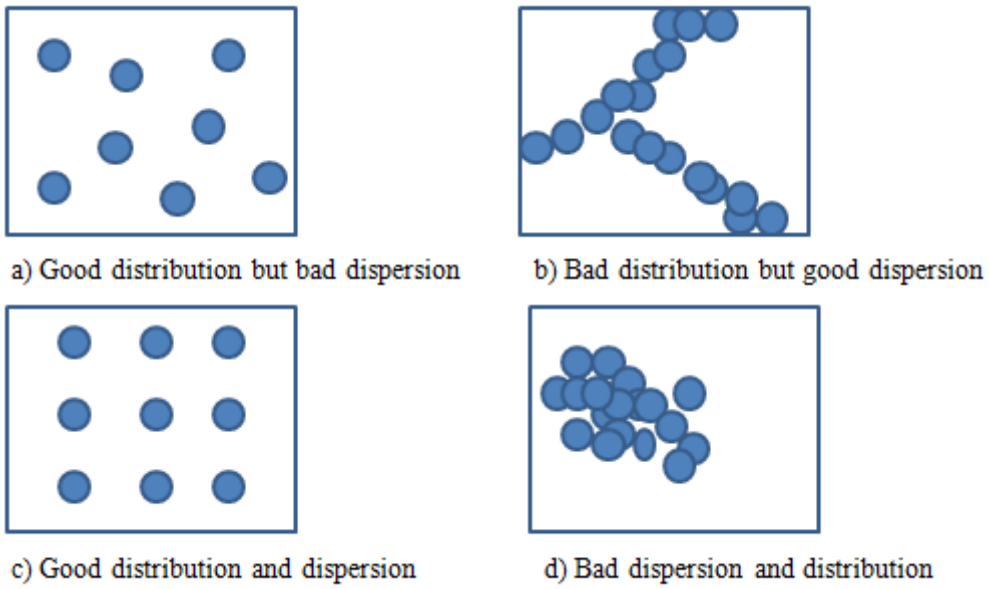

Figure 2.8 Schematic of filler distribution and dispersion in a polymer matrix.

Li *et al.* [60] dispersed carbon nanotubes (CNT) in epoxy under four different conditions and monitored the effect of filler distribution on percolation threshold

(table 2.4). The found that the composite with the lowest percolation threshold had some agglomeration and the CNT were uniformly distributed while the composite that exhibited the best dispersion state showed no apparent percolation threshold [60]. The lack of agglomeration by the well dispersed composite due to the damage to MWNT led to the lack of percolation threshold while the composites that showed some form of agglomeration displayed percolation behaviour [60]. Figure 2.9 shows the TEM images of the CNT filled epoxy under the four conditions. Figure 2.9a, shows the MWNT highly entangled but poorly dispersed in the epoxy matrix while figure 2.9b shows a better distribution of the CNT even though the CNT still shows some entanglement (agglomeration). It is observed in figure 2.9c that the CNT particles are less entangled but shows good distribution while figure 2.9d shows the least amount of entanglement for all the composites.

Saeed and Park [63] observed a similar decrease in percolation threshold when they modified the surface of MWNT through nitric acid treatment. The composite filled with the treated MWNT showed a better dispersion than the one filled with untreated MWNT. Martin *et al*. [56] also demonstrated that MWNT systems showing uniform distribution showed a higher percolation threshold compared to a system without uniform distribution.

Table 2.4 Dispersion method and percolation threshold for CNT/epoxy composite [60].

Condition	Dispersion method	Percolation threshold [wt%/vol%]
A	As-received CNTs + epoxy Shear mixing for 30 min at 3000 rpm	0.4/0.26
B	CNTs dispersed by ultrasonication for 1 h in acetone + epoxy Ultrasonication for 2 h at 60 °C	0.1/0.06
C	UV/ O_3 treatment of CNT for 1 h and ultrasonication for 2 h in acetone + epoxy Shear mixing for 30 min at 3000 rpm	0.25–0.3/0.16–0.19
D	CNTs were ball milled for 2 h, ultrasonicated in toluene for 1 h, and UV/O_3 treated for 2 h, followed by silane treatment [13] + epoxy Ultrasonicated for 2 h at 60 °C	No percolation

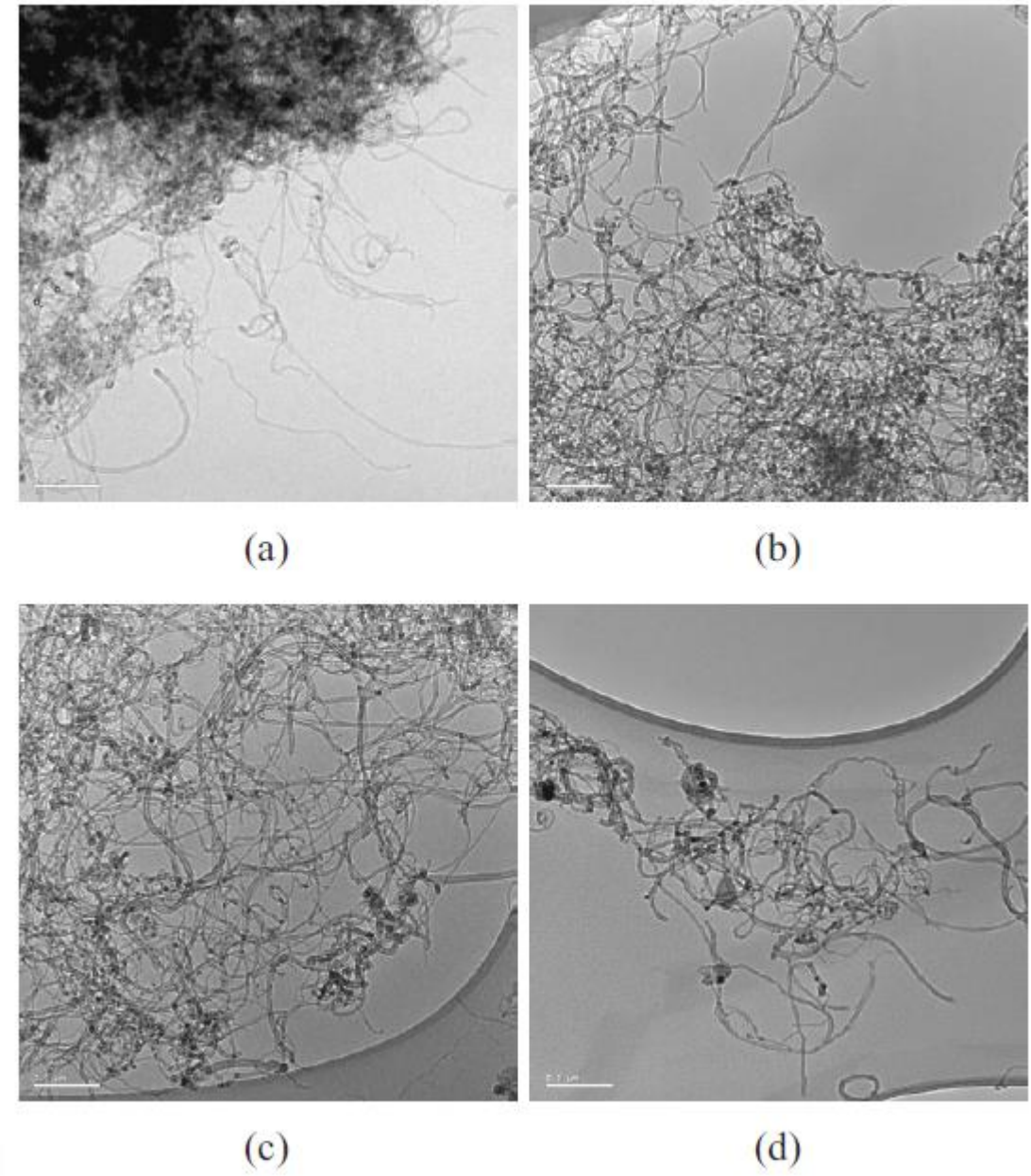

Figure 2.9 TEM image of CNT agglomeration dispersed according to condition A,B,C and D in table 2.4. Scale bar 0.2µm [60].

2.5 Effect of processing condition CPC

Although incorporation of conductive fillers into a polymer matrix can be achieved via different routes such as solution processing [59, 64, 70] and latex technology [71-73] but melt processing remains the preferred choice in the

polymer industry. Melt processing of CPCs is fast, cost effective and environmentally friendly when compared to some other processing methods such as solution processing. For example, CPCs can be produced in small or large quantities per hour using extruders. The extruder can be joined with a blow moulding or injection moulding machine to directly make the desired product therefore reducing the time needed to remove the solvent for instance in solution processing. CPCs produced using melt processing techniques are been extensively researched and reported in literature due to its alignment with industrial processing of polymers.

Distribution and dispersion of the fillers in the polymer matrix is achieved in melt processing by the shear forces generated during melt mixing. The distribution and dispersion of conductive fillers in a polymer matrix during melt processing is dependent on the mixing temperature, speed and time.

An increase in mixing temperature decreases the resistivity of the composite. Krause *et al.* [74] in a study using MWNT dispersed in polyamide 66 (PA66) showed that an increase in mixing temperature from 265 ^{o}C to 285 ^{o}C reduced the resistivity of the composite by more than two orders of magnitude. A non conducting composite prepared at a 240 ^{o}C using 5 wt% MWNT in polyamide 6 (PA6) became conductive when the mixing temperature was changed to 260 ^{o}C [74]. The decrease in resistivity with increasing mixing temperature was explained by the reduction in polymer viscosity. A decrease in polymer viscosity improves the dispersion of MWNT therefore a better filler network formation is achieved [74].

The resistivity of CPCs increases with increase in mixing speed and this is due to the damage suffered by the particles as the shear forces increases. For instance MWNT mixed at high speeds have been reported to suffer breakages leading to a reduction in their aspect ratio therefore increasing their room temperature resistivity [62, 74]. The shortening of MWNT particles also decreases the probability of the particles to form agglomeration. A reduction in the number of agglomerates for MWNT linked to an increase in screw speed increases the resistivity of the composite system [62, 68, 74].

This effect was observed by Krause *et al.* [74] and the difference in resistivity observed by changing the mixing speed from 50 rpm to more than 200 rpm was about six orders of magnitude higher. The number of agglomeration and their distribution in the polymer matrix is responsible for the huge change in resistivity. The composite mixed at 50 rpm included many big agglomerations of MWNT while small agglomerates were observed in the composite mixed at 300 rpm due to the increase in mixing energy [74].

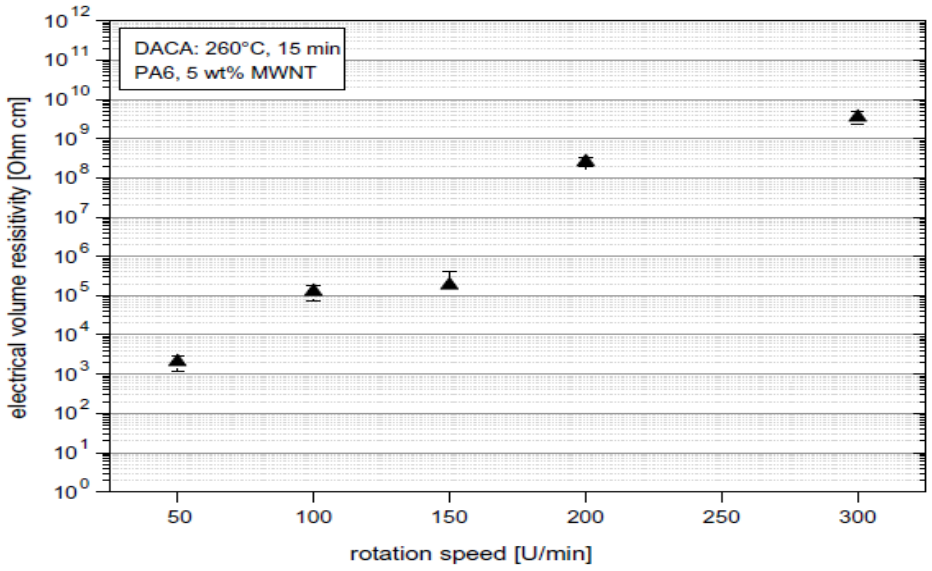

Figure 2.10 Effect of screw speed on the resistivity of MWNT/PA6 composite [74].

Potchke *et al.* [75] reported a reduction in resistivity for a composite system when the screw speed for the preparation of the composite was changed from high speed to a low speed. In melt mixing the shear stresses generated by the mixing screw provides the energy required in reducing the size of agglomeration and an increase in screw speed increases the energy hence a reduction in the number of agglomerates [76]. Generally an increase in mixing time results in a decrease in resistivity of conductive composites but contradicting results have been published in the literature [74, 75]. Potchke *et al.* [75] demonstrated that above percolation, an increase in mixing time at high shear rate (150 rpm) increases the resistivity of the composite although the opposite effect was reported for composites with filler concentrations below the percolation threshold. Using different screw speeds (50 and 150 rpm), Krause *et al.* [74] reported an increase in resistivity at high speed and a decrease in resistivity at low speed. It is possible that at low mixing speed, an increase in mixing time has less to no effect on damage to the conductive

fillers (i.e. agglomeration size is not affected) but the dispersion and distribution of the fillers in the polymer matrix is enhanced. This results in the decrease in resistivity while at high mixing speed, increasing the mixing time is most likely to damage the fillers (i.e. reduction in entanglement and agglomeration) therefore increasing the resistivity of the final composite.

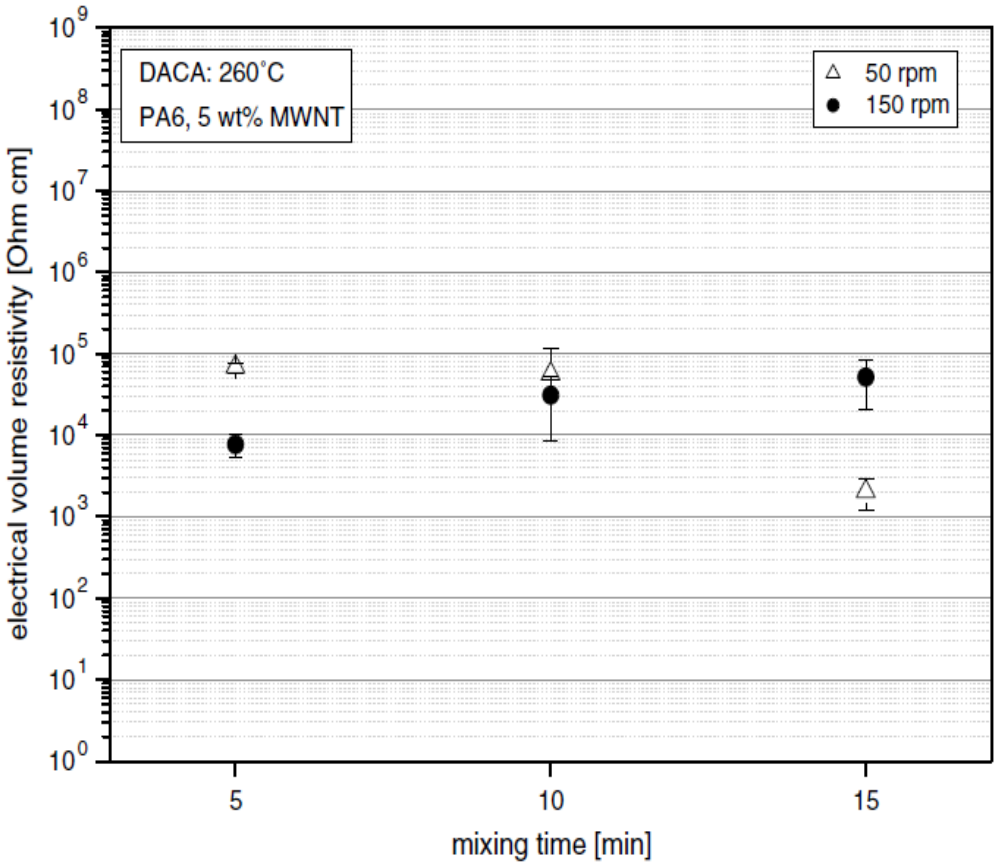

Figure 2.11 Effect of mixing time at high speed (filled circle) and low speed (unfilled triangle) on electrical resistivity of CPC [74].

2.6 Application of CPC

Electromagnetic interference (EMI) shielding is an application where conductive polymer composites are utilised [12, 54, 77]. Electronic parts that are susceptible to outside electromagnetic noise can be protected by using conductive polymer

composites. Different methods such as vacuum metalizing and electroless metal coatings compete in the EMI shielding field with conductive polymer composites but these composites offer low cost, lightweight and ease of producing complex shapes. The EMI shielding market is forecasted to reach $6.6 Billion in 2019 and conductive polymer composites are likely to be at the forefront of the market as the material of choice [78].

Prevention of harmful arcing discharges by continuous bleeding off charge (electrostatic dissipation) is another application of CPCs. Electrostatic dissipation (ESD) requires composites with lower conductivities compared to EMI shielding. ESD materials are employed in packaging of electronic machines and electronic components. Parts in weaving machines and conveyor belts where different materials are used require antistatic protection and CPCs provide the perfect solution to this [39].

Electroplating of plastics without metal coating is made possible when conductive polymer composites are used. Electroplating requires conductivity treatment to the surface to electroplated and surface treatment can be avoided by using CPCs. This makes the use of CPCs more cost effective in applications such as metal-plated automotive parts or cosmetic packages [39].

CPC can also be used to sense deformation (strain), [1, 73], damages [4-6], liquid and gases [2, 3] in materials by monitoring the change in electrical resistivity. When an external stimulus such as force is applied to CPC, the interparticle distance increases and this increases the resistance due to the difficulty in electron tunnelling as the gap increases (fig. 2.12). Levin et al. [73] prepared a strain sensor that had three times the gauge factor of classical metallic gauges and could

monitor strains above 5% using polyaniline (PANI) nanoparticles in a poly(vinyl acetate) (PVAc). The composite obtained was cheap, flexible, environmentally friendly and easily scalable therefore making the CPC very attractive [73]. CPC are also widely used in temperature sensitive applications such as heat trace cables and self regulated heaters and this area has attracted a lot of studies [8, 10, 11, 23, 24, 79-82].

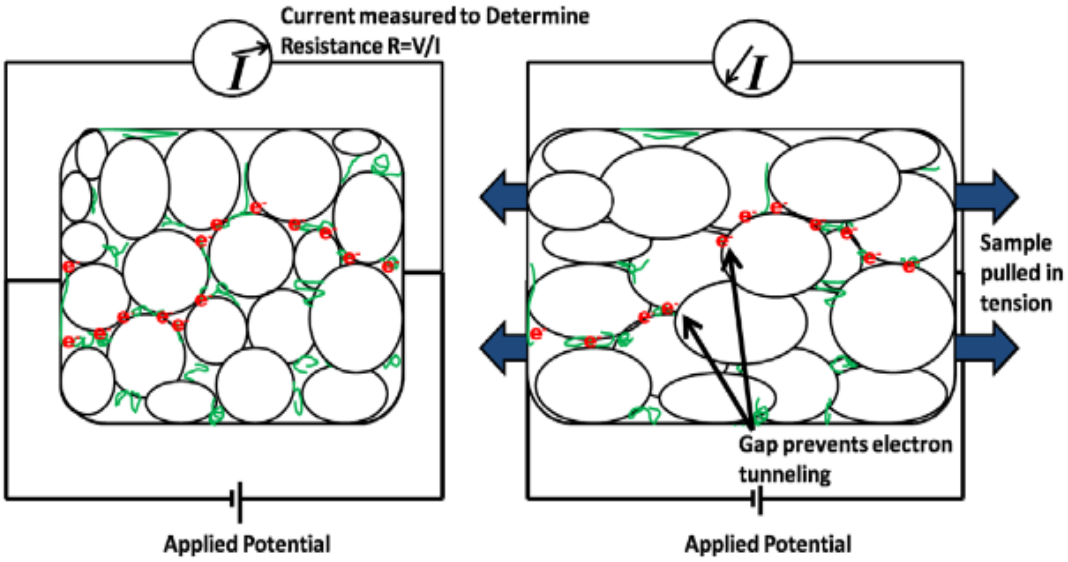

Figure 2.12 Schematic of resistance increase in CPC when deformed by uniaxial stress in tension [73].

Other applications employing conductive polymer composites include conductive adhesives, and over-current protectors. Conductive adhesives are employed in electronic application to join heat sensitive parts where welding or brazing will damage the material.

2.7 Positive temperature coefficient effect of CPC

Insulating polymers filled with conductive particles such as metals and carbon black usually show two changes in resistivity as temperature increases. The increases in resistivity over a small temperature range is known as the positive temperature coefficient (PTC) effect while the decrease in resistivity that usually follows the PTC effect is known as the negative temperature coefficient (NTC) effect (Fig. 2.13).

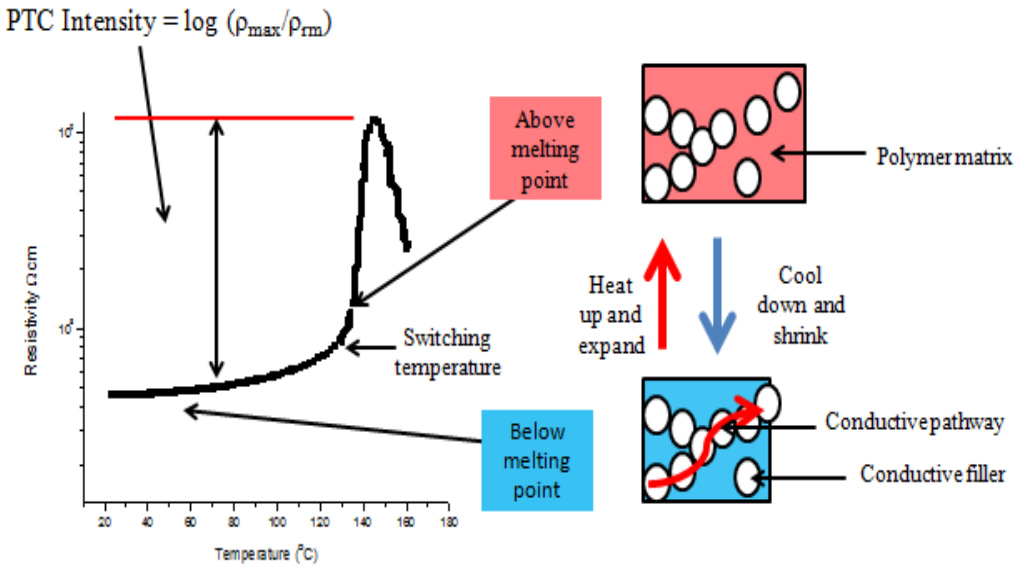

Figure 2.13 Resistivity against temperature behaviour of conductive polymer composites.

Composites that exhibit the PTC effect are of much interest due to their potential of being used as smart materials. The ability for these composites to change from conductive composites to insulating composites upon heating makes them interesting materials to study. The extent of this change in resistivity is defined by

the PTC intensity (PTC_I) which can be defined as the ratio of the log of the maximum resistivity (ρ_{max}) to the resistivity at room temperature (ρ_{RT}).

$$\boldsymbol{PTC_I = \log \frac{\rho_{max}}{\rho_{RT}}} \tag{3.1}$$

The first to report about large PTC intensity in conductive polymer composites was Kohler [79] although Frydman [83] had reported this behaviour earlier. An increase in PTC material research resulted in many applications such as heat trace cables.

In this chapter, the common explanation given for the PTC effect will be discussed along with the effect of the matrix polymer and conductive filler on the PTC intensity of the composite. Applications utilising the PTC phenomenon will be presented at the end of this chapter.

2.7.1PTC theory

Electrical conductivity in conductive polymer composites occurs due to the direct contact between conductive particles and electron tunnelling. As the concentration of the conductive particles increases, the electron tunnelling effect reduces and the conductive mechanism becomes dominated by the direct contact between particles. The disruption of the inter particle contact or electron tunnelling during heating of the composite causes the PTC effect.

Different theories have been proposed to explain how the PTC effect occurs but these theories are not fully supported by experimental results. The "true" mechanism for the PTC effect is not well established since most of these theories

cannot be verified experimentally but all the theories are somehow related to the thermal expansion of the polymer matrix close to the melting temperature. This has made it acceptable that the PTC effect is caused by the increase in inter particle distance due to the rapid volume expansion of the polymer matrix close to the melting point.

2.7.2 Difference in thermal expansion of polymer matrix and filler

Filling an insulating polymer with conductive particles will led to the polymer conducting at a critical volume of the particles. This is due to the conductive particles forming continuous conductive network within the composite. An increase in conductive particles increases the conductive networks within the composite. Polymers usually have higher thermal expansion coefficient compared to most conductive particles and according to Kohler [79], the difference in thermal expansion coefficient of the matrix and filler causes the PTC effect. As the composite is heated, the expansion of the polymer matrix disrupts the continuous conductive network formed by the conducting particles. This expansion of the polymer matrix causes the separation of particles in contact with each other therefore increasing the resistivity of the composite. The PTC temperature is the temperature at which the PTC effect occurs and for most composites this is linked to the phase transformation (i.e. Tg and Tm) of the polymer matrix. For semi crystalline materials, the biggest change in thermal expansion occurs close to the melting temperature therefore for many composites the PTC effect occurs at these temperatures [25, 46, 81, 84, 85]. Kar and Khatua

[33] showed that the PTC temperature does not depend on the polymer matrix by using fillers with a lower coefficient of thermal expansion than the polymer matrix. In a Ag/PMMA composite, they observed the PTC temperature at 92 ^{o}C which is 21 ^{o}C lower than the temperature at which PTC would have been predicted for PMMA.

Kohler's theory can explain the PTC effect of conductive composites but does not address the reduction in resistivity (NTC effect) with temperature that follows the PTC. Based on Kohler's theory, the resistivity of the composite should continue to increase with increase in thermal expansion but this is not supported by experimental results.

2.7.3 Tunnelling current

Electrical conductivity can occur in polymer composites when the distance between conductive particles are small enough to allow electron tunnelling. According to Ohe and Naito, the inter particle distances in a conductive polymer are uniformly distributed and this is what leads to electrical conductivity [8]. They proposed that, at temperatures close to the melting temperature of the polymer matrix, the uniformly distributed inter particle distances are destroyed and they become random. An increase in the inter particle distance also occurs close to the melting temperature of the polymer matrix therefore making electron tunnelling difficult (fig. 3.2). The increase in resistivity is caused by the decrease in electron tunnelling due to the break up in conductive pathways. Although Ohe and Naito were able to explain the PTC effect, the NTC effect remained unexplained. Also the idea of PTC effect occurring due to the random distribution of the distance between conductive filler cannot be acceptable as many researchers have shown

that the PTC effect can be stabilised by eliminating the redistribution of particles via crosslinking or using high viscosity polymer [86-88].

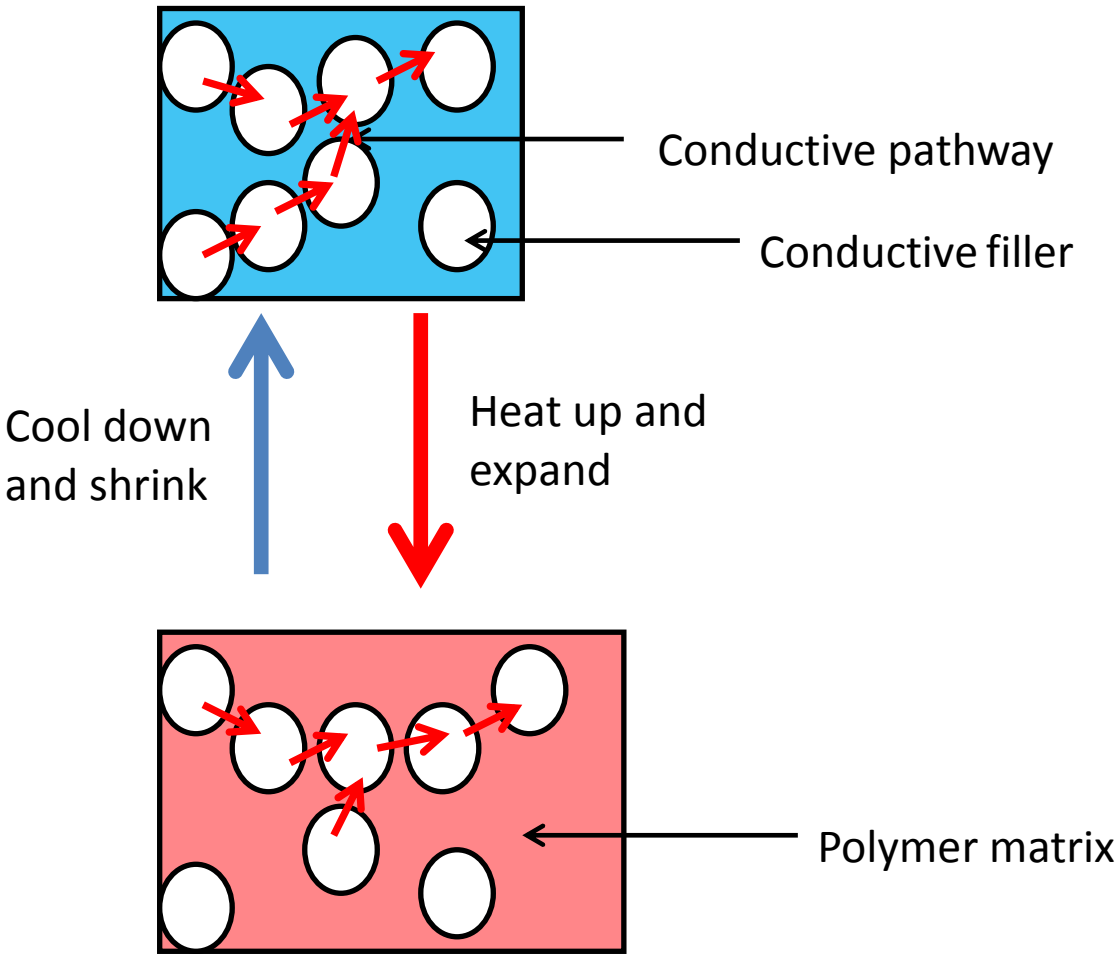

Figure 2.14 Schematic of effect of thermal expansion on tunnelling current of conductive polymer composites.

Meyer advanced the tunnelling current theory by studying the effect of polymer crystallinity [89]. Meyer proposed that conductive particles reside in the amorphous region separated by thin layer of crystallites in conductive composites. He assumed that the crystalline region of the polymer matrix is more conductive than the amorphous region therefore for electrical conductivity to occur, electrons have to tunnel through the crystalline film. According to Meyer, the sudden rise in resistivity with temperature is caused by the change in the state of the crystalline

region as the melting temperature of the polymer is approached. The melting of the polymer crystals affect electron tunnelling therefore increasing the resistivity of the conductive composite. Meyer's theory states that the PTC effect should occur before the melting temperature of the polymer matrix but in most cases the PTC behaviour occurs at the same time as melting and many researchers have shown that the PTC temperature is also dependant on the conductive filler concentration [80, 87, 90].

2.8 Polymer matrix effect on PTC behaviour

The thermal expansion associated with the polymer matrix is accepted as the driving force behind the PTC effect. This means that the PTC effect of a conductive composite depends heavily on the characteristics of the polymer matrix such as the crystallinity and thermal behaviour.

2.8.1 Effect of polymer crystallinity

The thermal volume expansion of semi crystalline polymers is bigger than amorphous polymers therefore the PTC intensity in semi crystalline polymer based composites should be higher when compared with amorphous based composites [21, 85, 89]. According to Meyer [89], the destruction of the crystallites leads to PTC behaviour therefore the PTC intensity is dependent on the crystallinity of the polymer. In an experiment conducted by Luo *et al*. [85] it was observed that as crystallinity decreased, the PTC amplitude decreased and this supports Meyer's theory.

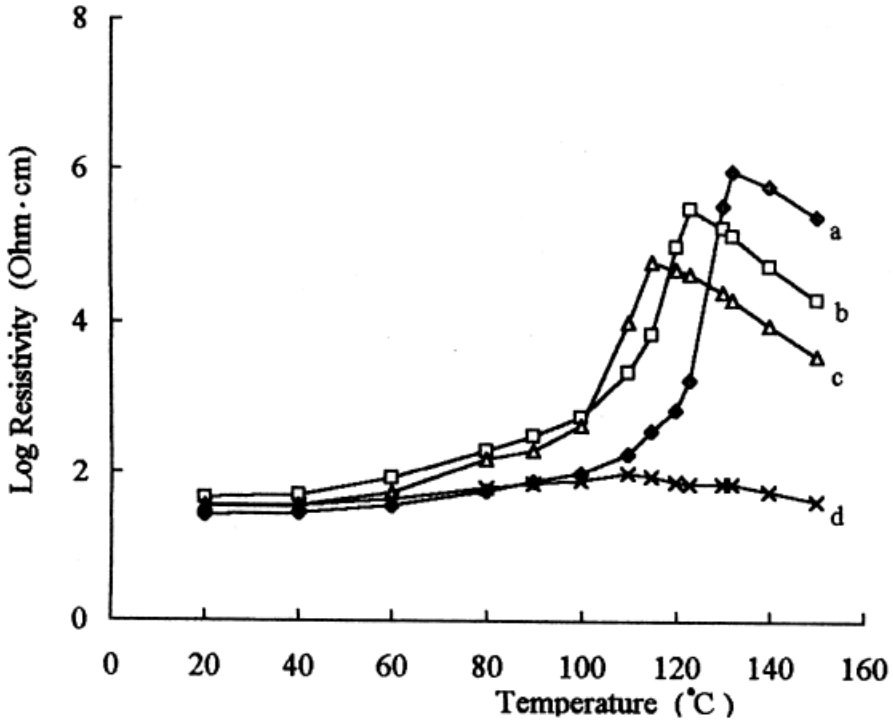

Figure 2.15 The dependence of PTC characteristics on crystallinity: (a) 38 phr CB/HDPE, (b) 30 phr CB/LDPE/CB, (c) 28 phr CB/EVA/LDPE, and (d) 27 phr CB/PMMA [85].

The crystallinity of the polymers used in the experiment by Luo *et al.* is shown in table 2.5. HDPE loaded with CB (sample a) showed the highest PTC intensity and this supports the idea that as crystallinity of the polymer matrix increases, the PTC intensity will also increase. PMMA filled with CB on the other hand which was amorphous showed little or no PTC effect.

Table 2.5 Crystallinity of the samples used by Luo *et al.* [85].

Sample	% Crystallinity
HDPE/CB (a)	63
LDPE/CB (b)	53.5
EVA/LDPE/CB (c)	42
PMMA/CB (d)	0

Although it is generally accepted that the crystallinity of the polymer has an effect on the PTC intensity, this claim has been challenged by some researchers [22, 91]. Fournier *et al*. demonstrated that the PTC intensity of an amorphous based polymer composite can reach three orders of magnitude using epoxy filled with carbon black [22].

2.8.2 Effect of polymer thermal behaviour

The PTC effect of conducting polymer composites occur around the melting temperature of the polymer matrix therefore the thermal property of the matrix is important. Semi crystalline polymers go through three reversible changes when heated. These changes include crystallisation and melting which occurs in the crystalline region and glass transition which happens in the amorphous region. These thermal transitions are associated with increase in specific volume of the polymer matrix and this will impact the PTC effect. Based on the models proposed for the PTC effect, the expansion caused by these thermal transitions of the polymer will break up the conductive network formed within the composite. This leads to a reduction in conductivity of the polymer composite. This suggests

that an increase in the degree of thermal transitions in the polymer matrix should increase the PTC effect of the composite.

Although for most semi crystalline CPC the PTC effect happens close to the melting temperature of the polymer matrix [8, 9, 18, 23, 87, 92], Kono *et al.* [90] when using nickel particles as a conductive filler in PVDF found out that for filler contents below 40 Vol %, PTC effect happened well below the melting temperature (Tm of PVDF = 167 ^{o}C) of the matrix. The low PTC temperature is caused by the concentration of the Ni particle being close to the percolation threshold (19 vol %). For instance the composite with 20 vol % Ni have fewer conductive paths formed within it when compared with the composite with 50 vol %. This means that any slight expansion in the polymer matrix even at temperatures below the melting temperature of PVDF will cause the conductive pathways to be broken therefore leading to an increase in resistivity (PTC effect).

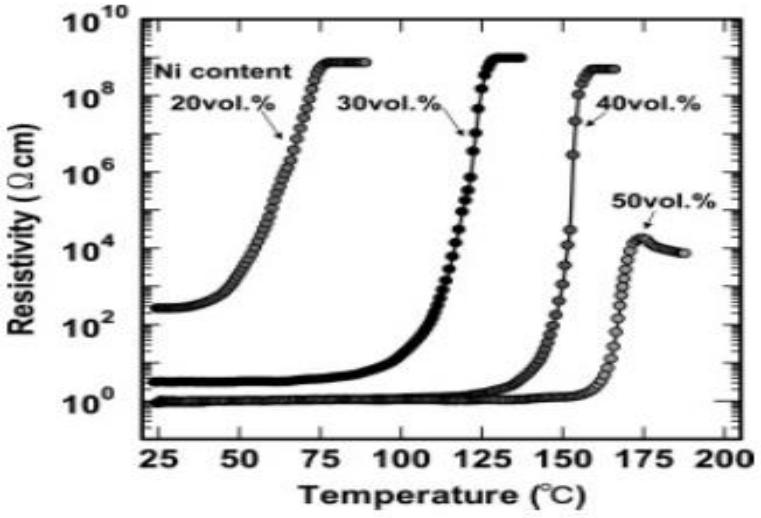

Figure 2.16 PTC curve of PVDF (Tm of PVDF = 167 ^{o}C) containing different amount of Nickel [90].

2.8.3 Polymer blend effect

The PTC behaviour of a composite can be modified by adding a second or third polymer to the composite to form a mixed polymer system.

The use of polymer blends as a matrix for conductive polymer composites (CPC) has many advantages including;

I. Low percolation threshold for the composite.

II. Multiple PTC behaviour of the composite [21].

III. Elimination of the negative temperature coefficient (NTC) [21].

Dispersion of conductive fillers into hybrid polymer systems can results in two morphologies as shown in figure 2.17. Figure 2.17 shows that conductive fillers can remain in one phase or be dispersed at the phase boundary between the two polymers although most systems reported in literature has the fillers dispersed only in one phase of the composite system.

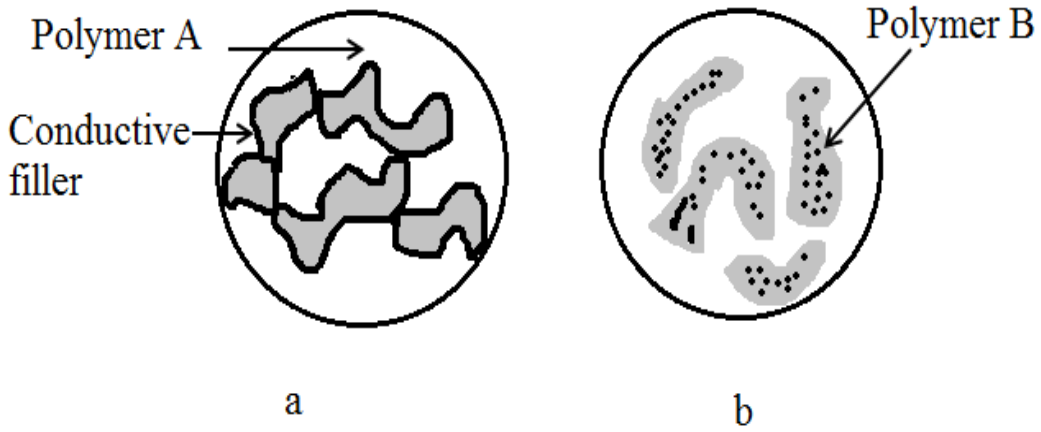

Figure 2.17 Schematic of filler dispersion in a mixed polymer composites.

The selective localization of conductive particles in one phase of the system leads to the formation of double percolation in the composite [82, 93-96]. The double percolation effect occurs when the amount of filler in one phase is percolated and the percolated composite phase spans the entire polymer blend (fig. 2.18b).

From figure 2.18a, it is observed that at low concentrations of the percolated phase, the resistivity of the composite will be high due to the increase in distance between the percolated phases. A 1:1 ratio of the percolated phase and the other polymer usually leads to a continuity of the percolated phase in the polymer blend therefore a decrease in resistivity while an increase in the polymer content of the percolated phase leads to a decrease in resistivity. This is caused by the increase in interparticle distance between the filler preventing physical contact or electron tunnelling.

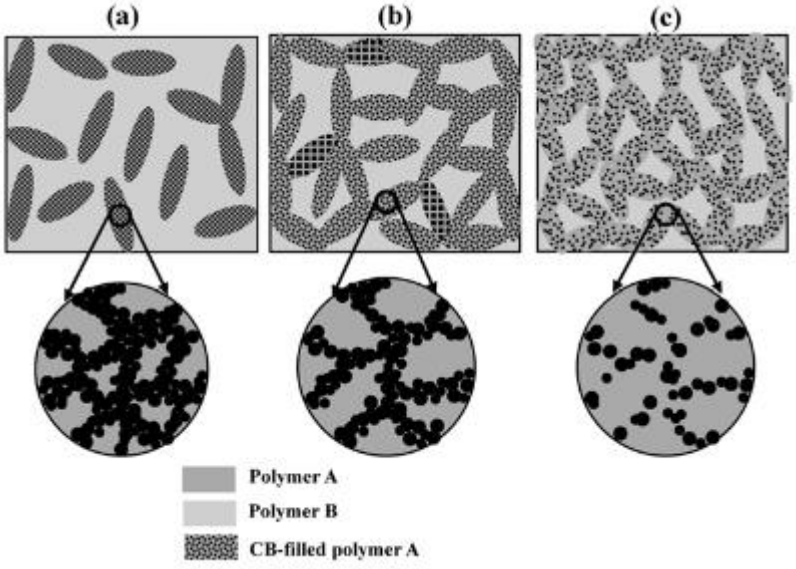

Figure 2.18 Schematic of increase in polymer content of the localised filler phase a) low content b) about 50 %wt and c) above 50 %wt [97].

Xu *et al.* [97] in a study involving CB particles dispersed in HDPE/PP polymer reported an increase in conductivity of about six orders of magnitude when the ratio of HDPE/PP was changed from 4:1 to 1:1. The CB particles were localised in the HDPE phase due to the low interfacial energy associated with HDPE compared to PP. The selective localisation of conductive fillers such as CB in a mixed polymer system can also be caused by the difference in melting temperatures or viscosities of the two polymers [82, 93, 94, 97]. Di *et al.* [93] also observe in a CB/HDPE/PP composite that an increase in HDPE/PP ratio up to 50 wt% decreased the resistivity of the composite but the resistivity increased when the CB localised HDPE phase exceeded 50 wt%.

The PTC behaviour of mixed polymer composites has yielded different results with some researchers reporting the presence of a double PTC effect while others did observe only a single PTC effect [9, 21, 82, 97-105]. The double PTC effect occurs in composites where the conductive fillers are dispersed at the interface between the two polymers. Selective localisation of conductive fillers at the interface between two polymers can be challenging due to the preferential localisation of fillers in one polymer phase because of the difference in interfacial energy and viscosities of the polymers [82, 93, 94, 97, 106]. This means that for most composites, the double PTC effect reported is as a result higher filler concentration in one phase. The increase in filler content in one phase leads to the migration of fillers into the phase boundary between the two polymers [21, 93]. The increase in thermal expansion associated with the melting of the polymer phase containing the conductive fillers causes the first PTC effect. The expansion of the polymer increases the conductive pathways within the polymer therefore increasing the resistivity of the composite. Around the melting temperature of the

second polymer, the conductive pathways formed at the interface between the two polymers are disrupted by the thermal expansion of the second polymer. This causes the second PTC effect. Di *et al.* [93] observed the double PTC effect when the used a high loading of CB (10 %wt) in HDPE/PP composite. The first PTC effect occurred at the melt temperature of the HDPE while the second PTC effect was observed at the PP melt temperature. Di *et al.* [93] argued that the CB particles although preferentially localised in the HDPE matrix, the particles begin to migrate to the interface as the CB content in HDPE exceed the percolation threshold. The double PTC effect was also observed by Feng and Chan [21] and Wei *et al.* [101] studying the PTC behaviour of CB/PP/UHMWPE . The amount of CB particles used in the study exceeded the percolation threshold for the mixed polymer composite (fig. 2.19).

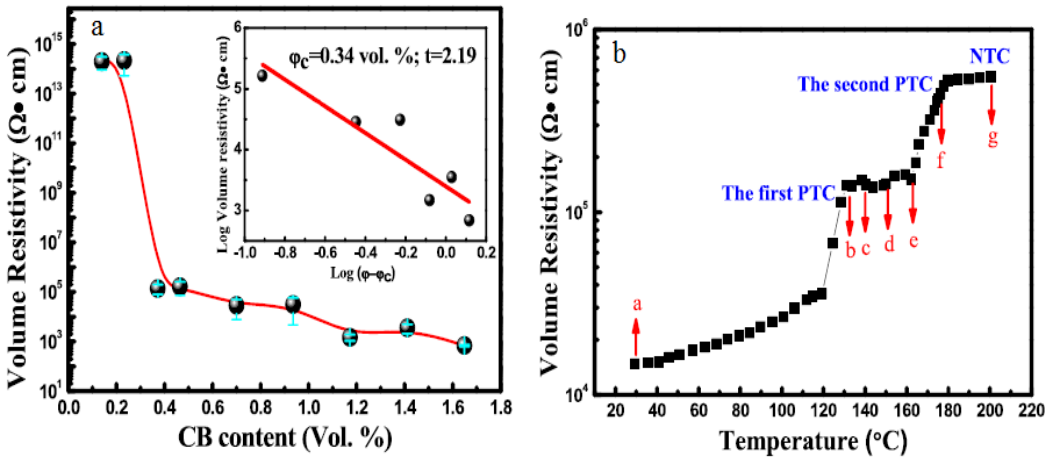

Figure 2.19 a) Percolation behaviour of CB/PP/UHMWPE and b) PTC effect for 0.9 Vol % CB filled PP/UHMWPE composite [101].

Conversely, Xu *et al.* [97] in their study of PTC effect on CB/HDPE/PP composite did not observe the double PTC effect. This was due to the selective

localisation of CB particles in the HDPE phase and the CB filler content being very close to the percolation threshold. This meant that CB migration into the polymer-polymer interface was not possible therefore the PTC effect was governed by the thermal expansion of the HDPE polymer. Pour *et al.* [105] reported the same effect when investigating the PTC effect of PMMA/LDPE composite filled with CB particles. The concentration of CB used was 2 wt% which was close to the percolation threshold of the CB/PMMA/LDPE composite.

The PTC intensity reported in literature for polymer blend composites are usually higher than the values for a single polymer [21, 82, 94]. The increase in PTC intensity maybe linked to the reduction in conductive fillers needed to percolate the composite. A reduction in conductive particles leads to a reduction in conductive network therefore disruption of the network causes a big change in resistivity. Addition of a second polymer has also been reported to lead to a reduction in PTC [100, 105]. Pour *et al.* [105] in a CB/PMMA/LDPE composite found that the PTC intensity for the mixed polymer composite was small compared to the either CB/PMMA or CB/LDPE composite even though the concentration of CB used was close to the percolation threshold. In a CB/HDPE/EVA composite, Yang *et al.* [100] observed no improvement in the PTC intensity of the composite compared to the CB/HDPE or CB/EVA. The observed PTC intensity was smaller as shown in figure 3.8.

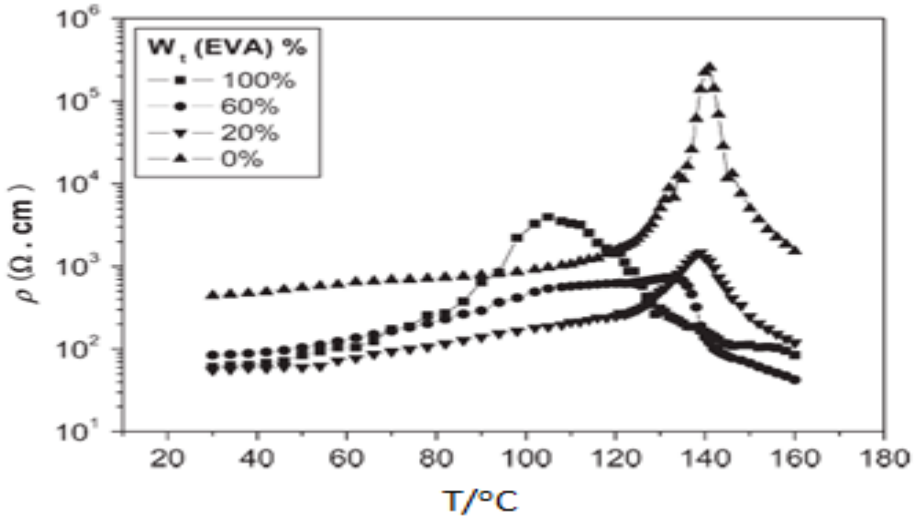

Figure 2.20 PTC behavior for CB/HDPE/EVA composite [100].

PTC intensity increases with an increase in polymer concentration of the polymer carrying the conductive fillers. Yu *et al.* [98] reported an increase in PTC intensity with increase in LDPE content in a CB/EVA/LDPE composite. The CB particles were localised in the LDPE phase therefore an increase in LDPE content is comparable to a reduction in CB concentration. The "reduction" in CB concentrations leads to a reduction in conductive networks relative to the polymer matrix hence an increase in PTC intensity. Xu *et al.* [97] found a PTC intensity of 8.3×10^7 for a CB filled HDPE/PVDF composite with a ratio of 1:1 for the two polymers. An increase in HDPE/PVDF ratio to 2:1 resulted in a decrease in PTC intensity to 6.5×10^6 for the mixed polymer composite. The same authors in a HDPE/PP filled CB composite reported a decrease in PTC intensity from 3.3×10^7 for a 1:1 ratio for HDPE/PP to 6.7×10^5 for a 2:1 ratio of the two polymers [97]. An increase in the amount of polymer in the filler localised phase reduced the PTC intensity of the mixed polymer composite. This effect is not expected since the PTC intensity relies on the concentration of the filler in the localised polymer matrix. The increase in the polymer content increases the volume of

"space" occupied by the conductive fillers. Around the melt temperature for the percolated polymer phase, the disruption of conductive pathway should increase with increasing amount of polymer for fixed filler content since the effective conductive network to polymer ratio is reduced.

Careful selection of the second polymer can lead to elimination of the NTC effect without crosslinking the polymer composite. Wei *et al.* [101] reported an elimination of the NTC effect when they used UHMWPE as the second polymer in a CB/PP composite. The CB/PP/UHMWPE composited formed had a segregated structure with CB particles dispersed at the interface between the two polymers. The high viscosity of the UHMWPE decreased the migration of the CB particles as the temperature increased therefore CB particles reagglomeration was prevented and this led to the elimination of the NTC effect [101]. Feng and Chan [21] observed the same effect in a CB/PP/UHMWPE composite which led them to suggest that a very high viscosity semicrystalline material can be used in a mixed filler to prevent the appearance of the NTC effect. CF/LMWPE/UHMWPE composite examined by Xi *et al.* [82] also showed the elimination of the NTC.

The reproducibility of the thermo-electrical behaviour of CPCs is challenging but the addition of a second polymer enhances the reproducibility of the composite as reported by Xi *et al.* [82] and Kar and Khatua [107]. The enhanced reproducibility of the composite according to Xi *et al.* [82] was caused by the high viscosity of the UHMWPE in the CF/LMWPE composite. Kar and Khatua [107] explained that the PCL used as the second polymer in the Ni-coated graphite/PC composite acted as a plasticizer. The PCL helped reduce the PTC temperature well below the T_g of PC therefore the mobility of the conductive fillers at PTC temperature was

hindered. This leads to the formation of the same conductive network after cooling to room temperature hence an enhanced reproducibility [107].

2.9 Conductive filler effect on PTC behaviour

Conductivity of the polymer composite depends to a large extend on the filler used therefore filler properties such as the filler conductivity and size will impact the conductivity of the final composite.

Carbon based fillers especially carbon black (CB) has been used extensively in PTC studies of conductive polymer composites due to their low cost and high PTC intensity when compared to other fillers [16, 17, 21, 84, 108]. Some metallic filler such as nickel and copper have been utilised in the study of CPC although their percolation threshold is much higher when compared to the carbon based conductive fillers [34, 90]. The problem of oxidation on the surface of metallic fillers affects conductivity of the composite. The high cost and high density of metallic fillers makes them limited in their use in a wide application.

2.9.1 Effect of filler shape and size

Many researchers have demonstrated that an increase in conductive particle size (i.e. diameter of the particle) increases the percolation threshold of a conductive polymer composite [49-52]. According to Ota *et al.* [51], the inter particle distance between conductive particles increases with increasing particle size when randomly dispersed in a polymer matrix (Fig. 2.21). Jing *et al.* [52] demonstrated that an increase in particle diameter increases the interparticle distance. This

relationship was used to prove that the percolation threshold depended on the distance between conductive particles by fitting experimental data for percolation threshold against particle size (fig. 2.22). This means that electron tunnelling or contact between particles is difficult when large particles are used as fillers. Wu [109] demonstrated that for the same particle volume fraction, the average distance between the particles is dependent on the size as shown in equation below.

$$\delta = D\left[\left(\frac{\pi}{6\varphi}\right)^{1/3} - 1\right] \tag{3.2}$$

Where δ is the average surface-to-surface interparticle distance, D is the diameter of the particle and φ is the volume fraction of the particles.

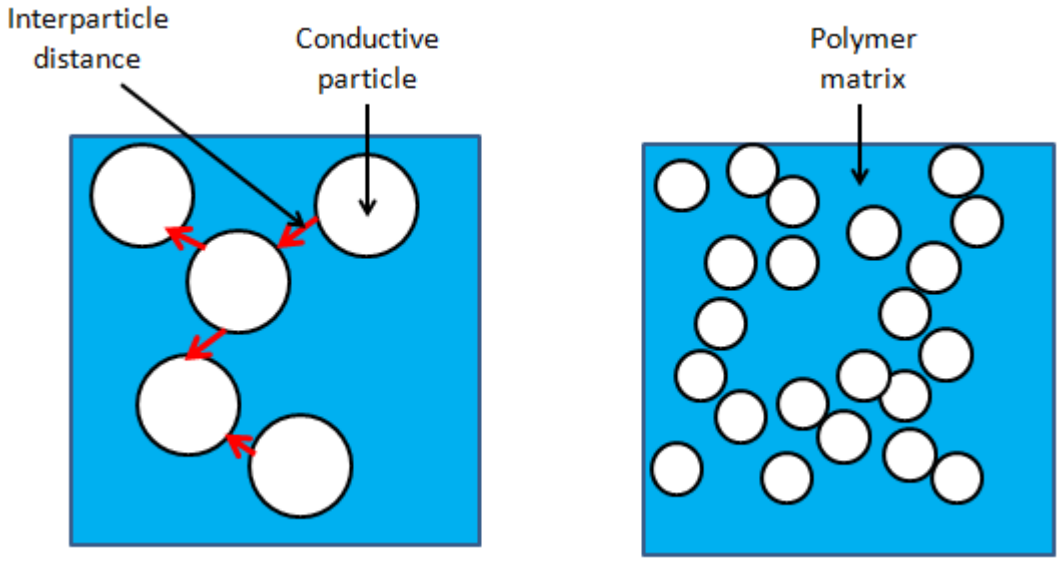

Figure 2.21 Schematic of size effect on average interparticle distance between conductive fillers.

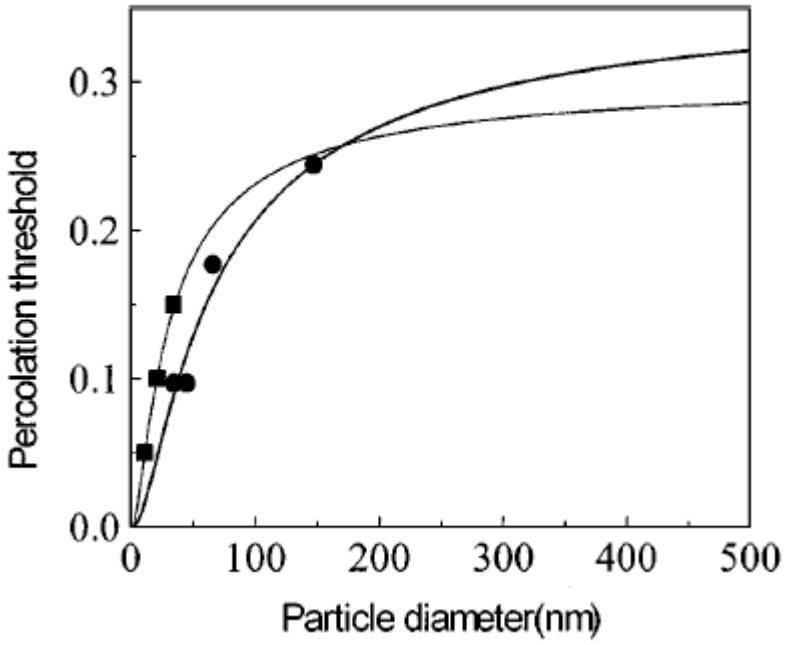

Figure 2.22 Percolation threshold as a function of particle diameter [52].

The PTC behaviour of conductive composites relies on the robustness of the conductive networks or pathways formed within the polymer matrix. At a given particle volume fraction, large particles dispersed in a polymer will show high PTC intensity or amplitude than smaller particles of the same conductive filler (fig.2.23) [53, 110]. This is caused by the ease with which the electron tunnelling distance can be affected due to the initial gap been bigger for large particles. Luo and Wong [38] observed that the PTC intensity was enhanced when they switched the filler in HDPE from a CB with smaller particle size (BP2000) to one with a larger particle size (N660). A more robust conductive network is formed by small particles due to the increase in the number of particles in contact with each other. The thermal volume expansion of the polymer matrix has a minor effect on the conductive network formed by smaller filler size and few conductive pathways are broken. This leads to a relatively small increase in resistance hence the small

PTC intensity. Although large particles increases the PTC amplitude, their large resistivity at room temperature acts as a disadvantage therefore a compromise between PTC intensity and resistivity at room temperature should be used.

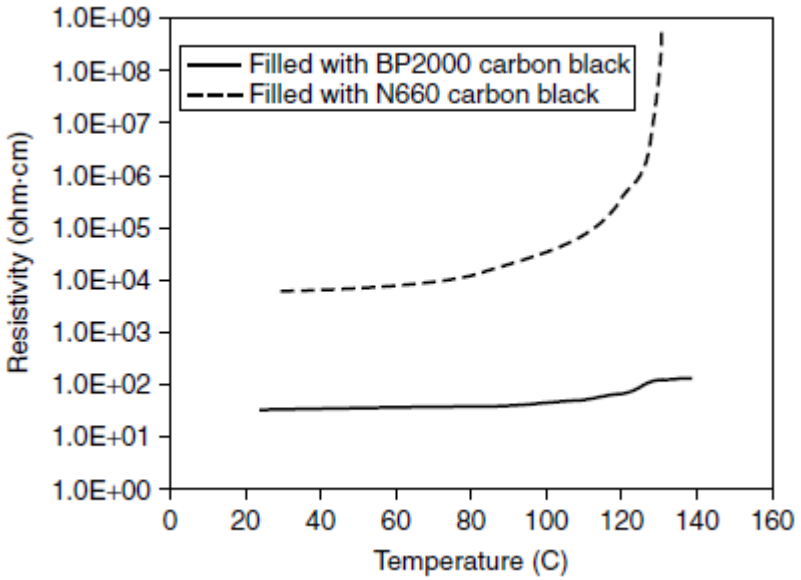

Figure 2.23 PTC curve for HDPE filled with different carbon blacks. BP2000: small particle size. N660: Large particle size [38].

2.9.2 Effect of mixed fillers

The percolation behaviour of CPC affect the PTC behaviour of the composite and this has lead many researchers into finding different ways to lower the percolation threshold of CPCs. CB based composites for example requires high loadings to conduct and this usually have implications on the processing and mechanical properties of these composites. One technique used in enhancing the room temperature resistivity as well as the PTC behaviour of a conductive composite is the introduction of a second filler into the composite [84, 88, 111-117]. The

second filler is usually high aspect ratio fillers such as MWNT or carbon fibre (CF) and the purpose of these fillers is to connect or bridge the gaps between the primary particles so that a conductive partway can be easily established (fig. 2.24). The repeatability of the thermo-electrical behaviour of the composite has also been reported to be enhanced when mixed fillers are used in a composite [84, 112, 114, 118] (fig. 2.25).

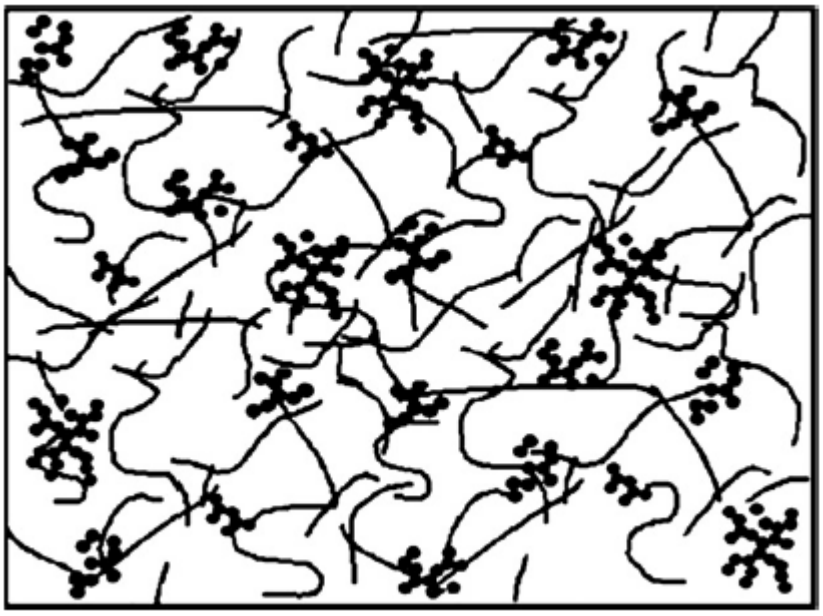

Figure 2.24 Bridging effect by addition of second filler on CPC [116].

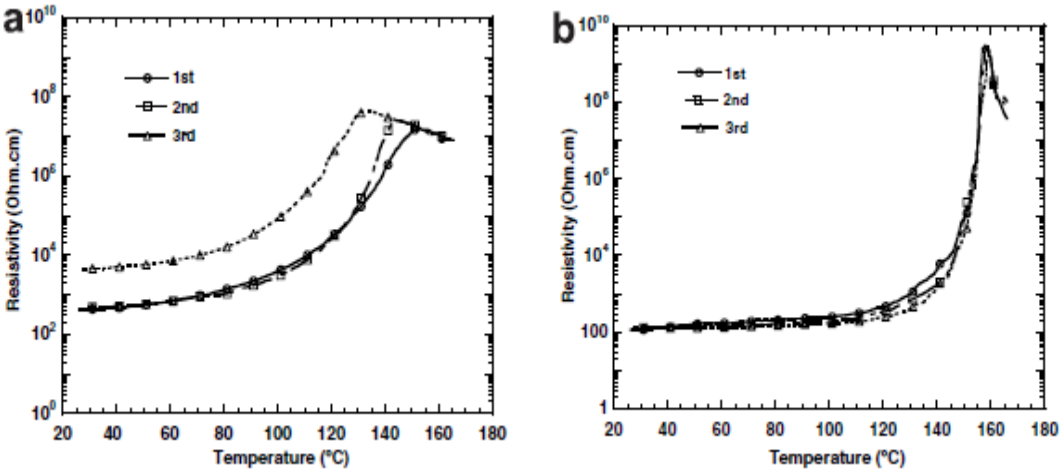

Figure 2.25. Thermo-electric behaviour of HDPE filled with a) CB and b) CB/MWNT [84].

The effect on PTC behaviour by the addition of second filler to CPC has yielded mixed results in the literature. Both increase and decrease in PTC intensity with addition of second filler has been reported in the literature [84, 111, 114, 119]. Table 2.6 show an increase with PTC intensity when second filler is added to the composite system. Dang *et al.* [111], reported an increase in conductivity when CF were added to a CB/HDPE composite. The CF particles bridged the gaps between the CB agglomerates therefore enhancing the conductive pathway as shown in figure 2.24. The same bridging effect was reported by Fang *et al.* [112] when MWNT was added to CB/EVA. The PTC intensity of the composite increased with increasing amount of CF and a reduction in NTC was also reported. The reduction in NTC is due to the difficulty in the movement of CF fillers in the polymer melt [111].

Table 2.6 PTC Intensity (PTC_I) for different mixed filler composites.

Polymer	Filler	PTC_I	Difference in PTC_I	Reference
HDPE	CB	2.5	3	[84]
HDPE	CB/MWNT	5.5		
HDPE	CB	5.2	2	[114]
HDPE	CB/GNF	7.2		
HDPE	CB	4.2	0.4	[42]
HDPE	CB/CF	4.6		
HDPE	CB	6.1	1.5	[111]
HDPE	CB/CF	7.6		
PP	CB	5.9	0.7	[111]
PP	CB/CF	6.6		
UHMWPE	MWNT	0.4	1.1	[120]
UHMWPE	MWNT/CB	1.5		

Li *et al*. [114], observed both an increase in PTC intensity and a decrease in PTC intensity when they studied the effect of addition of graphite nanofibers (GNF) on CB/HDPE composite system. They observed an increase in PTC intensity with the composite containing 20 wt% CB had GNF added to it. Although further increase in the amount of GNF decreased the PTC intensity, the PTC intensity did not drop below that of the CB/HDPE composite. The CB/HDPE composite filled with 25 wt% CB showed a slight increase in PTC intensity when GNF was added. An increase in the GNF content led to a decrease in PTC intensity below that of the CB/HDPE system. A similar effect was reported by Lee *et al.* [84], when MWNT was added to a CB/HDPE system. Lee *et al.* [84] observed that for the same CB/HDPE composite, an increase in MWNT content increased the PTC intensity but the intensity decreased with further addition of MWNT above a certain MWNT concentration. The decrease in PTC intensity with increasing MWNT above a certain concentration can be explained by the increase in conductive pathways due to the increase in filler concentration. The PTC intensity is hugely influenced by the amount of filler in the composite therefore based on

the observations of Li *et al.* [54] and Lee *et al.* [4], it could be argued that close to the percolation threshold, addition of second filler will increase the PTC intensity. Adding second filler to already percolated composite system is likely to reduce the PTC intensity. The percolation threshold for the CB/HDPE system in Li *et al.* [114] studies was 20 wt% and from table 2.7 it can be seen that the system that showed a decrease in PTC intensity had a CB content of 25 wt%. At low concentrations of the GNF, if the CB content is close to the percolation threshold, the number of conductive pathways increases slightly hence the decrease in resistivity but these pathways can be easily disrupted. Further increase in GNF increases the number of conductive pathways hence the difficulty in disrupting all the conductive pathways which leads to a decrease in PTC intensity. Further increase in GNF will result in a decrease in PTC intensity even below the CB/HDPE system since the conductive network increases even more compared to the CB/HDPE composite and this effect was also observed by Lee *et al.* [84].

Table 2.7 PTC intensity for the HDPE/CB/GNF composites [114].

Samples	I_{PTC}[a]	$\log \rho_{RT}$[b] (Ω cm)	$\log \rho_{max}$[c] (Ω cm)	T_s[d] (°C)
80/20	5.229	3.465	8.693	151
80/20/0.25	7.212	2.367	9.578	159
80/20/0.5	6.246	2.278	8.524	158
80/20/0.75	6.062	1.986	8.047	158
80/20/1.0	5.999	1.847	7.846	158
75/25	4.210	1.902	6.113	159
75/25/0.25	4.781	1.496	6.278	162
75/25/0.5	2.982	1.294	4.276	161
75/25/0.75	2.803	1.035	3.838	160

[a] PTC intensity, defined as the logarithm ratio of ρ_{max} to ρ_{rt}.
[b] Logarithm resistivity at room temperature.
[c] Logarithm resistivity at T_s.
[d] Switching temperature.

Figure 2.26 shows the percolation behaviour and PTC intensity for the composites used in the study by Lee *et al*. It is observed that for the system above the percolation threshold (i.e 25 wt% CB composite systems), the PTC increased with increase in MWNT up to 0.5 wt% MWNT. The PTC intensity starts to decrease after this concentration and this is caused by the increase in conductive pathways since the composite at this concentration is higher than the percolation threshold 0.5 wt% MWNT CB/HDPE composite. For the CB/HDPE composite containing 0.5 wt% MWNT, the percolation threshold is at 20 wt% CB and a CB content of 25 wt% is way above the percolation therefore any increase in MWNT content further enhances the robustness of the conductive networks. For the same loading of MWNT, an increase in CB content increases the PTC intensity and the same effect was observed by Cui *et al.* [120]. This is explained by the increase in the amount of CB particles taking part in the conductive network. The conductive network formed by high aspect ratio fillers such as MWNT are very robust and are slightly disrupted by the expansion of the polymer matrix during melting but the addition of spherical particles such as CB acts as weak points within the conductive network hence an increase in PTC intensity.

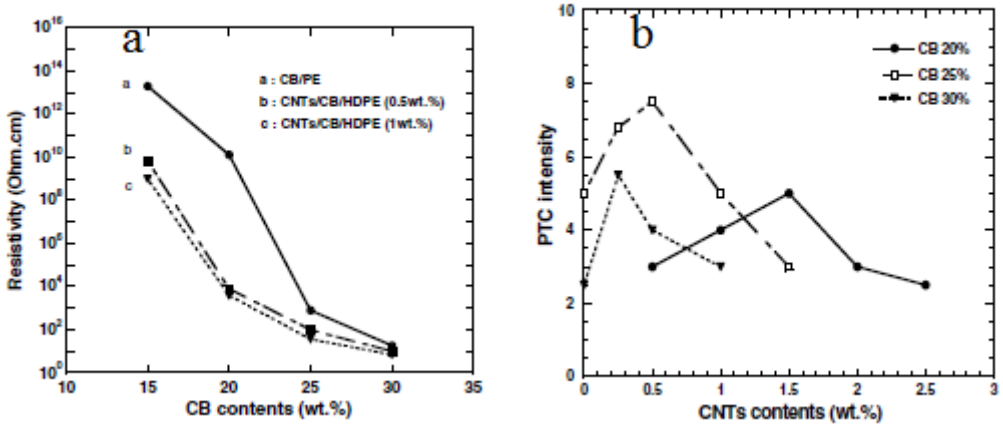

Figure 2.26 a) percolation behaviour of CB/HDPE filled with different MWNT and b) PTC intensity for CB/HDPE composites filled with different MWNT [84].

The second filler used in mixed filler composites can be non conductive as shown by Bao *et al.* [121] when they doped MWNT/PP system with montmorillonite (MMT). The percolation threshold of the composite increased with addition of MMT but an increase in PTC intensity was reported. An interesting observation by Bao *et al.* [121] was the increase in PTC temperature with increasing MMT concentration. This phenomenon is due to the increase in viscosity of the composite when MMT was added. The increase in viscosity restricted the movement of the polymer chains therefore more energy was needed to cause a disruption in the conductive network. The change in PTC temperature with addition of MMT to the MWNT/PP demonstrates a technique that can be used to tune the PTC temperature for CPCs [121]. Sridhar *et al.* [37] observed a slight decrease in room temperature resistivity when they added a MMT modified clay to a CB/HDPE composite. The change in PTC intensity and temperature remained minimal when MMT was added to the CB/HDPE composite (fig. 2.27). It is observed in figure 2.27 that the addition of MMT to HDPE filled with silver

coated glass bead causes an increase in PTC temperature and this is in agreement with the observation by Bao *et al.* [121]. Again no significant change in PTC intensity was observed for the composite when MMT was added to the composite.

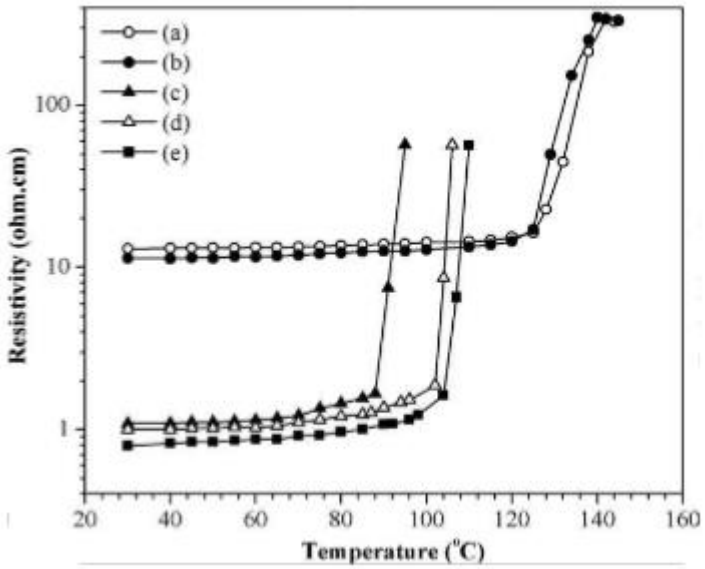

Figure 2.27 PTC behaviour for a) CB/HDPE b) CB/MMT/HDPE c) Ag-coated glass bead/HDPE d) Ag-coated glass bead/MMT/HDPE [37].

2.10 Summary of factors affecting PTC intensity

The positive temperature coefficient (PTC) intensity which describes the extent of the change in resistivity during the PTC effect is important in determining the suitability of a composite for the selected application. The PTC intensity is affected by all the factors that affect the electrical conductivity of the polymer composite from the type of matrix and filler all the way to the processing method. Although the PTC intensity is affected by several factors, the most important factors are the ones that directly affect the polymer matrix (such as the phase

structure of the polymer, polarity of the polymer and filler (interfacial interactions)) and filler (packing density or factor of the filler and the oxidation of the conductive filler for metallic fillers).

Semicrystalline polymers can experience three reversible transitions when heated which are linked to a volume change in the polymer [39]. These transitions are crystallisation, melting and glass transition and they affect different phases of the polymer. Crystallisation and melting affects the crystalline phase while glass transition is linked to the amorphous phase. The PTC effect of most polymer composites occurs in correspondence of one of the phase transition temperatures, due to the volume change of the polymer causing a disruption in the conductive filler network.

The PTC intensity depends on the polymer matrix structure with many researchers reporting a higher PTC intensity for crystalline polymers compared to amorphous ones [85, 89, 94]. The difference in PTC intensity is linked to the smaller thermal expansion of amorphous polymers compared to the thermal expansion experience by semi crystalline polymers during melting [36]. Meyer [89] demonstrated that a crystalline polybutadiene had a higher PTC intensity compared to the amorphous version of the same polymer and this same effect was observed by Lou *et al*. [85].

Although there is a general acceptance that amorphous polymers will have lower PTC intensities, some experiments do not support this. Fournier *et al*. [22] for instance produced an amorphous composite with three orders of magnitude change in PTC intensity which is similar to some semicrystalline polymers [122].

Chemical or irradiation can be used to crosslink the polymer composite resulting in elimination of the NTC effect and increase in PTC intensity. Irradiation is best since it is conducted at room temperature after the conductive networks have formed. This crosslinked network prevents the migration of the conductive filler outside the network and this enhances the reproducibility of the PTC effect [87]. Crosslinking causes an increase in the melt viscosity of the composite and an increase in irradiation dose increases the PTC intensity as demonstrated by Seo *et al*. [87].

The dispersion of conductive fillers in a polymer matrix and the interfacial interaction between the filler and the matrix are dependent on the polarities of the polymer and the filler [122]. Polar fillers are dispersed more evenly in polar polymers while they partially agglomerate in nonpolar polymers. Nonpolar fillers on the other hand disperse more homogeneously in nonpolar polymers. The homogeneous dispersion in polar polymers by polar fillers results from the interfacial restricted layer formed by the strong interactions between the polar groups of the filler and the polymer. The existence of a strong interaction between the polymer and filler prevents the filler from agglomerating as temperature increases [123]. This strong polymer-filler interaction (interfacial adhesion) restricts the movement of conductive fillers and this increases the PTC temperature and causes a reduction in NTC effect. A decrease in PTC intensity is expected from improvement of interfacial adhesion due to the increase in energy required to disrupt the conductive network formed within the composite but mixed effects have been reported for the PTC intensity [122, 123].

Jia *et al*. [123] reported an increase in PTC intensity when the interfacial adhesion between carbon black (CB) and LDPE/EPDM was improved by changing the

polarity of the CB filler in LDPE/EPDM composite. Zhang and Pan [122] showed a decrease in PTC intensity with increase in interfacial adhesion for HDPE polymer filled with an alloy of tin (Sn) and lead (Pb).

The shape and special distribution of the conductive fillers within the polymer matrix affects the PTC intensity of the composite. The packing density or factor (F) according to Mamunya *et al* [10], is the parameter that describes and takes into considering the shape and spatial distribution of the conductive fillers within a polymer composite. The packing factor (F) is equal to the maximum possible filler volume content within the polymer:

$$F = \frac{V_F}{V_f + V_P}$$

where V_f is the volume occupied by the filler particles at the highest possible filler fraction and V_p is the volume occupied by the polymer between the filler particles [34].

For monodispersed spherical fillers packed statistically, the packing factor will be 0.64 regardless of the particle size [34]. The packing density decreases with increase in aspect ratio of the conductive fillers and this leads to a reduction in percolation threshold.

A decrease in packing density decreases the PTC intensity of the composite due to the deviation of the particle shape from the spherical one. The interparticle distances between spherical particles within a composite is bigger when compared to non-spherical particles (high aspect ratio particles) [52]. This result in the formation of weak conductive network by the spherical particles therefore the conductive pathways can easily be destroyed resulting in a higher PTC intensity

than non spherical particles. CB filled PP composites are reported to have a higher PTC intensities compared to MWNT filled PP and this is due to the robustness of the conductive networks formed by the high aspect ratio MWNT as a result of the low packing density associated with it [67]. Luo and Wong [53] demonstrated that HDPE filled with CB particles of less aggregated structure (closer to spheres) have higher PTC intensities when compared with CB of more aggregated structure in the same polymer and this is again due to the packing density of the particles.

Metal fillers such as copper which has high conductivity and low cost can be used in PTC application but the susceptibility of these fillers to oxidation make them unsuitable. The oxidation of the conductive filler surface causes an increase in room temperature resistivity.

The PTC intensity of oxidised conductive fillers is higher compared to fillers whose surfaces are not covered by an oxide layer. Oxidation of conductive fillers increases the PTC intensity of the composite due to the increase in resistivity of the fillers. This is due to the weakness in the conductive network and is synonymous with a reduction in conductive filler content since the conductivity of some of the conductive fillers is reduced by the oxidation.

Yim *et al.* [124] protected the surface of copper particles from oxidation by treating the surface of the particle with a silane coupling agent before dispersing in an epoxy matrix to investigate the effect of oxidation on thermo-electrical properties. The PTC intensity reduced with an increase in silane coupling agent concentration due to an increase in protection of the copper particles from oxidation as temperature increases [124].

2.11 Negative temperature coefficient (NTC) effect

The sharp decrease in resistivity with temperature (NTC effect) that usually follows the PTC effect of conductivity polymer composite is a detrimental property for applications employing PTC materials such as self regulated heaters and overcurrent protectors [23, 87, 119]. The NTC effect is reported to be caused by the reagglomeration or rearrangement of the conductive particles during the melt process of the polymer matrix [14, 15, 23, 119, 125]. Above the melting temperature of the polymer matrix, the conductive particles gain mobility and can reassemble to repair the disrupted conductive pathways within the composite [87].

Due to the undesirable nature of the NTC effect in PTC materials, the elimination of the NTC effect has started to become a topic of interest. Many techniques have been proposed for the elimination of the NTC effect but one of the most effective ways is the crosslinking of the polymer matrix [15, 87, 88, 92]. Crosslinking can be achieved via the radiation or chemical crosslinking route depending on the polymer matrix. Radiation crosslinking can be performed at room temperature while chemical crosslinking requires temperatures usually above the melting point of the polymer [87]. This makes radiation crosslinking more appealing as a means of eliminating the NTC effect. The mobility of polymer chains in the melt encourages agglomeration of the conductive fillers and this leads to the NTC effect but during crosslinking, this effect is reduced significantly [87]. This reduction in polymer chain movement hinders the mobility of the conductive particles therefore eliminating the NTC effect.

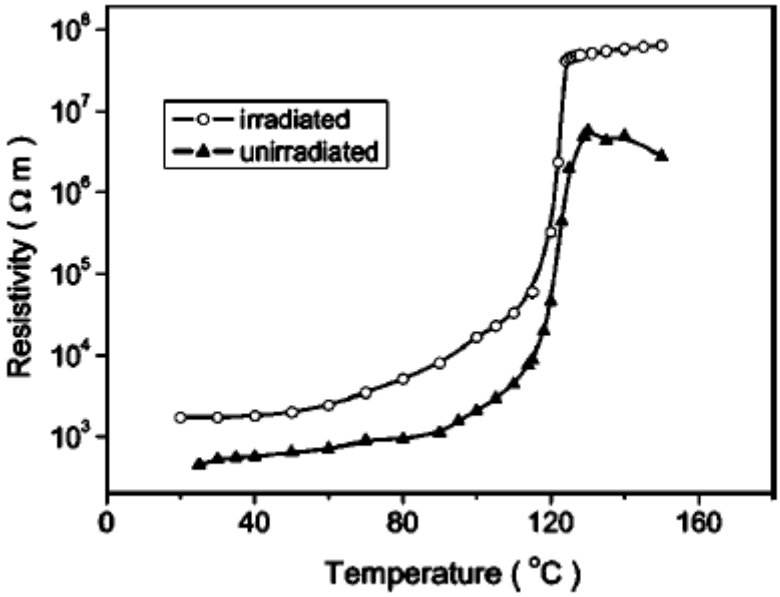

Figure 2.28 effect of irradiation crosslinking on NTC behaviour of MWNT/HDPE [23].

Seo *et al.* [87] investigated the effect of electron beam irradiation on the NTC effect of CB/HDPE composite. They found that the NTC effect was eliminated after crosslinking the polymer via the irradiation method. The elimination of the NTC effect was linked to the trapping of CB particles in the crosslinked network. According to Seo *et al.* [87], crosslinking of HDPE occurs in the amorphous region of the polymer and since the CB particles are located within the amorphous region, the CB particles are more likely to be entrapped during crosslinking. They also observed an increase in PTC intensity with irradiation dose.

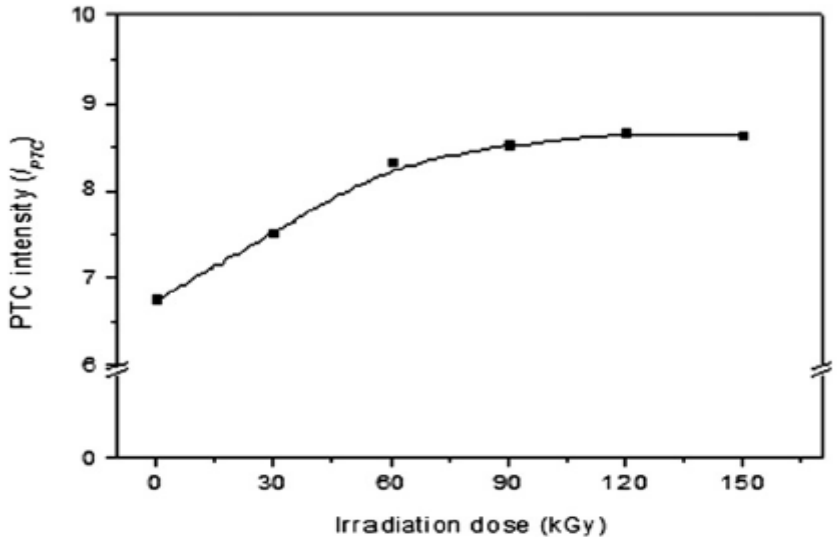

Figure 2.29 effect of irradiation dosage on PTC intensity for CB/HDPE composite [87].

^{60}Co γ-ray radiation was used by Tsao *et al*. [88] to crosslink CB/HDPE. They observed the elimination of the NTC effect and an increase in PTC intensity with radiation dose but one of the interesting discoveries in their studies was the reduction in PTC temperature with an increase in radiation dosage. Tsao *et al.* [88] stated that the decrease in PTC temperature was caused by the scission of the molecular chains into small crosslinking density molecular chains during the increase in radiation dosage. This presents not only a way to eliminate the NTC effect but to tune the PTC temperature of conductive polymer composites.

The use of high viscosity polymer either as polymer composites or a second polymer in a mixed polymer composites has also been reported to eliminate the NTC effect [16, 21, 93, 101, 125]. The high viscosity linked to these polymers restricts the movements of conductive particles therefore preventing them from reagglomerating.

Wei *et al.* [101] dispersed CB particles at the interface between PP and UHMWPE and observed no NTC effect when the investigated the pyroresistive properties of the composite. According to Wei *et al.* [101], the elimination of the NTC effect was caused by the high viscosity of UHMWPE which decreased the mobility of the CB particles therefore making reassembly of the CB particles difficult.

PVDF polymer filled with carbon fiber (CF) in a study by Wang *et al.* [125] did not show the NTC effect. The increase in viscosity of the polymer matrix was responsible for the elimination of the NTC effect.

The NTC effect can be reduced if not eliminated by the addition of second filler to a composite system (hybrid filler systems) [119, 125]. The addition of second filler increases the viscosity of the composites and this leads to a reduction or elimination of the NTC effect [119, 126]. Mobility of high aspect ratio fillers require high thermal energy therefore around the melting temperature of the polymer matrix, the polymer chain movement is hindered by these particles [119]. This is similar to an increase in viscosity of the polymer matrix and an increase in aspect ratio increases the viscosity of the polymer as reported by Kitano *et al.* [126].

CF were used as second filler in a CB/LDPE composite by Di *et al.* [119] to reduce the NTC intensity of the composite. The addition of CF to the CB/LDPE composite reduced the NTC intensity due to the increase in viscosity of the composite. The NTC effect was eliminated when CF was added to GF/PVDF composite.

Chapter 3. Materials and experimental procedures

3.1 Introduction

In order to investigate the positive temperature coefficient (PTC) effect of conductive polymer composites, the polymer matrix and the conductive filler properties have to be carefully considered. The materials selected for this project were based on their widespread use, availability and cost effectiveness. High density polyethylene is commonly used in PTC applications such as heat trace cables and the semi crystalline nature of the polymer makes it a good candidate for a polymer matrix. Glass coated silver particles not only have good conductivity but the shape and size of the particles can be controlled easily.

Industrial polymer processing method is employed in the preparation of the composites and several characterisation methods are used to investigate the final composites.

This chapter will detail the properties of the materials used in this project and the experimental methods used.

3.2 Materials

3.2.1 Polymer matrices

High density polyethylene (HDPE) was obtained from Ineos Polyolefins under the trade name Rigidex HD5218EA. For the polymer blend composites, a plastomer based on propylene-ethylene (PPE) copolymer (Versify®) produced by Dow was mixed with HDPE. The polymer according to the manufacturer has a unique chain microstructure which makes it an excellent candidate to induce

flexibility and can be easily blended with other polyolefins. The properties for the HDPE and Versify are shown in table 3.1.

Table 3.1 Properties of the polymers used in this study as provided by the suppliers.

Property	**HDPE**	**PPE**
Melt Flow Index (2.16 Kg Load)	18g/10mins	2
Density	0.952 g/cm^3	0.876 g/cm3
Flexural Modulus @ 23 ^{o}C	1050 MPa	100MPa
Melting Temperature (DSC)	131 ^{o}C	
Softening Temperature		107 ^{o}C

3.2.2 Fillers

Three different sizes of silver coated spherical glass spheres (AgS), with a relatively narrow size distribution were supplied by Potters Industries Limited, Germany. Silver coated glass flakes (AgF) of different sizes (20 µm and 100 µm) were procured from Glassflake Limited while Nippon Glass Flake supplied the smallest (5 µm) Ag coated glass flakes.

The silver coated poly(methyl methacrylate) (PMMA) (AgP) was purchased from Cospheric LLC, USA.

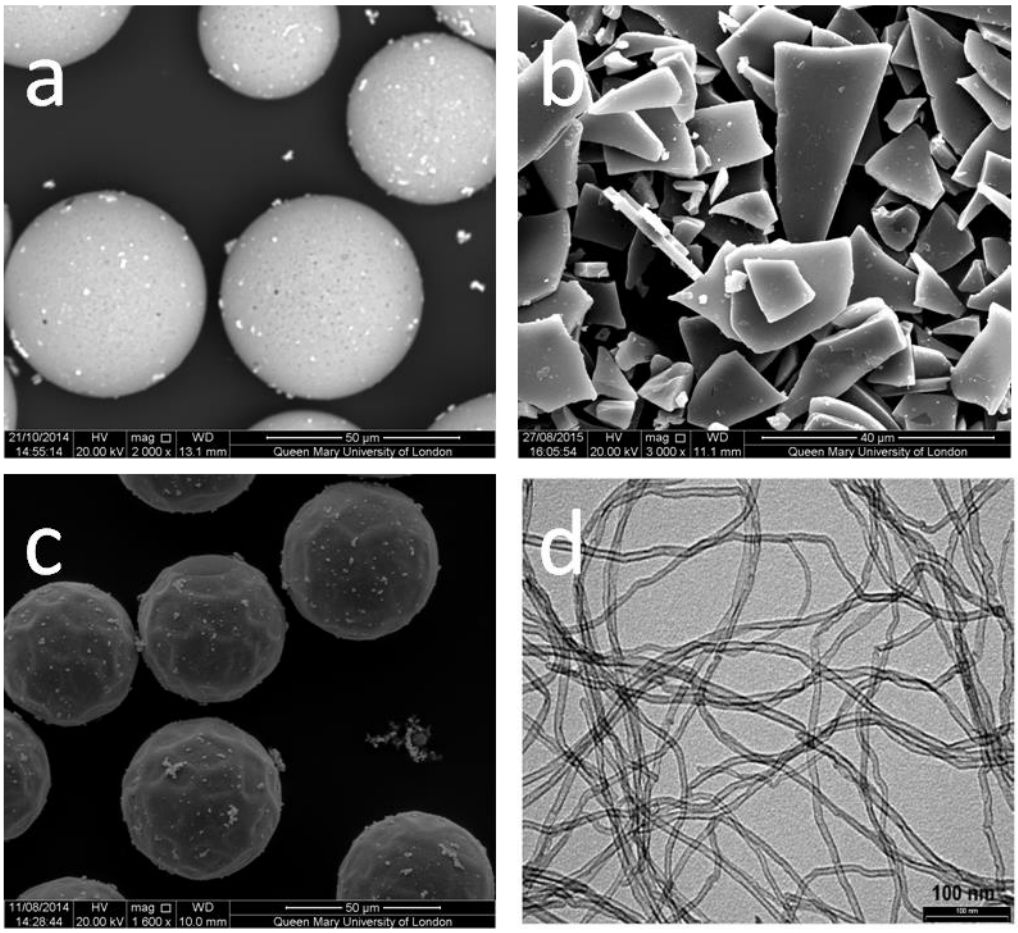

Figure 3.1 Shape of particles used in the experiment a) AgS, b) AgF c) AgP and d) MWNT.

Multiwalled carbon nanotubes (MWNT) (NC7000) supplied by Nanocyl S.A in Belgium were also used in this study. The carbon nanotubes had an average length and diameter of 1.5 µm and 9.5 nm respectively with carbon purity greater than 90 percent.

The dimensions of the fillers as supplied by the manufacturers are shown in the table 3.2.

Table 3.2 Conductive filler dimensions as provided by the suppliers.

Particle	Diameter/µm	Thickness/µm
AgS_S	8	N/A
AgS_M	50	N/A
AgS_L	100	N/A
AgF_S	5	08 - 1.2
AgF_M	20	1.01 – 1.3
AgF_L	100	1.01 - 1.3

3.3 Composites preparation

All composites were prepared via a melt extrusion method using a mini twin screw extruder (DSM Xplore Micro 15) with a processing temperature of 170 ^{o}C, screw speed of 50 rpm and mixing time of 15 mins (unless otherwise stated). The extruded strands were pelletized and hot pressed into rectangular bars using a Collins P300E hot press. The pellets were placed in a rectangular mould (25 mm × 4 mm × 2 mm) and hot press for 3 mins using a pressure of 60 bars after holding it at a temperature of 200 ^{o}C for 5 mins.

Figure 3.2 Mini extruder used in composite preparation.

For the mixed filler composites, the composites were prepared using the dilution method where a higher concentration of the composite is prepared and different amounts of polymer are added to achieve the required concentrations. The dilution of the composite was done at the same conditions as the master-batch. The composites were prepared by using the individual composites of the fillers as feeder stock.

MWNT/HDPE master-batch was prepared using a screw speed of 50 rpm to mix the polymer and filler at 170 ^{o}C for 3 mins.

The MWNT/AgS/HDPE hybrid composite was prepared under the following conditions of 170 ^{o}C temperature, 50 rpm for the screw speed and a mixing time of 5 mins while the AgF_S/AgF_L/HDPE hybrid composites were prepared using a screw speed of 50 rpm, temperature of 170 ^{o}C and a mixing time of 3 mins. The mixing time for AgF_S/AgF_L/HDPE was reduced to prevent damage to the silver coated glass flakes.

Polymer blend composites were prepared by predispersing the AgF_S in HDPE using the conditions stated above. The AgF_S/HDPE composite was pelletized and then mixed with PPE in a mini extruder. The conditions for the mixing of the composite with the PPE were a temperature of 170 ^oC, screw speed of 50 rpm and a mixing time of 5 minutes.

Table 3.3 Preparation of composites and the concentrations used for PTC studies. a and b are shown in chapter 5 and 6.

Materials				**Processing Condition**		
Composite	Vol % of Filler			Screw Speed/rpm	Mixing time/mins	Temp/^oC
HDPE + AgS_S	10	12.5	25	50	15	170
HDPE + AgS_M	12.99	16.44	19.59	50	15	170
HDPE + AgS_L	13.54	16.44	19.59	50	15	170
HDPE + AgF_S	4.3	5.13	7.12	50	15	170
HDPE + AgF_M	6.91	7.12	9.24	50	15	170
HDPE + AgF_L	7.5	8.91	9.04	50	15	170
HDPE + MWNT	0.8	1.2	2.9	50	3	170
HDPE + MWNT + AgS	a	a	a	50	5	170
HDPE + AgF_S + AgF_L	a	a	a	50	3	170
HDPE + PPE + AgF_S	b	b	b	50	5	170

3.4 Composites Characterization

Particle size distribution for the silver coated glass particle were characterised before and after melt mixing using an optical light microscope and a scanning electron microscope (SEM). The particles were dispersed on a glass slide and images taken from different parts before measuring the particles. Estimation of the particle size after melt processing was conducted by isolating the particles from the polymer by dissolution in xylene at 90 ^oC and filtering.

Morphology of the composites was studied using FEI Inspect-F scanning electron microscope (SEM). Samples for SEM image are fractured in liquid nitrogen. Fractured surface was analysed with a sputter coating of gold.

Thermal analysis on the samples was performed using a Differential Scanning Calorimeter (Mettler Toledo DSC-882). Samples were heated, in N_2 atmosphere, from room temperature to 250 ^oC at a heat rate of 10 ^oC/min and then cooled back to room temperature at the same rate. The second heating curve is used in examining the melting behaviour of the composite to eliminate differences in thermal history.

Dynamic Mechanical Analysis (DMA) was used to study the behaviour of the hybrid composites when subjected to periodic force. DMQ800 TA Instrument machine under a single cantilever mode was used during the test. Samples were tested from room temperature to 100 ^oC at a heat rate of 3 ^oC/min and a scanning frequency of 1 Hz. A hot pressed rectangular shaped sample with the dimensions 30 mm × 10 mm × 4 mm was used for the test.

Netzsch DIL 402 PC- Horizontal pushrod dilatometer was used to study the changes in linear dimension (coefficient of thermal expansion) with temperature of the hybrid polymer composites and the AgF_S/HDPE composite. The sample size for the dilatometry test was 25 mm in length and diameter of 5mm. The test was performed in a nitrogen environment from room temperature to 65 ^oC.

Direct current (DC) electrical resistivity of the samples was measured by the two point technique. A voltage scan was performed for each sample from 0.1 to 0.5 V with 0.01 V steps. The sample ends were coated with silver paste to reduce contact resistance between the sample and electrodes (fig.3.3). The resistance of

the samples were measured using a Keithley picoammeter and Agilent 6614C programmable voltage source. A Labview software allows the current (I) and voltage (V) to be recorded on a computer linked with the equipments. The region of the I-V curves obtained that obeyed Ohm's Law is used to calculate resistivity of the samples.

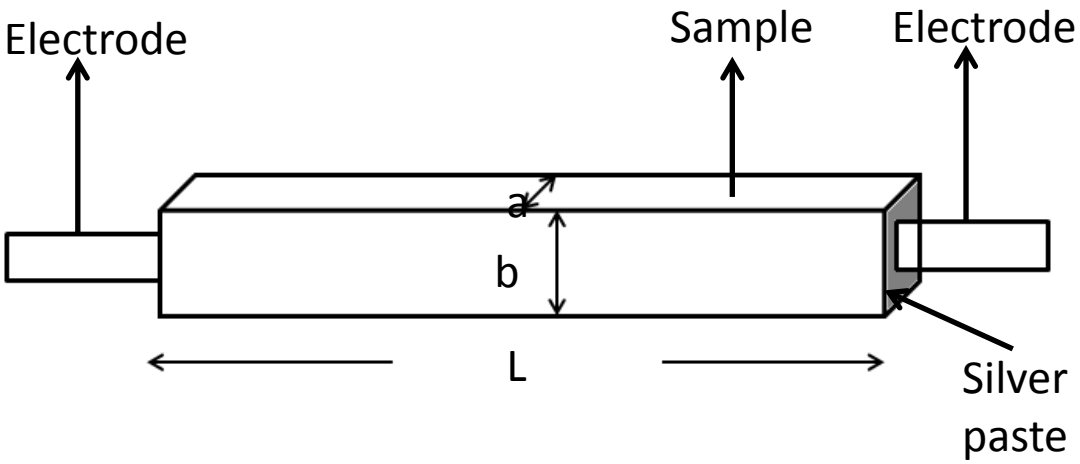

Figure 3.3 Sample dimensions for calculating electrical resistivity.

The resistivity (ρ) of the samples is calculated using the equation

$$\rho = \frac{R\ (a \times b)}{L} \tag{3.1}$$

where R is the resistance of the sample (found from the slope of the I-V curve), (a × b) is the cross-sectional area of the sample and L is the distance between the two electrodes. The reported resistivity is an average of a minimum of 3 measurements on different specimens.

Positive temperature coefficient (PTC) effect of the samples was examined by placing the samples in a heating chamber (fig 3.4). The chamber is heated from room temperature to 300 ^{o}C using a mini hot stage. Concurrently, under an applied voltage of 0.5 V, a reading of the current and the sample temperature was taken after every 1 s. A minimum of three samples are tested and the average PTC intensities are reported.

The samples selected for PTC investigations were composites with filler concentrations higher than the electrical percolation threshold of the composite. Two composites with filler concentration at the start and close to the end of the electrical percolation curve plateau were also selected for PTC investigation. This was done in order to understand the effect of filler concentration on the PTC behaviour of the composites.

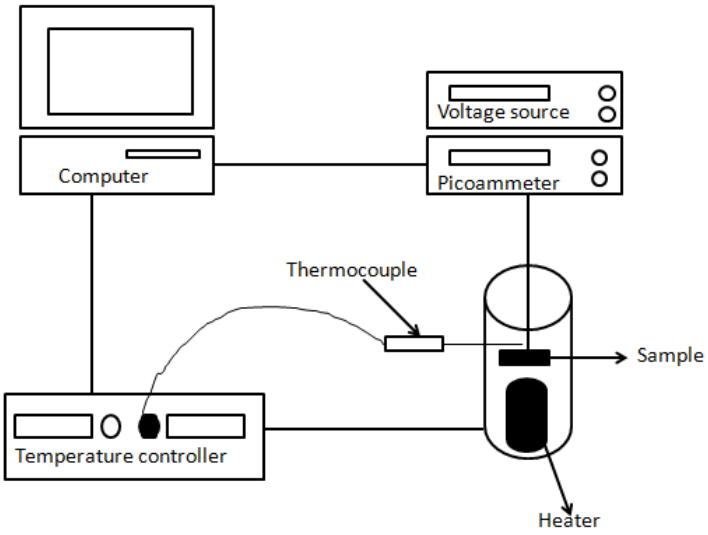

Figure 3.4 schematic of electrical and PTC effect examination.

Chapter 4. Effect of Particle Size and Shape on PTC of CPC

4.1 Introduction

In this study, silver coated glass particle (spheres and flakes) of different sizes are used to determine the relationship between the filler shape and size and the positive temperature coefficient intensity of the composite.

The experimental technique used in this chapter is described in chapter 3.

4.2 Results and discussion

4.2.1 Particle size distribution

The distribution of diameters of silver coated glass flakes and spheres are shown in Figure 4.1. The distributions of the particle diameter seem to be a normal distribution.

The mean which is the average of the data set and the median which is the centre or middle score for the data set were almost the same which confirms that the distribution of the particles was normal distribution (tab 4.1). The mean is affected by outliers therefore for skewed distributions, the median is a better choice in describing the midpoint of the data set but this was not the case for this data set. The median which is the same as the D50 of the particles is the midpoint of the data set where half of the data is below and above. The mode which describes the number which occurs frequently was also found to be closer to the

mean and the median for all the particles (tab 4.1). This also confirms the normal distribution of the silver coated glass particles.

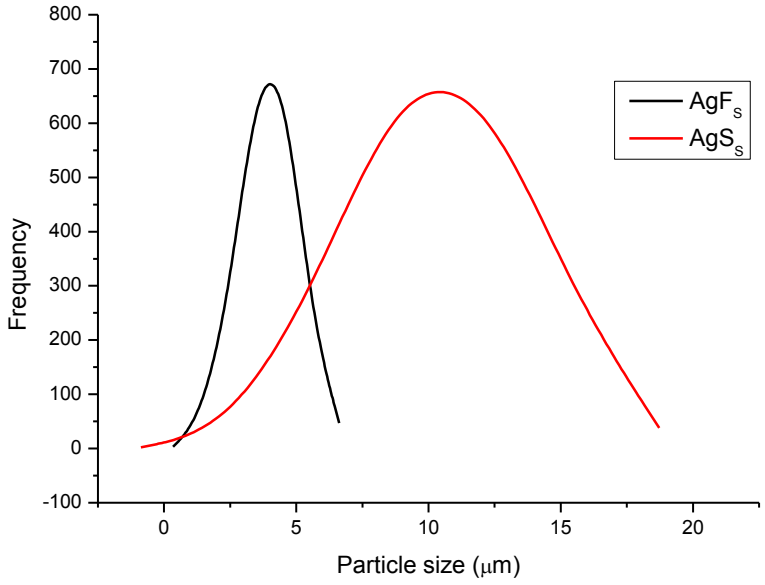

Figure 4.1 Size distribution (diameter) for silver coated glass flake (AgF_S) and silver coated glass sphere (AgS_s).

The skewness of the distribution was used as another measure of checking the normal distribution of the particle diameter. It was found that the skewness of the particles was closer to zero with no high positive or negative values for any of the particles (tab 4.1). This again confirms that the distribution for all the particles was normal distribution.

Table 4.1 Statistical analysis of the silver coated particles.

Particle	Mean/µm	Median/µm	Mode/µm	Skewness
AgS_S	8.92	8.47	8.7	0.07
AgS_M	48	47.87	49.58	-0.11
AgS_L	87.69	87.93	88.1	-0.07
AgF_S	4.26	3.97	3.49	0.56
AgF_M	26.9	24.07	25.4	0.11
AgF_L	80	79.62	75.54	0.36

Most of the particles diameter was between 40 µm and 60 µm and a D50 of 48 µm, in agreement with data sheet values from manufacturer. The measured values for the conductive particles are compared to the values claimed by the manufacturers (tab 4.2). The D50 value measured for the silver coated glass sphere particles were comparable to the average particle size given by the manufacturers. No major damage of the spheres was observed after melt compounding.

Table 4.2 Diameters of the three silver coated glass spheres.

Particle	D10 (µm)		D50 (µm)		D90 (µm)	
	Supplier	Measured	Supplier	Measured	Supplier	Measured
AgS_S	N/A	5	8	9	N/A	13
AgS_M	N/A	40	50	48	N/A	56
AgS_L	N/A	80	100	87	N/A	95

Silver coated glass flakes as expected were more sensitive to the compounding process. Figure 4.2 shows the particle size distribution before and after compounding for the large flakes (AgF_L). The bigger flakes experienced the

largest extent of damage with the D50 of AgF_L reducing by approximately 50 percent (tab 4.3). Interestingly, though, the size distribution curve becomes narrower, leading to a more uniform flake size (Figure 4.2).

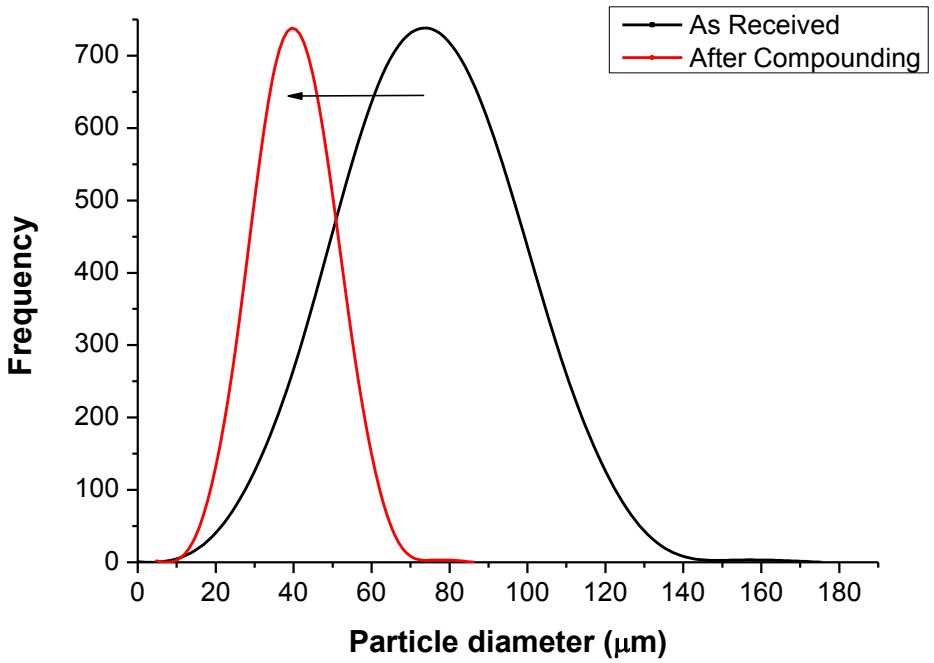

Figure 4.2 Graph showing particle size (lateral dimension) distribution of AgF_L before and after compounding. The average size decreases but the distribution curve becomes narrower.

Table 4.3. Lateral dimensions of the three silver coated glass flakes, before and after melt compounding. Where S is the supplier, B is before compounding and A is after compounding.

Particle	**D10 (µm)**			**D50 (µm)**			**D90 (µm)**		
	S	Measured		S	Measured		S	Measured	
		B	A		B	A		B	A
AgF_S	N/A	2	2	5	4	3	N/A	6	5
AgF_M	N/A	9	-	20	27	-	N/A	45	-
AgF_L	N/A	57	22	100	80	36	N/A	104	50

4.2.2 Morphology

Figure 4.3.a shows the SEM image of high density polyethylene (HDPE) filled with AgF_L. The orientation of the silver coated glass flakes in the polymer matrix was observed to be random and this was evident for all the different sized particles. No damage to the silver coating was observed on the lateral surfaces of the flakes even though the size was reduced after melt compounding. Dispersion of silver coated glass spheres in HDPE is shown in figure 4.3.b. Damage to the silver coating on the glass spheres was observed after cold fracture of the composite. A poor interfacial interaction was noticed for all composites, with clear signs of failure at the interface and debonding (void formation).

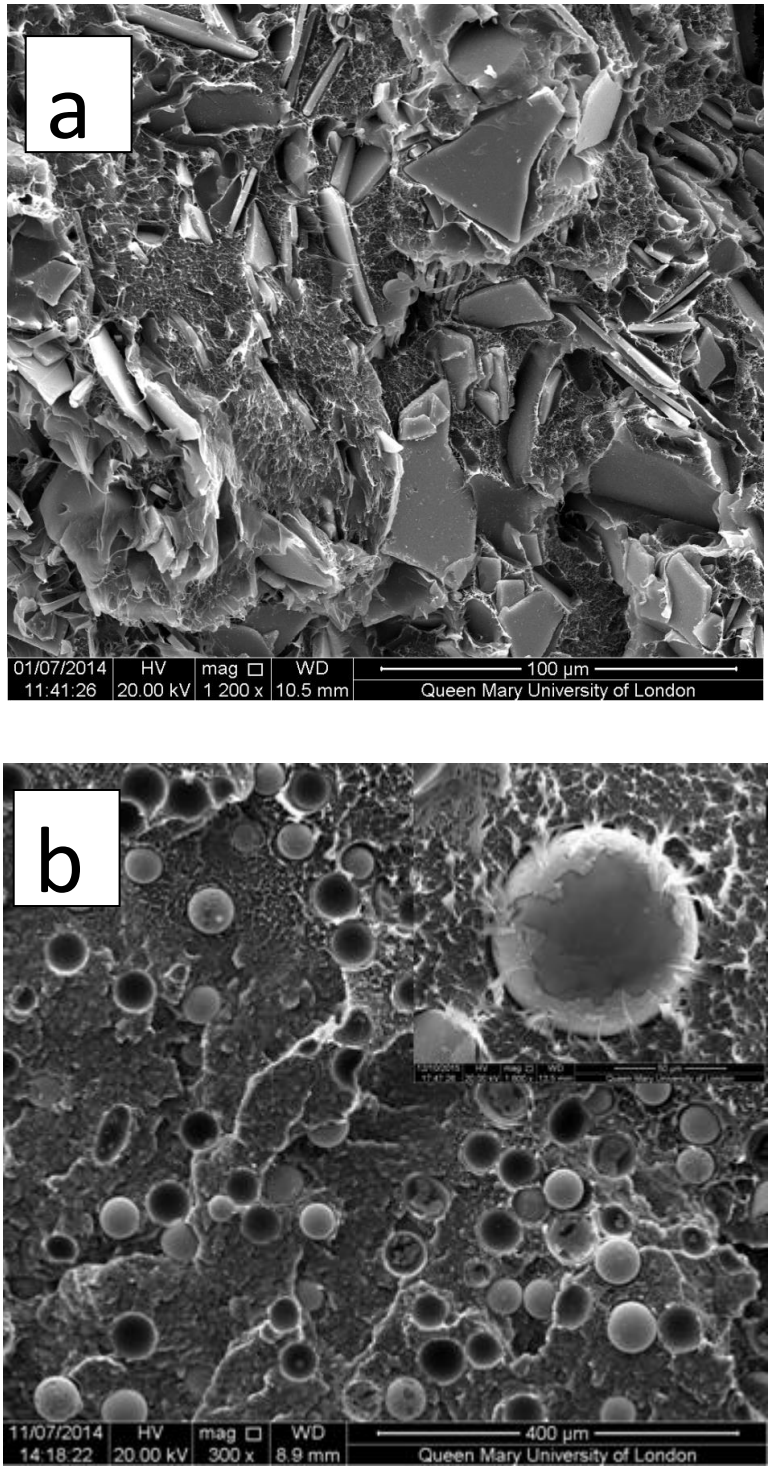

Figure 4.3 SEM images of cold-fractured cross-sectional areas of a) 30 wt% AgF_L/HDPE and b) 35 wt% AgS_M/HDPE with an insert of higher mag (50 µm) image the particle showing damage to the particle surface.

Elemental analysis was performed on the silver coated glass spheres to confirm the damages observed on the particle surface using an energy-dispersive X-ray spectroscopy (EDS). EDS analysis was performed on the particles before and after extrusion to tract changes in the percentage weight of silver. The results are displayed in figure 4.4. The silver coated particle before extrusion was 37 %wt. for the silver content while the silver content reduced to about 27 %wt. after extrusion. The reduction in weight percentage of silver content indicates that the silver coatings were partially damaged during extrusion. The damage to the particles was about 27 % and this would affect the percolation behaviour of the AgS/HDPE composites.

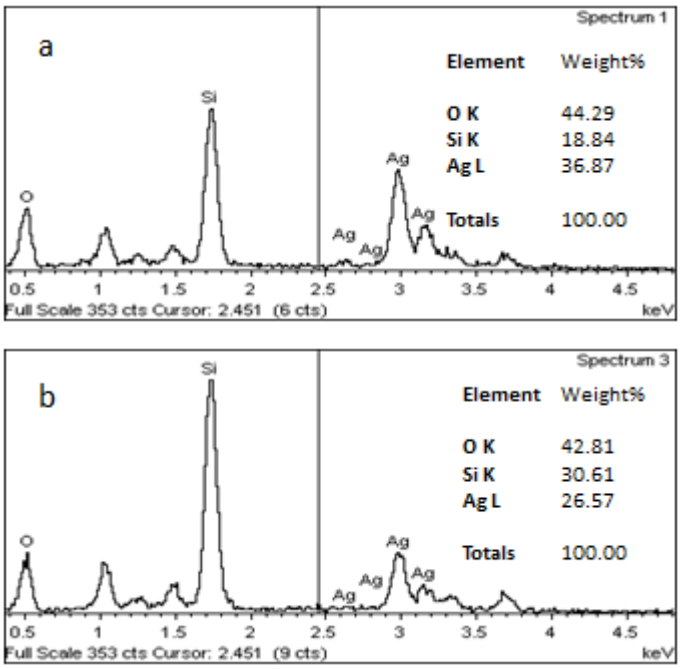

Figure 4.4 EDS analysis of the AgS particles a) before extrusion and b) after extrusion.

4.2.3 Electrical properties

Figure 4.4 shows the electrical percolation curves of composites containing each of the six conductive fillers. As expected, all the prepared composites showed a

similar trend of an increase in electrical conductivity with filler content, with a typical exponential increase after a threshold value.

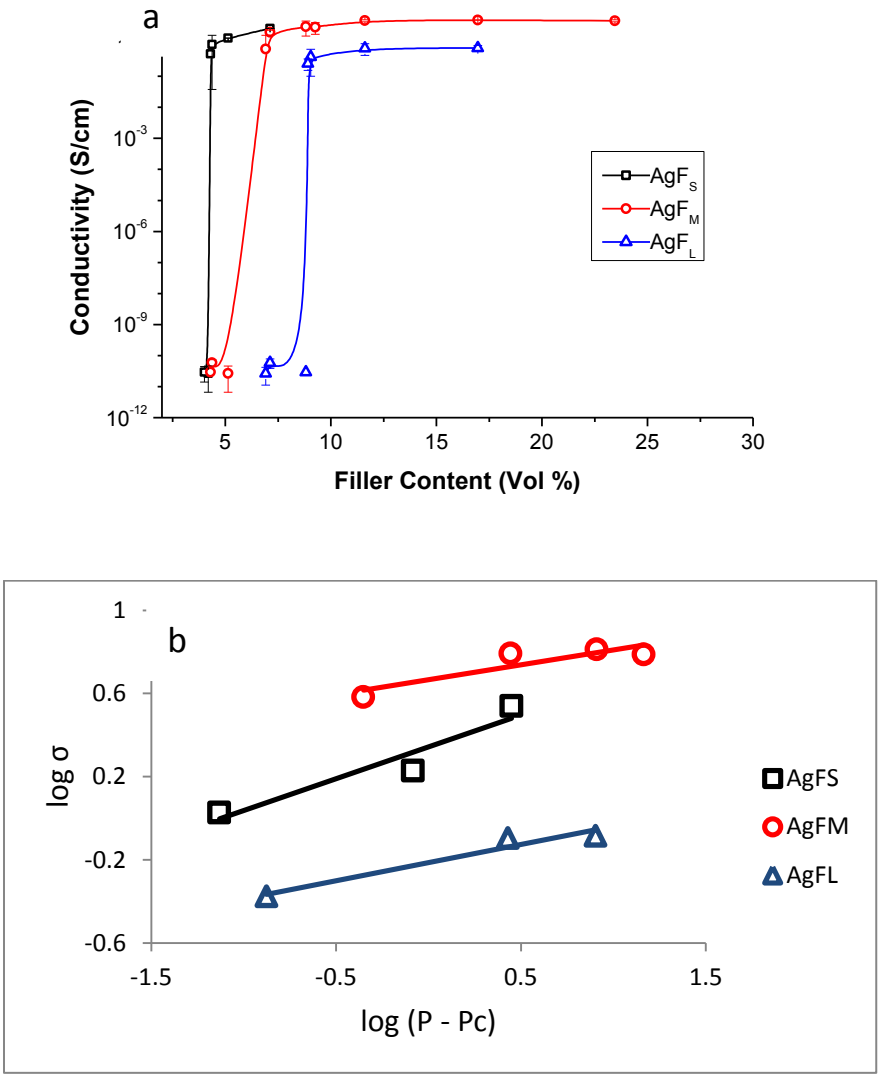

4.5 Electrical percolation curves of HDPE filled with: a) Ag coated spheres and b) graph of log σ against log (P – Pc), percolation threshold for AgF_S = 4.3 Vol. %, AgF_M = 8.8 Vol. % and AgF_L = 8.9 Vol. %.

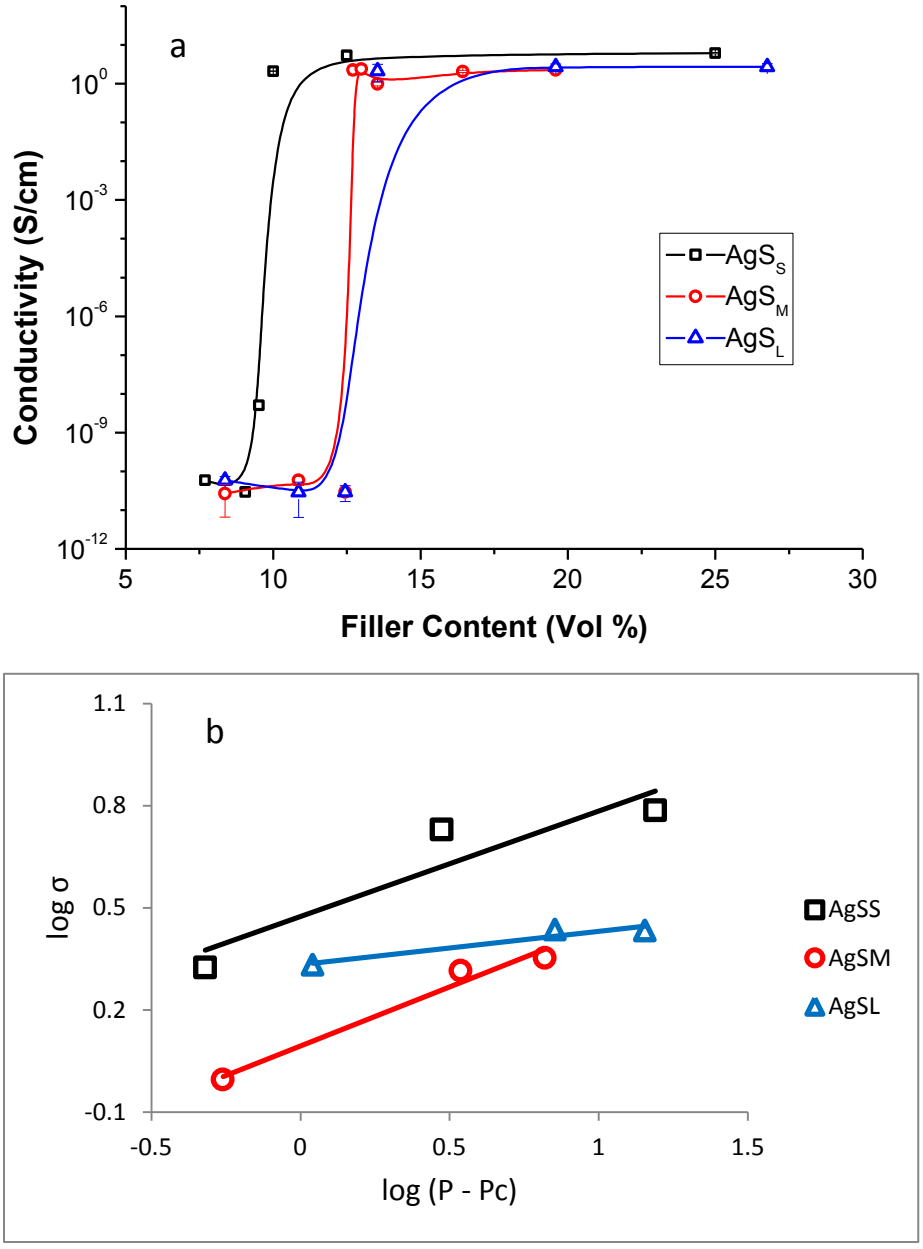

Figure 4.6 Electrical percolation curves of HDPE filled with: a) Ag coated spheres and b) graph of log σ against log (P – Pc), percolation threshold for AgS_S = 9 Vol. %, AgS_M = 12 Vol. % and AgS_L = 13 Vol. %.

The percolation threshold, i.e. the minimum volume fraction of conductive particles needed to establish a conductive network, increases with particle size for both spheres and flakes. A similar phenomenon was previously reported for composites based on different conductive fillers [7]. The increase in percolation threshold with particle size is associated to the increase in specific surface area [53, 110]. In other words smaller particle size leads to higher specific surface area of the conductive particle and therefore a larger number of possible conductive pathways, which means a more 'robust' conductive network at the same filler volume fraction.

4.2.4 PTC behaviour of different sized Ag particles in HDPE

Figure 4.5 shows the change in electrical resistivity with temperature of composites filled by each of the six model conductive fillers. All the composites exhibited a sudden increase in electrical resistivity with temperature (i.e. PTC effect). From Figure 4.5 it can be observed that the PTC effect occurred at temperatures in proximity of the melting temperature (Tm = 131 ^{o}C) of the polymer matrix, when the thermal expansion of the polymer is the greatest. This is in agreement with some of the past literature, which associates the PTC effect to the thermal expansion coefficient mismatch between filler and polymer [33].

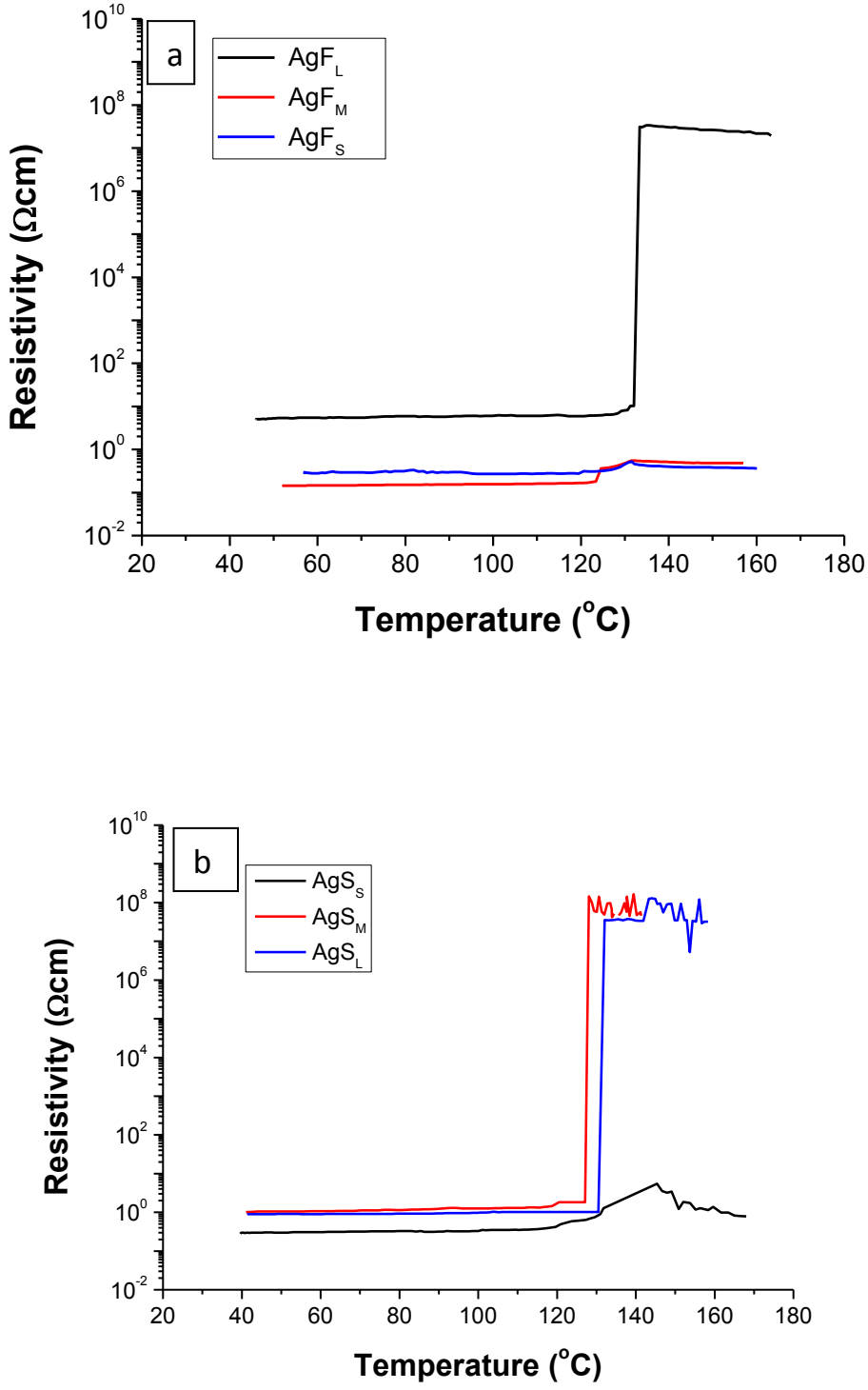

Figure 4.7 PTC behaviour of HDPE filled with: a) Ag coated flakes (4 Vol. % AgF_S, 7 Vol. % AgF_M and 9 Vol. % AgF_L) and b) Ag coated spheres (10 Vol. % AgS_S, 13 Vol. % AgS_M and 14 Vol. % AgS_L).

Interestingly an increase in particle size causes a dramatic increase in the PTC intensity of the composite, with up to 8 order of magnitudes change over a relative small particle dimension range (Figure 4.6). Moreover, the PTC intensity increased with a decrease in filler content, regardless of the filler type, but following a rather smooth and linear tendency curve.

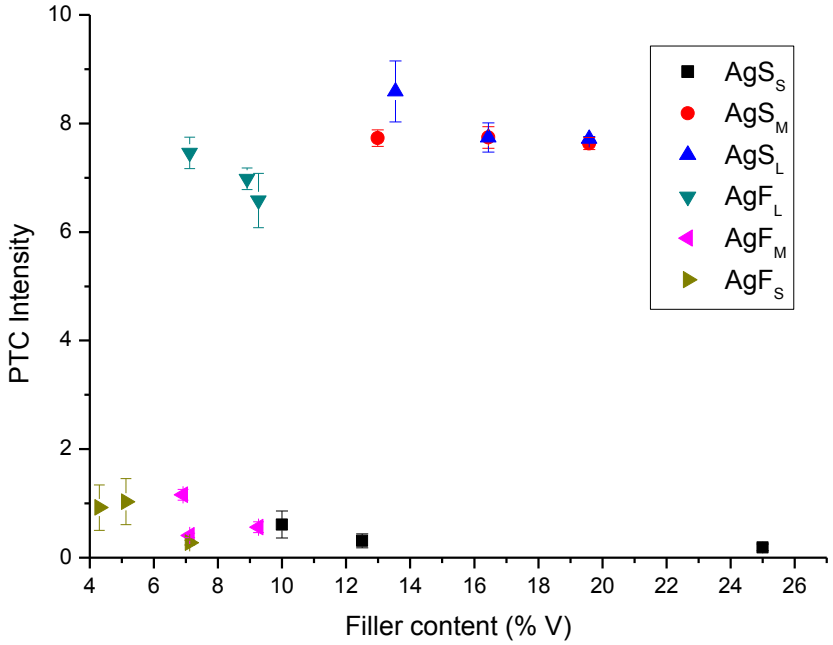

Figure 4.8 PTC intensity of HDPE filled with Ag coated flakes and Ag coated spheres.

This observation can qualitatively be explained by the concept of 'robustness' of the conductive network. Both a smaller filler (spheres and flakes) size and higher filler content contribute to a more 'robust' conductive network, with an increased number of conductive pathways formed (fig. 4.8). The more 'robust' the conductive network, the more difficult it is to disrupt it, hence the smaller the PTC intensity.

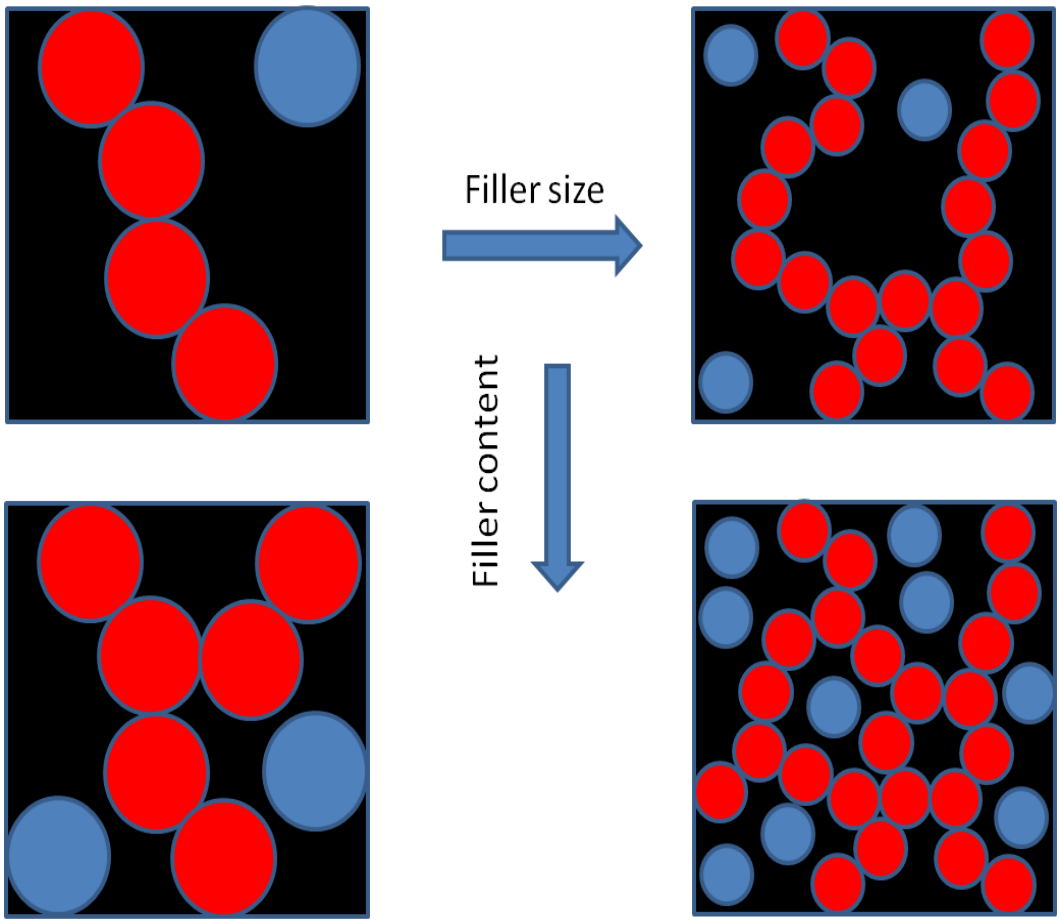

Figure 4.9 Schematic of how a reduction in filler size and an increase in filler content (direction of arrows) increases the number of conductive pathways (red spheres) and reduces the PTC intensity in a CPC.

4.3 Conclusions

In this study silver coated glass particles (spheres and flakes) were used as model conductive fillers to establish for the first time a relationship between the filler size and shape and PTC intensity. HDPE composites were prepared via melt extrusion and their morphology, electrical percolation and resistance-temperature relationship was studied. The electrical percolation threshold of the composites

increased with increasing filler size both for spheres and flakes, in analogy with previous studies.

Resistance-temperature tests revealed that the PTC intensity increases with decreasing filler content and with increasing filler size. Interestingly this observation was true for both spherical and flake-like conductive filler. This is phenomenologically consistent with the concept of ‘robustness’ of the conductive filler network. The higher the filler content and the lower the filler size (for a specific shape), the more ‘robust’ the conductive network is. As the number of specific conductive pathways increase, it is more difficult for the conductive network to be disrupted and therefore the PTC intensity is lower. Being a model system, with conductive fillers relatively homogeneous in shape and size, it lends itself to future modelling studies.

Chapter 5. Effect of Mixed Fillers on PTC of CPC.

5.1 Introduction

Silver coated glass particles (spheres and flakes) are used as model conductive fillers due to the ease in controlling size and shape.

In particular two mixed fillers systems are studied. In one system both fillers are model conductive flakes of different lateral dimension (5 μm and 100 μm). In the other system MWNT is used as the minority filler, in combination with a model conductive spherical filler (50 μm). The selection of MWNT, though slightly departing from the model system approach, serves as a limit case of a conductive filler of very high aspect ratio and hence low percolation threshold.

5.2 Results and discussion

5.2.1 Morphology

Figure 5.1a shows the SEM images of high density polyethylene (HDPE) filled with the different silver coated glass particles and/or MWNT.

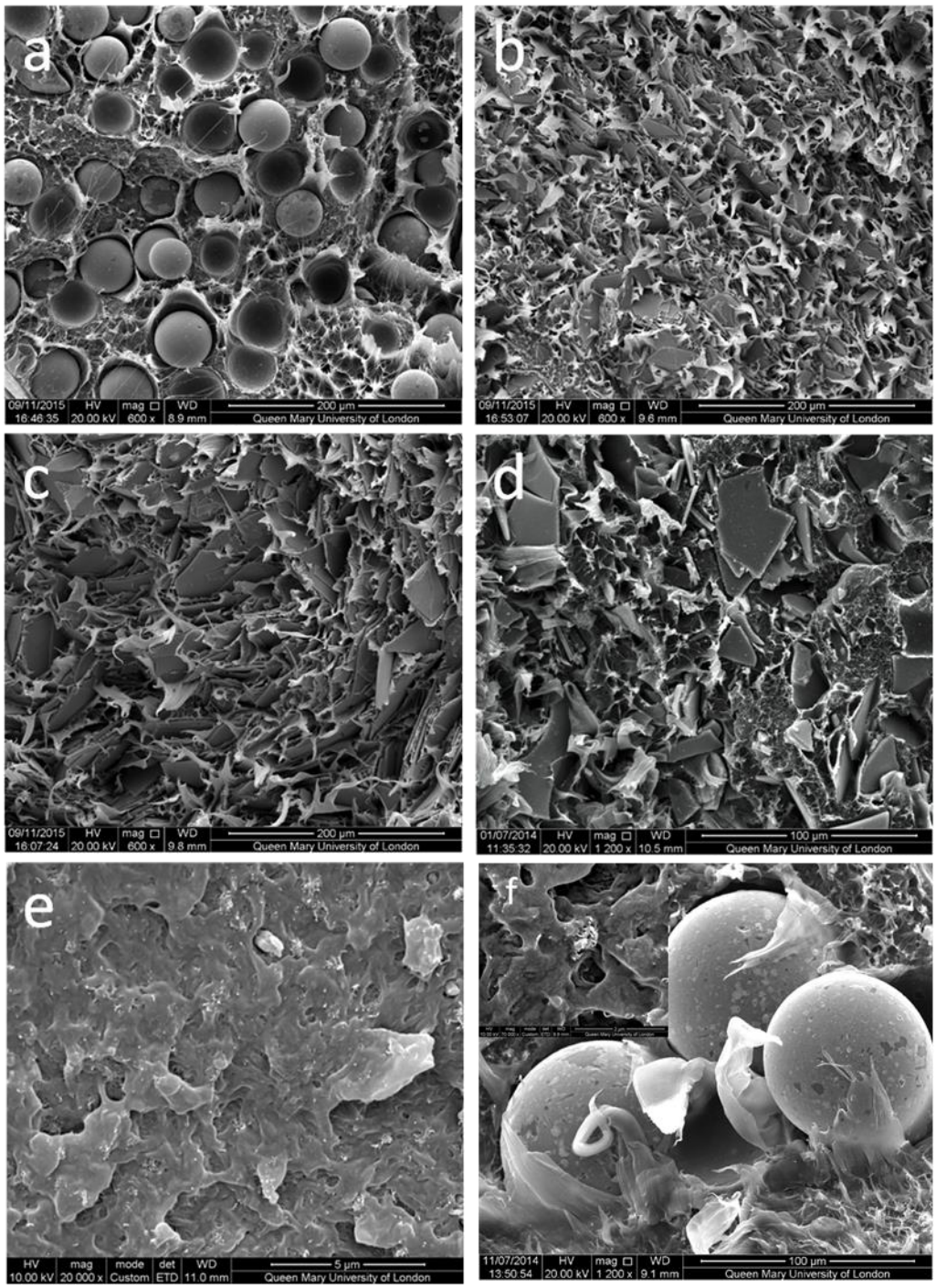

Figure 5.1 SEM pictures of: a) HDPE / 28 wt.% AgSM, b) HDPE / 40 wt.% AgFS, c) HDPE / 50 wt.% AgFL, d) HDPE / 22 wt.% AgFL + 7 wt.% AgFS, e) HDPE/2.5 wt.% MWNT f) HDPE / 20 wt.% AgSM + 0.7 wt.% MWNT.

Silver coated glass particles (AgF_L, AgF_S, AgS_M) all show poor interfacial interaction with HDPE (Figure 5.1.a-c, e), with clear signs of failure at the interface and debonding (void formation). The effect of melt processing on the damage of the particles (particularly AgF_L) as well as the silver coating have previously been reported [127]. No preferential orientation of the particles was observed. Figure 5.1e shows a relatively good dispersion of MWNTs in HDPE matrix with isolated MWNTs among micron-size agglomerates. The mixed filler polymer composite in Figure 5.1d (AgF_L + AgF_S/HDPE) presents two populations of glass flakes in HDPE, though a bimodal distribution is not obviously observable.

5.2.2 Single filler HDPE pyroresistive composites

Figures 5.2a shows the percolation curves of the four conductive fillers individually dispersed in HDPE. As expected the percolation threshold decreases with particle aspect ratio and particle size. MWNT the particle of smallest size and highest aspect ratio presents the lowest percolation threshold, with a value below 1 Vol. % in filler content. AgS_M shows instead the largest percolation threshold, at about 13 Vol. %. The difference in particle size between AgF_L (100 μm) and AgF_S (8 μm) explains the decrease in percolation threshold, respectively, from below 9 Vol. % to about 4.5 Vol. %.

Figures 5.2b shows typical resistivity-temperature curves for the four single filler composites.

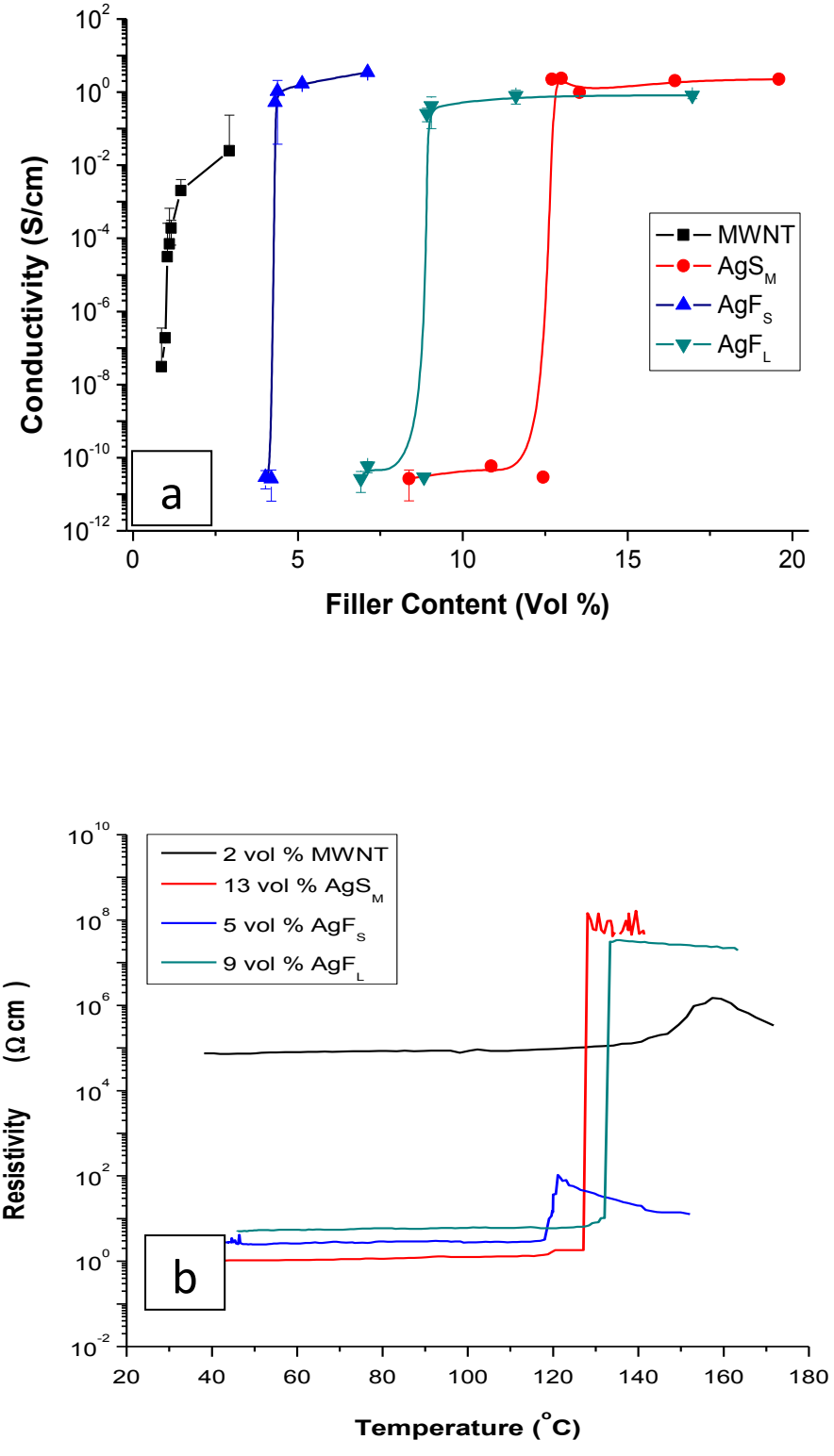

Figure 5.2 a) Percolation curves of four fillers (MWNT, AgS_M, AgF_S and AgF_L) and b) Resistivity-temperature curves of all four single fillers HDPE composites.

The PTC intensity increases with increasing particles size and decreasing aspect ratio. MWNT/HDPE presents the lowest PTC intensity and the least sharp transition as well as an evident NTC effect (usually explained by particle re-agglomeration). The transition temperature for all composites is approximately in correspondence with the melting temperature of the polymer matrix, with the exception of MWNT/HDPE. This might be a consequence of a more robust conductive and rheological network established by MWNTs as well as a lower thermal conductivity when compared to the other silver coated particles at substantially higher filler content.

5.2.3 Mixed filler HDPE pyroresistive composites

After having studied the pyroresistive behaviour of the single filler composites in the previous section, two different fillers combinations have been selected and investigated: AgS_M + MWNT and AgF_L + AgF_S.

AgS_M and MWNT were chosen because of their most extreme difference in terms of percolation threshold and PTC intensity. Several series of composites were prepared at fixed AgS_M contents, starting from just below percolation threshold. A minority phase of MWNT was added to re-establish a continuous conductive network (fig 5.3a).

For a fixed AgS_M content, increasing the MWNT Vol. % resulted, as expected, in a decrease in PTC intensity (fig. 5.4.b). Overall the different series of mixed filler composites showed values of PTC intensity between the values of single filler composites but very much skewed toward the lower end of the range, closer to the values of MWNT/HDPE composites. Adding even a minute amount of MWNT (e.g. 0.17 Vol. % MWNT) to a concentration of AgS_M just below its percolation

(12 Vol. %) resulted in a dramatic decrease in PTC intensity, from almost 8 to 2.5 orders of magnitudes (fig. 5.4.b). In other words the pyroresistive behaviour seems to be dominated by the conductive phase with lowest PTC intensity (and percolation threshold), even at very small Vol. %.

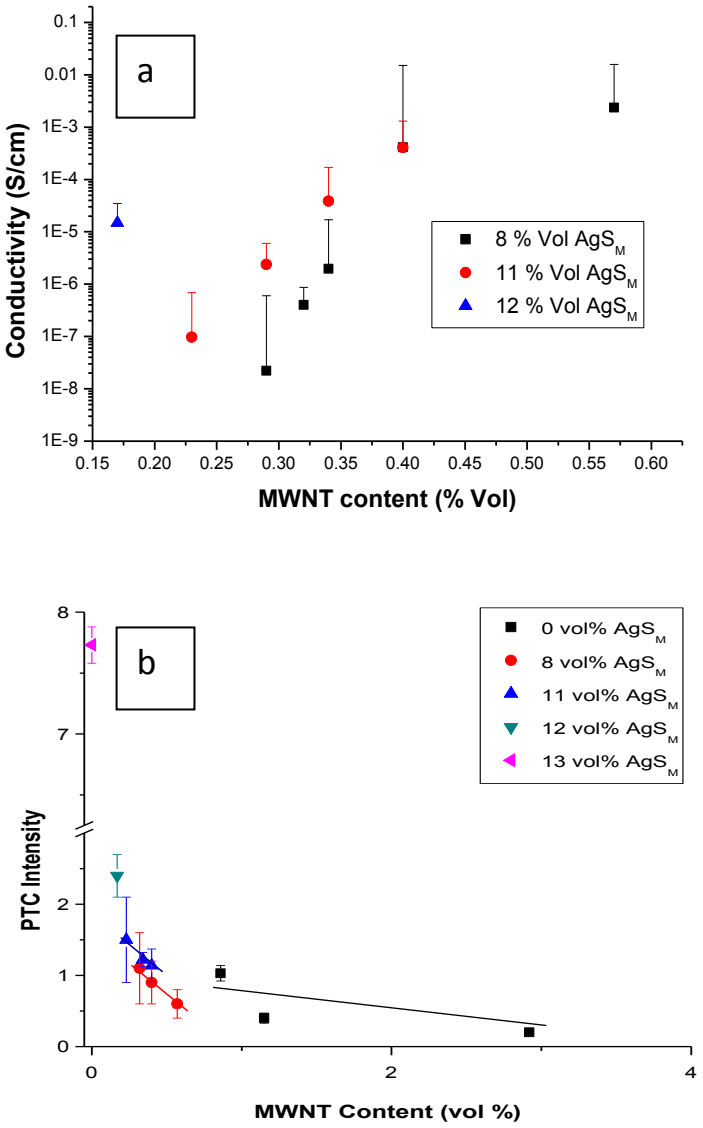

Figure 5.3 Mixed fillers composites AgS_M+MWNT/HDPE: a) percolation curves and b) PTC intensities as a function of MWNT vol % for several fixed AgS_M content.

To confirm and generalise the results obtained on AgS_M + MWNT/HDPE, a second group of mixed fillers composites was prepared by combining AgF_L and AgF_S. This constitutes a model system in which both fillers are of relatively homogeneous size and shape. The fillers have got the same shape (flake-like) and nature and just differ in size (and aspect ratio).

Also in this case the majority filler phase was constituted by the filler with highest PTC intensity (AgF_L). For a fixed AgF_L content, starting from just below its percolation threshold, a small amount of AgF_S was added to re-establish a continuous conductive network (Figure 6.4a).

As for the MWNT+AgS_M/HDPE, also in the case of AgF_L+AgF_S/HDPE the PTC intensity was dominated by the conductive phase with the lowest PTC intensity (percolation threshold) even at small Vol. %.

Adding about 2 Vol. % of AgF_S to 8 Vol. % of AgF_L resulted in a dramatic decrease in PTC intensity, from about 7 to 1.5 orders of magnitudes, when compared to the single filler composite 9 Vol. % AgF_L/HDPE (Figure 6.4b).

This is a very interesting result because, to the best of our knowledge, it is the first demonstration of how, in essence, the distribution of conductive filler size affects the PTC intensity. Adding small amounts of AgF_S to a majority of AgF_L effectively means modifying the distribution of AgF_L particle size by adding a tail in the region of small particle size. This modification of size distribution is sufficient to compromise the PTC intensity which becomes dominated by the small tail of the distribution curve.

Hence, the important underlying message here is that the PTC intensity is not only influenced by the conductive particle size, as previously demonstrated [127], but also by its distribution.

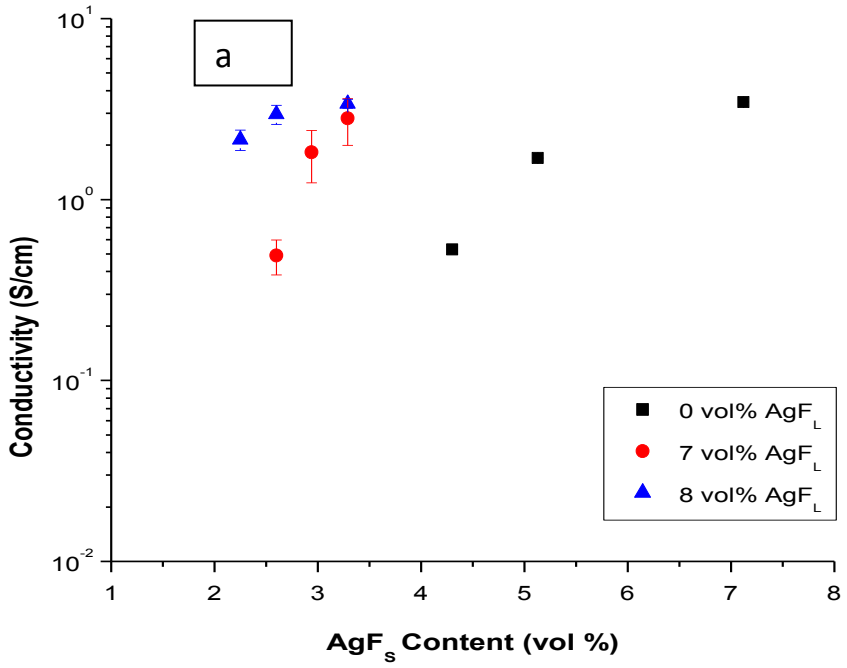

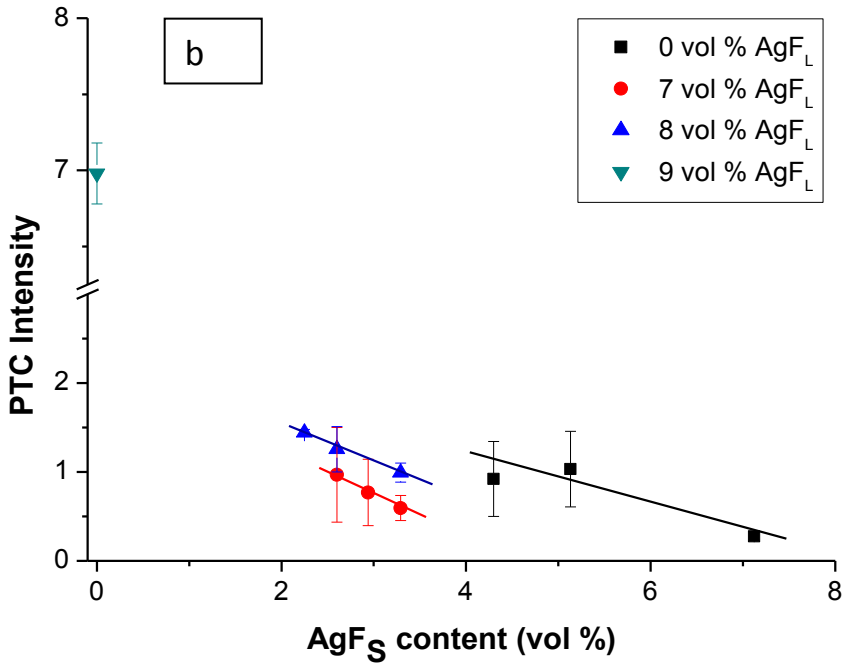

Figure 5.4 Mixed fillers composites AgF_L+AgF_S/HDPE: a) percolation curves and b) PTC intensities as a function of AgFS Vol. % for several fixed AgF_L content.

At the same time these results pose doubts on the simplistic - but generally accepted - view that a thermal expansion coefficient (CTE) mismatch between polymer and filler is the main governing mechanism for the pyroresistivity effect. In our case, AgF_S and AgF_L have got the same CTE but they, as well as their combinations, induce very different pyroresistivity behaviours. We believe that a better understanding could come from the study of the 'quality' and 'robustness' of the conductive network and how the latter is affected by a number of disruptive mechanisms generated upon increase of temperature, one of which could certainly be thermal expansion.

It is possible to imagine two extreme conductive network morphologies in a mixed filler composite (fig. 5.5b), as opposed to a single filler composite (fig. 5.5a).

The first case (blue arrows path in fig. 5.5b) assumes two independent and interpenetrating conductive networks. The second case (red arrows path in fig. 5.5b) assumes the two fillers constituting a hybrid conductive network in which one filler occupies the interstitial sites of the network of the second filler.

Both our mixed fillers composites are believed to be exhibit predominantly hybrid network morphology (red arrows path in fig. 5.5b) also because the two fillers contents are very different from each other. But, within the framework of this case, one could imagine a host of network morphologies, which could be described by a combination of series/parallel electrical connections between fillers. The specific network morphology assumed by the fillers could well explain the dramatic decrease in PTC intensity in both our mixed filler conductive composites. Recently, Chu *et al.* [128] have demonstrated an interesting CPC architecture with a zero temperature coefficient of resistance, by stacking two distinct layers, one showing PTC effect (CB/PDMS) and the second showing NTC effect (MWNT/PDMS). The authors were able to calculate the optimal layers thickness ratio in correspondence of which the PTC and NTC effect were effectively cancelling each other out, hence giving a zero temperature coefficient of resistance. The mixed filler composites can be seen as just a more complicated case of a bilayer stacked structure. By modelling the actual series/parallel connection morphologies of the two fillers, one could predict the overall PTC intensity, once the PTC intensity of the two single fillers is known.

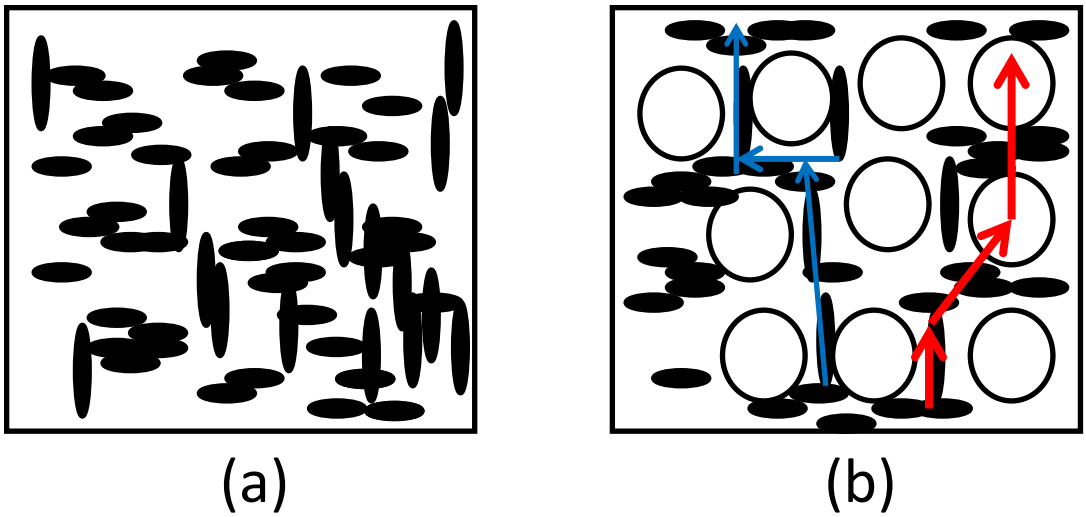

Figure 5.5 Schematic of conductive pathways in (a) single filler composites or (b) mixed filler composites: independent and interpenetrating conductive network (red arrow) and hybrid conductive network (blue arrow).

5.3 Conclusions

Two series of mixed filler conductive composites were studied, to explore the possibility to combine low percolation threshold with large PTC intensities. In both series, two fillers were combined, the principal filler, exhibiting a large PTC intensity, and secondary filler, exhibiting a low percolation threshold. At least one of the two conductive fillers (the principal filler) was selected to be of relatively homogenous size and shape (silver coated glass spheres or flakes) to help clarifying the relationships between (mixed) conductive fillers and the PTC effect.

For the first time it was demonstrated in a universal manner that the PTC intensity of mixed fillers composites is dominated by the filler with the lowest PTC intensity, even at very low volume fractions.

Chapter 6. Effect of change in filler core on PTC Intensity

6.1 Introduction

The materials properties, sample preparation method and characterisations used in this experiment are described in chapter 3.

6.2 Results and discussion

6.2.1 Particle properties

Figure 7.1 shows the SEM images for AgS_M and AgP particles. It can be observed that both particles are coated a uniform layer of silver. The silver coating on the PMMA beads had a wrinkly surface and this might have been caused by poor adhesion between the silver and the PMMA surface (fig. 6.1). Such effect was not observed on the AgS_M particles.

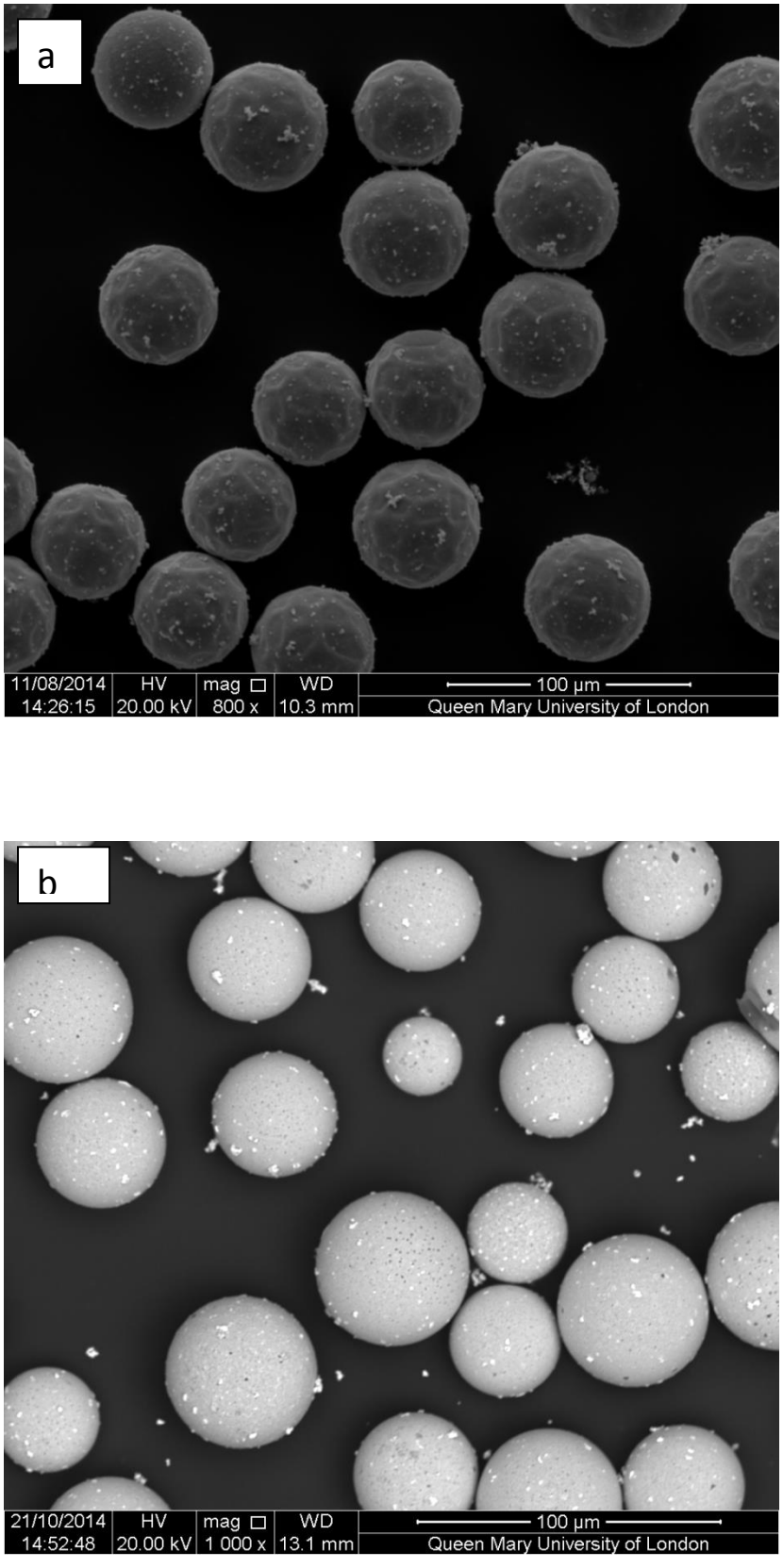

Figure 6.1 SEM image of silver coated a) PMMA beads and b) glass spheres

Table 6.1 presents the measured values for the particles compared to the manufacturers' data. There was a strong correlation between the measured values for both particles and the data supplied by the manufacturer. The D50 for both particles (AgS_M = 48 and AgP = 51) did not differ by much therefore the particle diameter can be assumed to be equal for both particles. The distribution of conductive particles are important in the PTC behaviour of a composite as demonstrated in Chapter 6 hence a narrow and similar distribution of the particles is important. AgS_M and AgP had similar distribution as shown in figure 7.2.

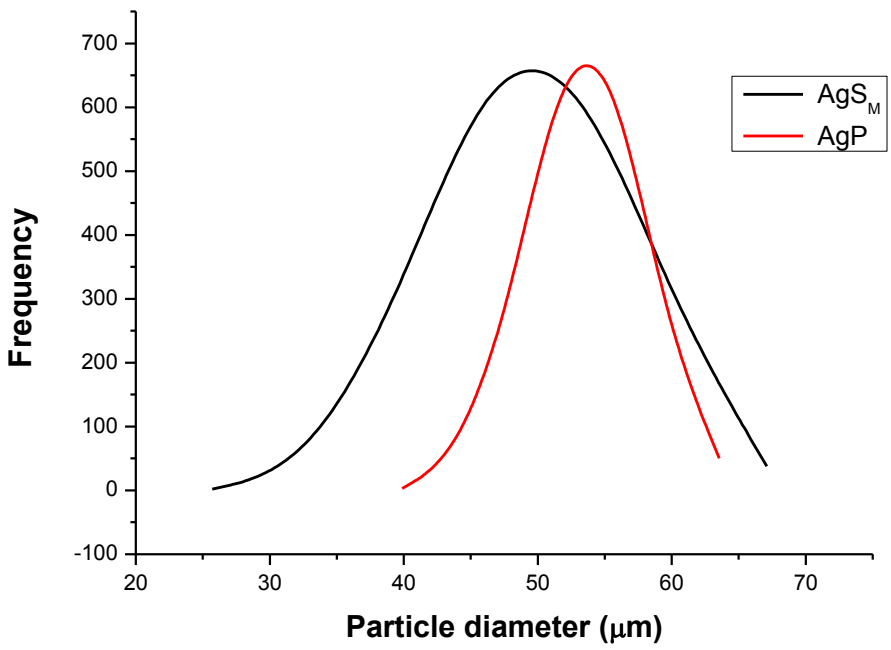

Figure 6.2 Particle distribution curve for silver coated glass spheres (black) and silver coated PMMA (red).

Table 6.1 Measured particle dimensions as compared to the data provided by the supplier.

Particle	D10/µm		D50/µm		D90/µm	
	Supplier	Measured	Supplier	Measured	Supplier	Measured
AgS_M	N/A	40	50	48	N/A	56
AgP	N/A	46	50	51	N/A	57

6.2.2 Morphology

The distribution of the AgP fillers in HDPE was observed to be better than that of AgS_M as shown in figure 6.3.

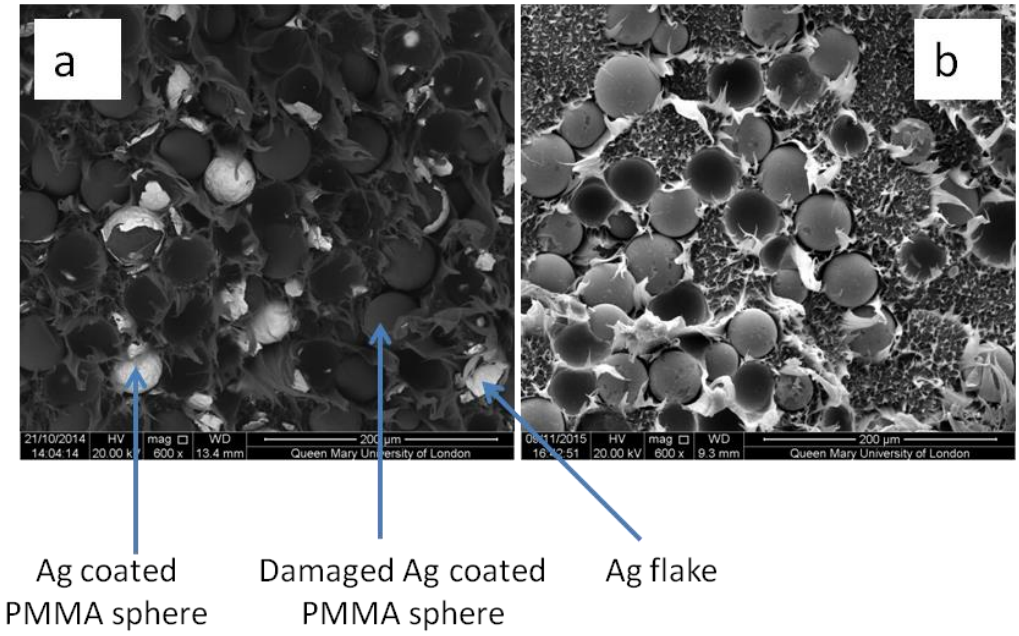

Figure 6.3 SEM image of HDPE composite filled with a) 32 %wt AgP and b) 28 %wt AgS.

It was observed in figure 6.3a that the silver coatings on the AgP particles were damaged during extrusion. The damages experienced by the conductive particles were caused by the poor adhesion between the silver coating and the PMMA core evident by the wrinkly surface of the particle (fig. 6.1), the silver coating was easily damaged compared to the glass core particles.

6.2.3 Electrical properties

The electrical percolation behaviour of the composites is shown in figure 6.4. The AgS_M/HDPE and AgP/HDPE composites showed no change in conductivity until a critical concentration (percolation threshold) of 13 vol. % and 23 vol. % respectively. An increase in AgS_M and AgP particles in the HDPE polymer matrix did not change significantly the conductivity of the composite after the percolation threshold. An increase in conductive particles is expected to increase the physical contact between the particles and also enhance the tunnelling effect by reducing the distance between the particles.

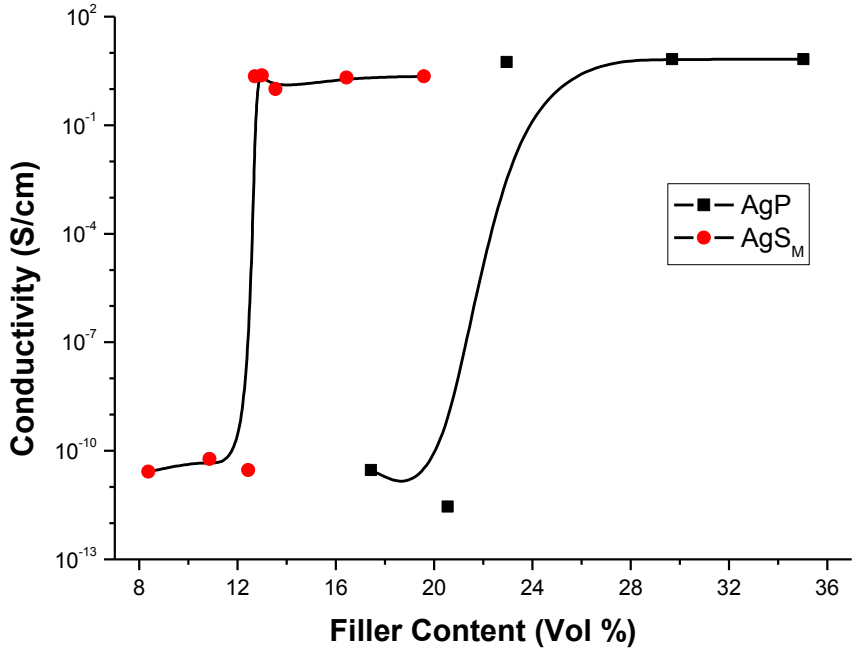

Figure 6.4 Electrical percolation behaviour of AgP/HDPE and AgS_M/HDPE composites.

The electrical percolation for AgS_M/HDPE was lower than that of the AgP/HDPE composite. The high percolation threshold of the AgP/HDPE composite is likely to have been caused by the damage suffered by the particles during extrusion. The

number of AgP particles in the composite was reduced and the composite behaved like a mixed filler composite (fig. 6.4).

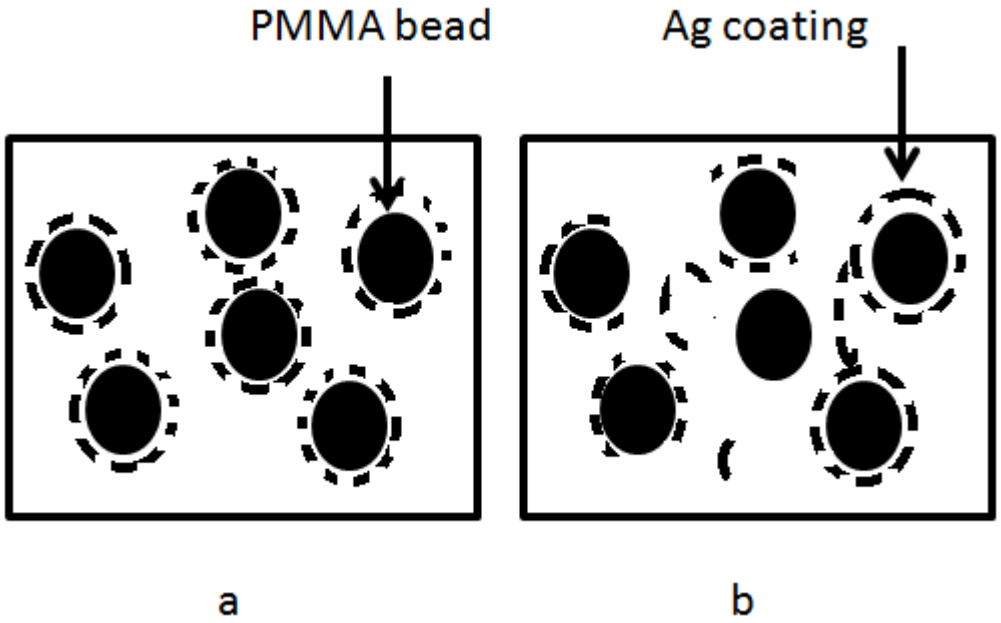

Figure 6.5 Schematic of conductive pathway for AgP a) undamaged and b) damaged in a polymer matrix.

Different sized silver flakes, fully and partially coated PMMA beads were present in the AgP/HDPE composite hence would have participated in the percolation behaviour of the composite. This makes the percolation threshold reported "untrue" for the AgP/HDPE composite (fig. 6.3a) due to the formation of hybrid conductive network (fig. 6.5b). Figure 6.5a shows the ideal situation for the composite and the actual situation where conductive pathway is formed by only the AgP particles. The effect of filler shape and size is eliminated therefore the percolated threshold for such system will be true for the particles.

6.2.4 PTC behaviour

Figure 6.6 shows the PTC behaviour of AgS_M/HDPE and AgP/HDPE composites. It was observed that the AgP/HDPE composite displays a gradual increase in resistivity up to a temperature around 135 ^oC when suddenly the resistivity increases sharply. The sharp increase in resistivity for AgP/HDPE composite is immediately followed by a sharp decrease in resistivity (NTC effect).

Although some researchers have reported a decrease in PTC temperature for polymers filled with low CTE particles [113, 129], the PTC temperature for the AgS_M occurred close to the melting temperature of the HDPE. The same effect was observed for the AgP/HDPE as shown in figure 6.6. This means that for these composites, the PTC temperature is governed by the drastic increase in specific volume associated with polymer matrix near the temperature. Conductive particles such as CB are expected to be situated in the amorphous regions of a polymer matrix [89, 130]. Around the melting temperature of the HDPE matrix, the amorphous phase increases as the crystalline region decreases and this leads to a reduction in the ratio of conductive particle content to amorphous region. The increase in amorphous region of the polymer matrix leads to a break up in physical contact or increase in distance between the particles hence the sharp increase in resistivity (PTC effect) witnessed in the AgS_M/HDPE and AgP/HDPE composites.

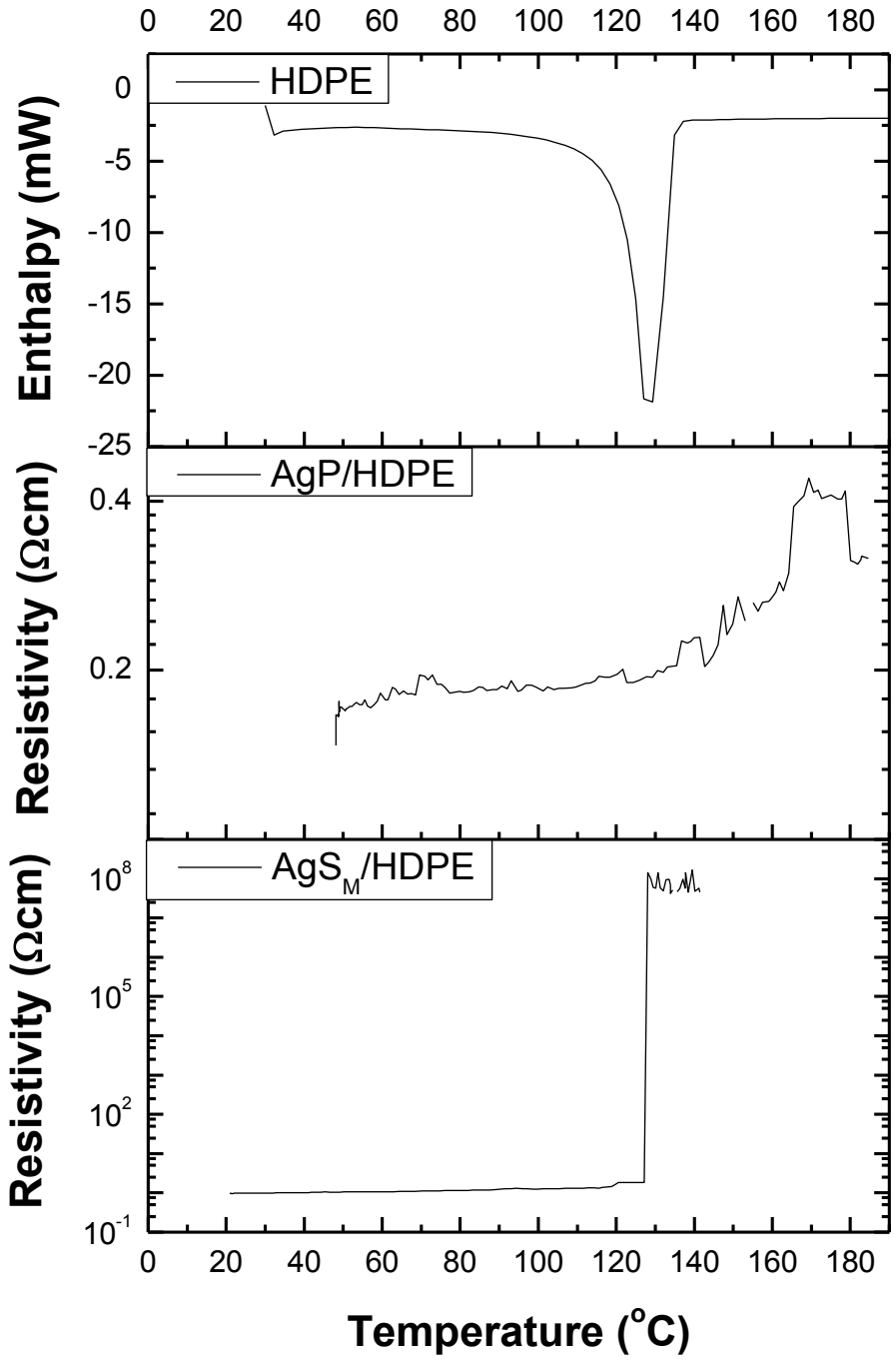

Figure 6.6 PTC behaviour for 35 vol. % AgP/HDPE and 13 vol. % AgSM/HDPE plus the DSC curve for HDPE.

The difference in CTE is responsible for the high PTC intensity observed for the AgS_M/HDPE composite. A combined effect of interactions between the fillers (i.e. thermal expansion of the fillers) and the disruption caused by the thermal expansion of the polymer matrix is responsible for the huge PTC intensity witnessed in the AgS_M/HDPE composite.

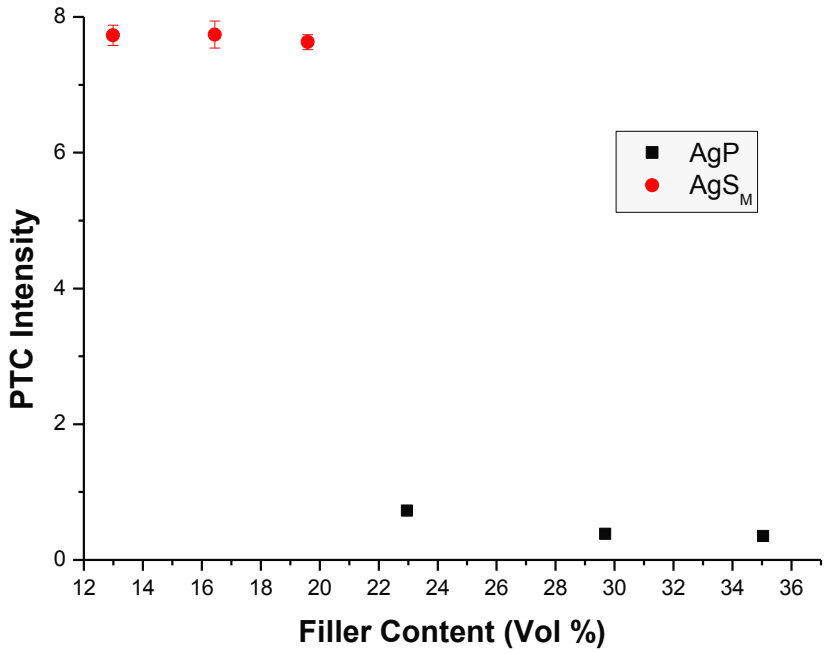

Figure 6.7 PTC intensity for AgP/HDPE and AgS_M/HDPE composites.

A small PTC intensity is observed for the silver coated PMMA/HDPE composite (fig. 6.7). This low PTC intensity might have been caused by the formation of hybrid conductive pathways within the polymer matrix (fig. 6.5). The high shear forces experienced by the AgP particles during extrusion shaved off the silver coatings on some particles, either partially or wholly as evident in figure 6.3a. These silver (Ag) shavings could have helped formed a hybrid conductive

pathway by bridging the gaps between AgP spherical particles. Due to the high aspect ratio of these particles, the conductive network formed by them is more robust when compared to the network formed by the AgS_M particles due to their spherical shape. Is already been reported by different researchers that an increase in filler aspect ratio reduces the distance between the particles hence a more robust network is formed [51, 52]. The decrease in distance between the silver shavings means that physical contact or electron tunnelling within the composite is enhanced. This means that disruption of the conductive network becomes difficult compared to the low aspect ratio and large particles such as AgS_M.

The PTC behaviour observed for the AgP/HDPE composite is similar to the one observed in the mixed fillers studied in Chapter 5. As demonstrated in Chapter 5, addition of high aspect ratio fillers to CPCs can reduce the PTC intensity and even present the NTC effect.

The presence of the NTC effect in the AgP/HDPE composite might have been caused by the rearrangement of the conductive particles in the composite [23, 119]. Rearrangement of the conductive particles requires movement of the polymer chains close to the particle therefore the large AgP particles will require more energy to rearrange [23]. The silver shavings on the other hand might be small enough to agglomerate easily due to the less energy required compared to the AgP particles.

An increase in filler concentration corresponded to a decrease in the PTC intensity for both composites as previously reported in Chapter 4 and 5. This effect can be explained by the increase in conductive networks linked to the increase in particle concentration. The increase in conductive network is a result

of an increase in physical contact and a reduction in the distance between particles. This increases the robustness of the conductive networks therefore thermal expansion in the polymer matrix disturbs the network less compared to low particle loaded composites. The PTC intensity was governed by the difference in CTE value of the conductive fillers and the amount of fillers in composites.

6.3 Conclusions

The effect of difference in linear coefficient of thermal expansion (CTE) of conductive fillers and polymer matrix based on a change in filler core on the electrical and PTC behaviour CPCs has been investigated using AgS_M/HDPE and AgP/HDPE composites.

The electrical percolation threshold for the AgS_M/HDPE was lower than that of AgP/HDPE. This increase in percolation threshold might have been caused by the damage to the AgP particles during processing due to the poor adhesion between the silver coating and the PMMA bead.

The PTC intensity observed for the AgS_M/HDPE composite was higher than that of the AgP/HDPE composite. The mismatch in CTE values between the AgS_M particles and the HDPE polymer matrix is responsible for the huge PTC intensity while the damages caused to the AgP particles might have caused the small PTC intensity. The damaged AgP particles (Ag shavings) could have helped form a hybrid conductive pathway which is more robust than the conductive pathway

formed by spherical particles as demonstrated in the mixed filler composites in the previous chapter.

NTC effect was observed in the AgP/HDPE composite but not obvious in the AgS_M/HDPE composite. The NTC effect for the AgP/HDPE composite might have been caused by the formation of new conductive pathways by the rearrangement of the silver shavings at high temperatures (i.e. reagglomeration of Ag shavings).

Chapter 7. Effect of hybrid polymer composites on PTC of CPC

7.1 Introduction

The materials and preparations methods for the conductive composites used in this experiment are described in chapter 3. HDPE was filled with 16 wt% AgF_S and 40 wt% AgF_L. The hybrid composites were made by addition of two different concentrations of polypropylene-ethylene based plastomer (PPE) (10 wt% and 20 wt% PPE).

7.2 Results and discussion

7.2.1 Morphology

The structure of the conductive polymer composites were investigated using scanning electron microscopy after fracturing in liquid nitrogen. The SEM migrograph (fig. 7.1a) shows a segregated structure with silver flakes dispersed in the HDPE phase. Dispersing the silver coated glass flakes in the HDPE first before further mixing with the PPE might have helped the fillers to remain in the HDPE phase. The high viscosity of the PPE compared to the HDPE might have also played a part in the fillers not migrating into the plastomer. An increase in HDPE content in the composite decreases the phase separation and it becomes difficult to see a clear phase separation when the PPE phase changes to 10 wt% (fig 7.1b).

No preferential orientation of AgF particles was observed in the composite.

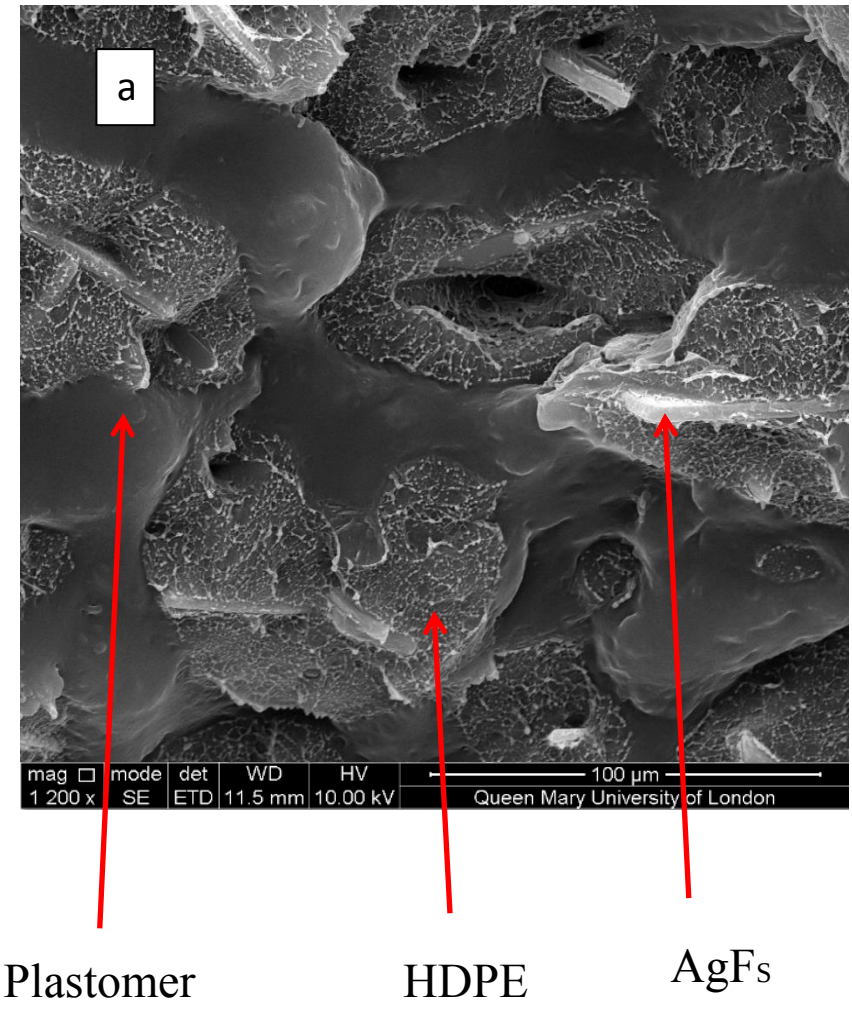

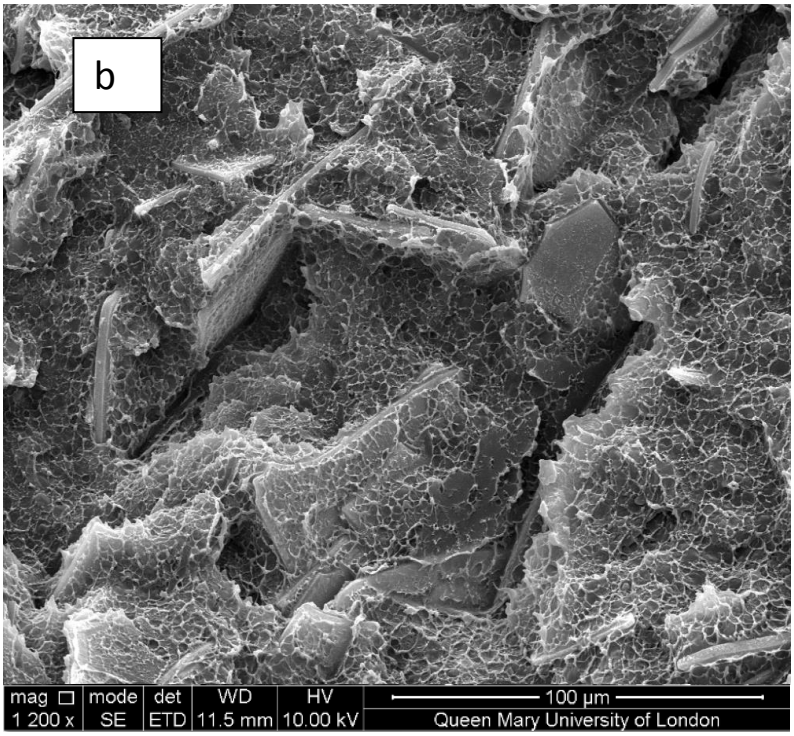

Figure 7.1 SEM micrograph of 16 wt% AgF_S/HDPE composite with a) 30 wt% PPE b) 10 wt% PPE.

7.2.2 Dynamic mechanical analysis of the composites

The miscibility of the two polymers can be investigated by utilising a dynamic mechanical analysis (DMA). DMA results will aid in understanding the blend behaviour and phase morphology of the blends. Probably the most direct method to estimate the blend morphology is by selectively removing each of the two phases, one at the time, and observing the remainder structure. In this case both polymers are dissolvable in the same solvents therefore this approach was not suitable.

The effect of adding PPE to HDPE on the stiffness of the composites is shown in figure 7.2. An increase in temperature decreased the storage modulus of all the composites and this was caused by the softening and relaxation of the polymer

chains [131]. The storage modulus which is related to the stiffness of the composite decreased with increase in PPE content (fig. 7.2) but the reduction in storage modulus is less pronounced at higher temperatures. HDPE showed the highest value in the storage modulus while the lowest value was observed in the PPE.

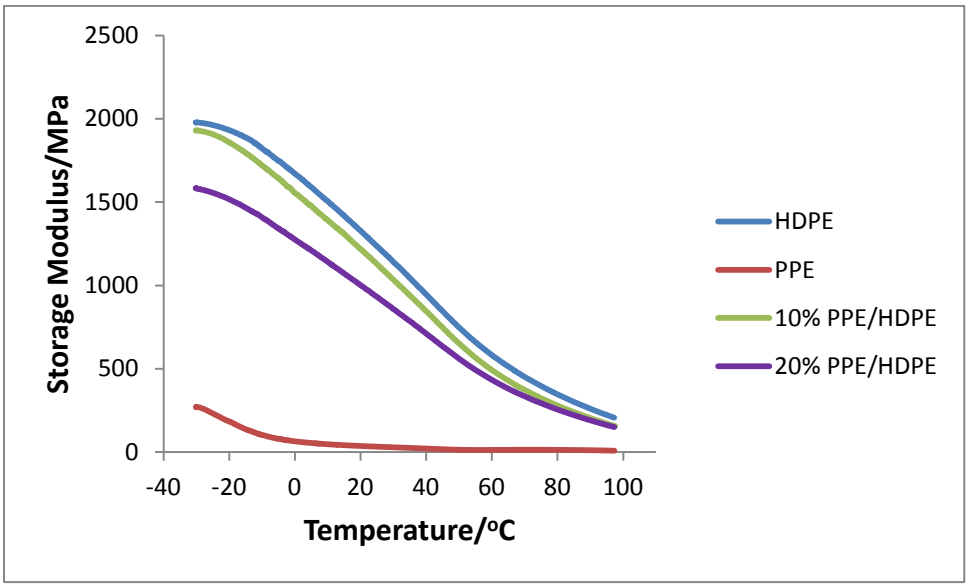

Figure 7.2 Storage modulus against temperature for the composites.

Addition of 10 %wt. PPE to HDPE leads to a disperse phase morphology and this is shown in the difference between the storage modulus of the blend and HDPE. The storage modulus of the blend is less than 10 % lower than that of HDPE as temperature increases. This indicates that the addition of PPE had less effect on the storage modulus of HDPE hence the modulus of the blend is dominated by the HDPE component [132].

The change in storage modulus with temperature observed in the blend with 20 %wt. PPE defers more from the pure HDPE sample. This is caused by the increase in contribution of the PPE polymer in the polymer blend. For instance at

20 ^{o}C, the reduction in storage modulus of HDPE was 24 % compared to 8 % for the blend with 10 %wt. PPE.

The loss modulus (E") which is linked with the damping effect of the polymer measures the energy absorbed due to the polymer relaxation [131]. Figure 7.3 shows the loss modulus against temperature curve for the HDPE, PPE and their blend in the temperature range -30 to 100 ^{o}C. The peak of the loss modulus corresponds to the maximum heat dissipation per unit deformation [133]. Addition of PPE to HDPE decreased the E" as temperature increased and had a peak in the transition region around 40 ^{o}C. The relaxation peak observed in HDPE and PPE/HDPE blends is linked to a complex multi-relaxation process caused by the molecular movement of the HDPE crystalline region [131, 134]. The E" at the relaxation temperature decreased with an increase in PPE concentration.

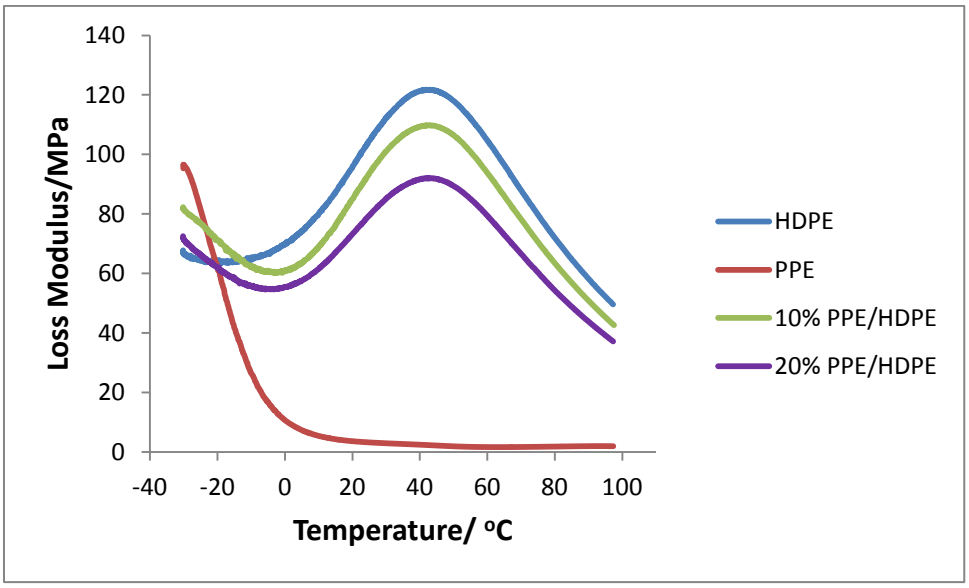

Figure 7.3 Loss modulus against temperature curve for the composites.

The E" for PPE decreased sharply at low temperatures up to 0 ^{o}C with the curve resembling the end of a transitional peak. This decrease in E" was also observed in the blends. The observation of characteristic transition of HDPE and PPE in the polymer blends indicates the immiscibility of the polymers [133, 135]. This is confirmed by observations in the SEM images (fig. 7.1a).

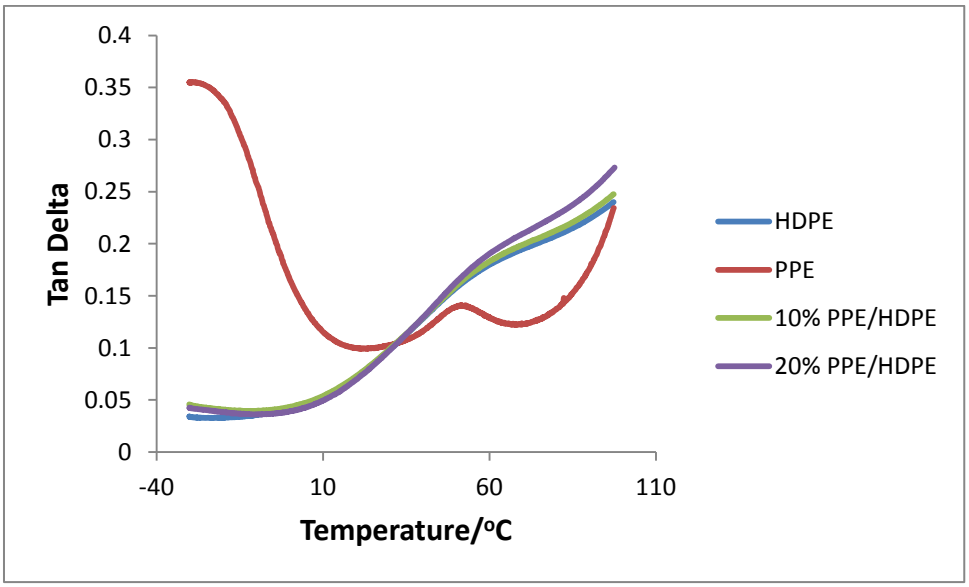

Figure 7.4 Tan delta against temperature for the composites.

The tan delta (δ) or damping factor is defined as the ratio of the loss modulus to the storage modulus. Tan δ is used to study the viscoelastic behaviour of the material and is not affected by the stiffness of the material. Tan δ of HDPE and blends of HDPE and PPE are shown in figure. The damping curves moved towards a higher value as the PPE content increased in HDPE. At low temperatures, the damping curves showed no mayor change in tan δ values but a significant difference in tan δ value was observed in the blend containing 20 %wt. PPE after 50 ^{o}C. 10 %wt. PPE in HDPE showed a slight increase in tan δ value after 50^{o}C. This indicates an increase in damping effect with increase in PPE

content in the HDPE. The relaxation peak observed in the E" curves were less distinctive in tan δ curves.

DSC technique can be used to investigate the miscibility of two or more polymer. Usually detection of a single glass transition temperature (Tg) for the polymer blends, positioned at a temperature between the Tg of the single polymer phases, is an indication of molecular homogeneity. On the other hand, observation of multiple Tg for polymer blends, in correspondence of the Tg of the single polymer phases, indicate immiscibility and a phase separation of the blend components [135, 136].

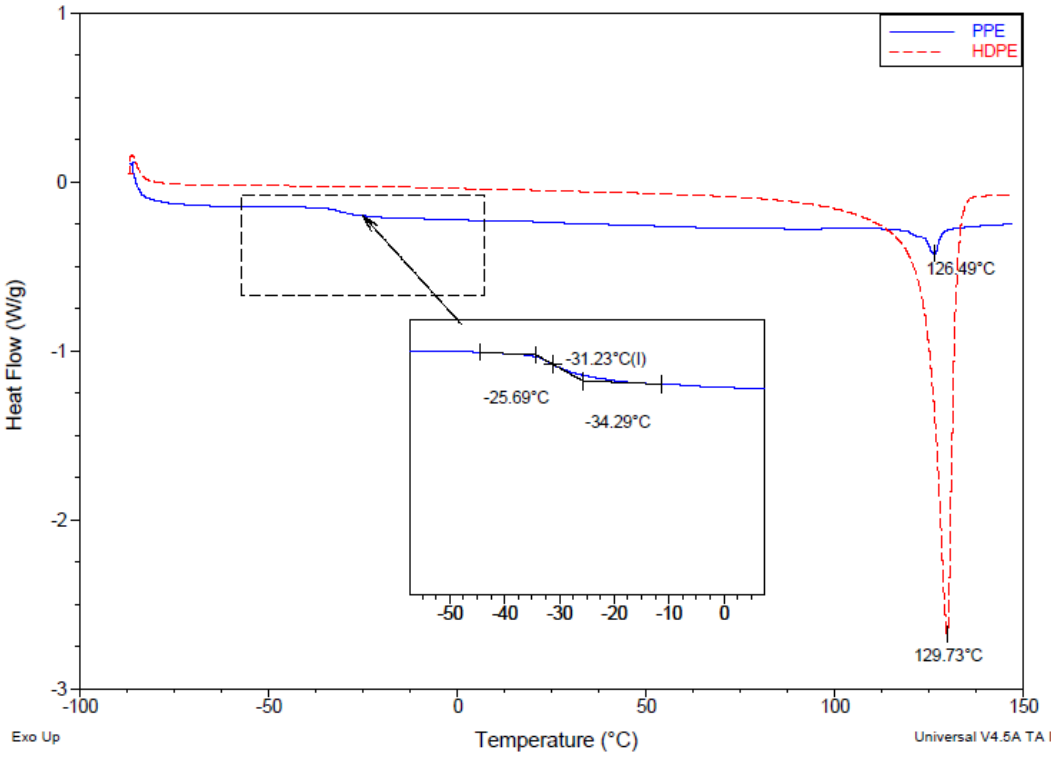

Figure 7.5 DSC curve for the pure PPE and HDPE polymers

Figure 7.5 shows the DSC curves for the pure polymer components (HDPE and PPE). The Tg for HDPE is below -90 ^{o}C and, unfortunately, it is beyond the measurement range of our DSC. A melt peak was observed for the HDPE

polymer at 129.7 ^{o}C which is in agreement with the data supplied by the manufacturer. PPE showed a Tg at -31.2 ^{o}C and a small melt peak at 126.5 ^{o}C and this is in agreement with manufacturer's data.

The DSC curve for the blend at 20% wt. of PPE is shown in figure 7.10. The DSC curve shows a Tg at -31.3 ^{o}C and a single melt peak at 129.8 ^{o}C. The Tg observed in the polymer blend correspond to the Tg of the pure PPE phase, which suggest immiscibility of HDPE and PPE. This is in agreement with the SEM images (fig. 7.1a). The melt peak observed in the polymer blend corresponds to that of HDPE. The weak melt peak observed for PPE (fig 7.5) was masked by the strong melt peak of HDPE in the blend.

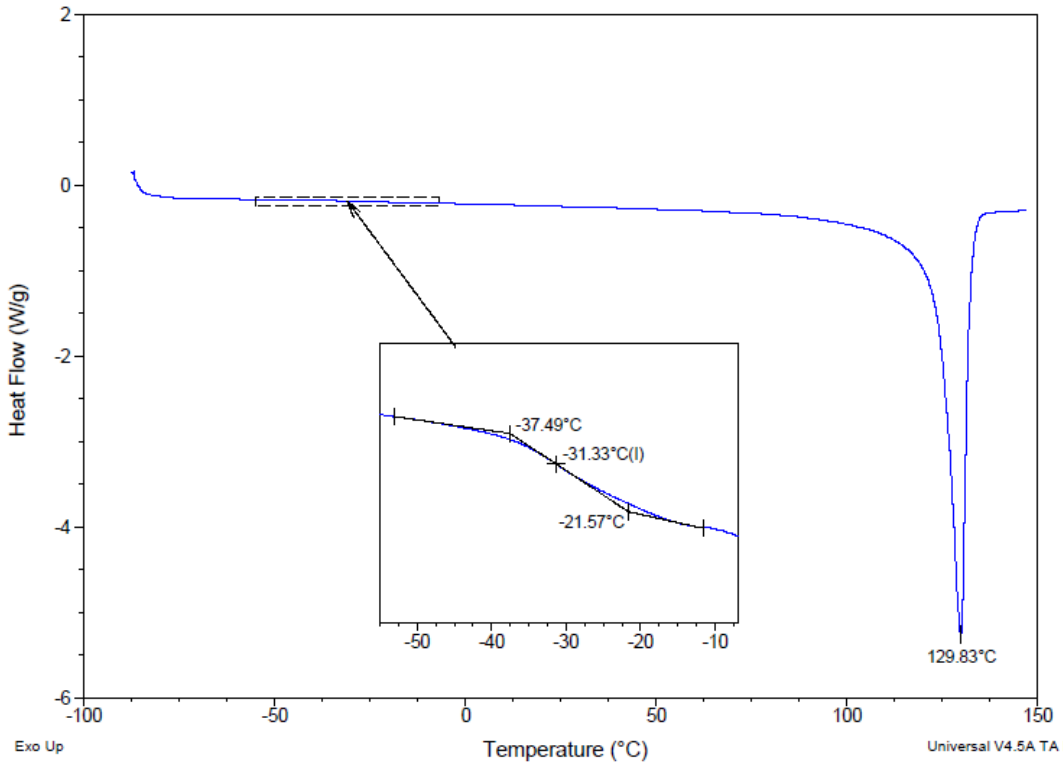

Figure 7.6 DSC curve for 20 %wt. PPE/HDPE polymer blend.

7.2.3 PTC effect of the composites

Figure 7.7 shows the resistivity-temperature behaviour for the AgFs/HDPE composites with different PPE contents. It was observed that the hybrid composite (PPE/HDPE/AgF_S) did not exhibit the classical double positive temperature coefficient (PTC) effect reported in literature. Only one PTC behaviour was observed for the AgF_S/HDPE/PPE composites with the PTC effect occurring around a temperature of 135^oC. This temperature is close to the melting temperature of HDPE and this was confirmed by DSC studies of the pure polymers and the composites. The increase in resistivity of the composite around the melting point of the HDPE might have been caused by the thermal expansion associated with the melting of the polymer crystallites. The increase in resistivity with temperature was immediately followed by a decrease in resistivity also known as the negative temperature coefficient (NTC) effect for both hybrid composites. This was caused by the reagglomeration of the conductive fillers [101].

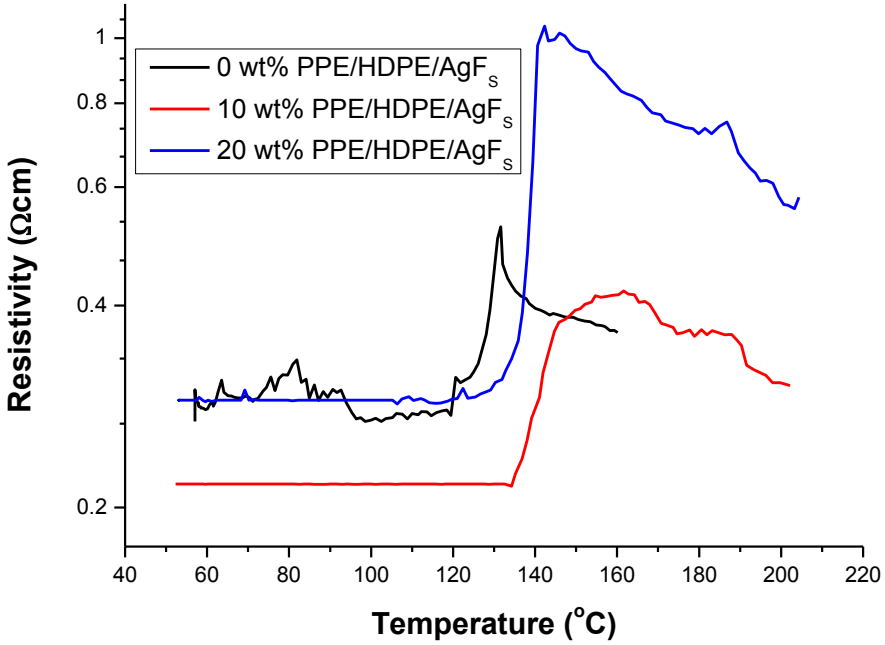

Figure 7.7 Resistivity-temperature for the AgF_S/HDPE polymer composite filled with different amounts of PPE.

Addition of PPE to HDPE/AgF_S composite increases the temperature at which the PTC effect happens. For HDPE/AgF composite (fig 7.8a), the PTC behaviour is depended on the thermal expansion of HDPE while addition of PPE to HDPE/AgF might results in the behaviours shown in figure 7.8b and 7.8c and this explains the increase in PTC temperature.

PPE forms a disperse phase in HDPE due to their immiscible nature and this was confirmed by SEM images (fig 7.1a), DMA and DSC studies. AgF_S particles stay in the HDPE phases when PPE is added to the HDPE/AgF composite and this confirmed by the absence of a double PTC behaviour of the PPE/HDPE/AgF composite. For the same filler content, substitution of HDPE concentration with PPE causes an increase in the local concentration of AgF_S in the HDPE phase due

to the reduction in HDPE (i.e. the ratio of HDPE to AgF decreases). An increase in local filler concentration results in a more robust network which is more difficult to be disrupted, hence the increase in PTC temperature.

The thermal expansion of PPE occurs at a lower temperature and is higher than that of HDPE.The expansion of PPE causes a reduction in interparticle distance between fillers in the HDPE phase (fig 7.8c). This decrease in interparticle distance causes an increase in interaction between particles therefore more energy is required to break the interaction hence an increase in PTC intensity.

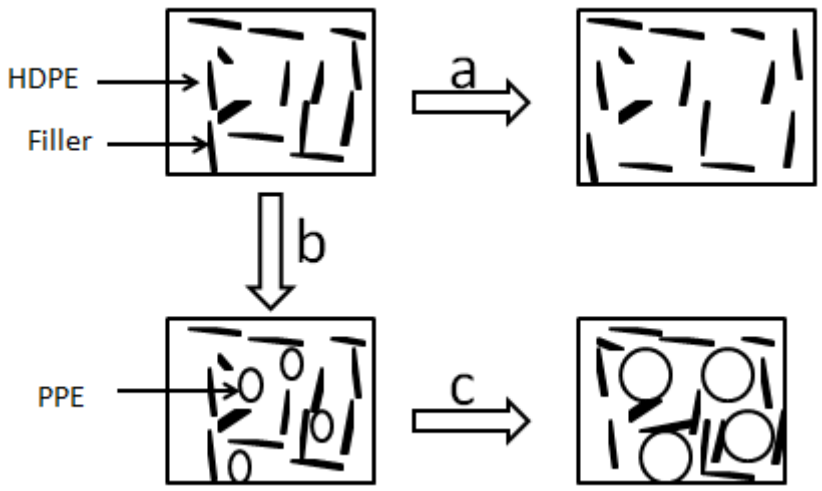

Figure 7.8 PTC behaviour of a) HDPE/AgF, b) adding PPE to HDPE/AgF and c) Expansion of PPE phase as temperature increased.

The PTC intensity increased with increasing PPE content as observed in figure 7.3. Increasing the amount of PPE in the composite gives the same effect as increasing the concentration of AgF_S in the composite. SEM imaging showed that the AgF_S particles were located in the HDPE phase of the composite. Increasing the amount of PPE reduces the amount of HDPE in the system therefore decreasing the available space for the conductive particles. Further increase in

PPE for instance at 20 wt% PPE will shrink the interparticle space even further due to the reduction in HDPE volume. This increases the concentration of AgS in the HDPE polymer matrix and this can lead to the particles migrating into the interphase between the HDPE and PPE polymer [21, 93]. The conductive particles found at the interphase will be affected by the thermal expansion of the polymers during heating hence an increase in the PTC intensity.

The effect on PTC intensity by the addition of PPE was also investigated for AgF_L/HDPE composite. It was observed that the PTC intensity increased when 10 wt% of PPE was added to the composite although the error bar suggested no "real" increase in PTC intensity. The PTC intensity seems to decrease slightly upon increase in PPE content.

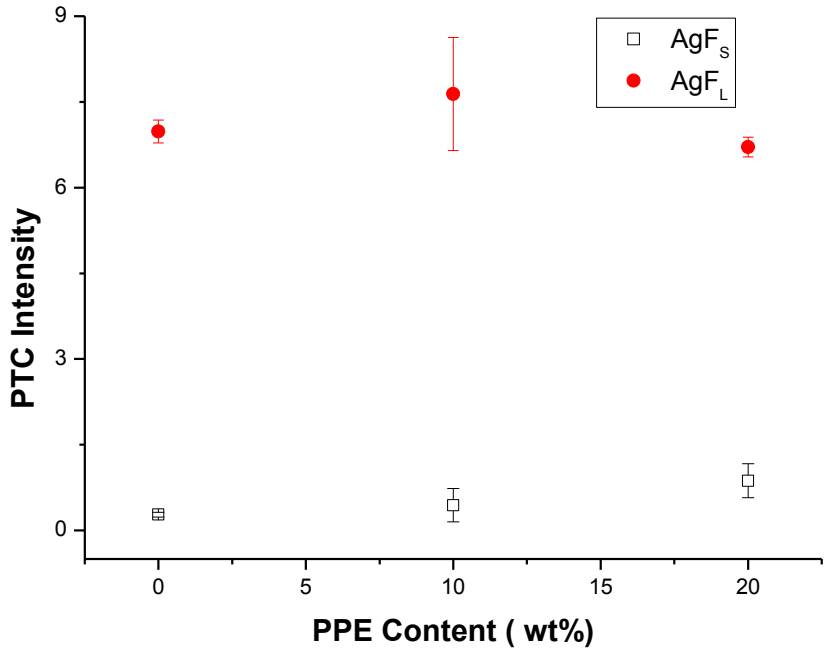

Figure 7.9 PTC Intensity versus amount of HDPE/AgF_S.

.

Examination of the thermal behaviour of the composites via DSC is shown in figure 7.4. HDPE showed a melt transition at a temperature of 130 ^{o}C. Only one transition which corresponded to the melting temperature of the HDPE polymer was observed in the DSC curves for the AgF_S/HDPE/PPE composites. The PTC temperature (135 ^{o}C) for the mixed polymer composites occurred around the temperature observed in the DSC curve for the composite.

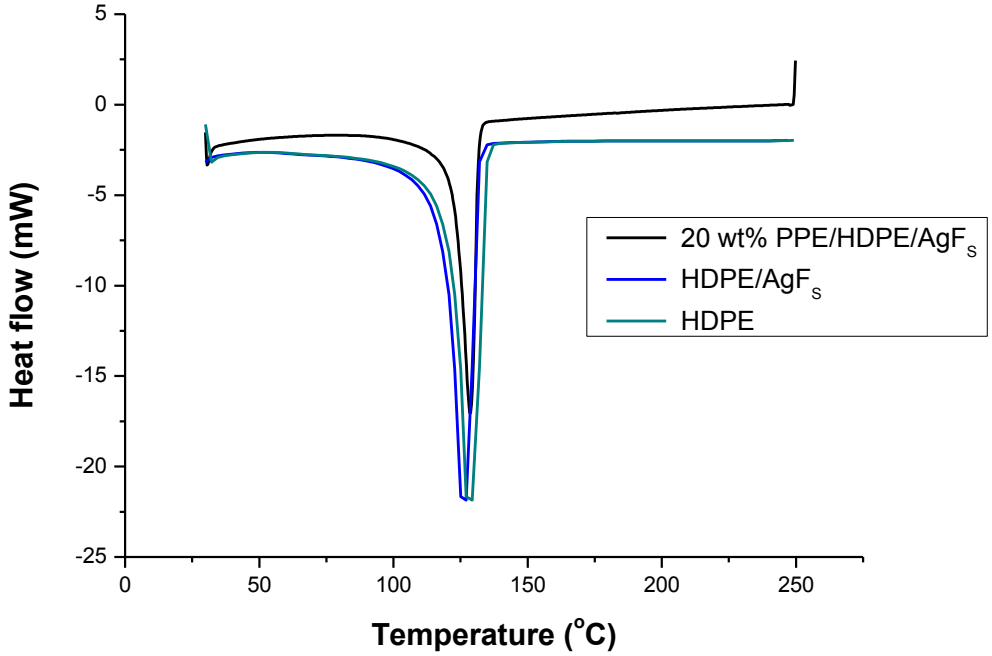

Figure 7.10. DSC curve for 20 %wt PPE in HDPE/AgF_S , HDPE/AgF_S and HDPE.

The linear coefficient of thermal expansion (CTE) of the composite was investigated to check if there was a change in CTE of the HDPE/AgF_S and the mixed polymer composite. From figure 7.5 it was observed that the CTE of the mixed polymer composite is bigger that the CTE of pure HDPE. The increase in CTE might have caused the increase in PTC intensity due to the increase in inter-

particle distance as the polymer expands. The maximum temperature for TMA analyses was 100 ^{o}C and this temperature was not enough to see the melt transition in the composites.

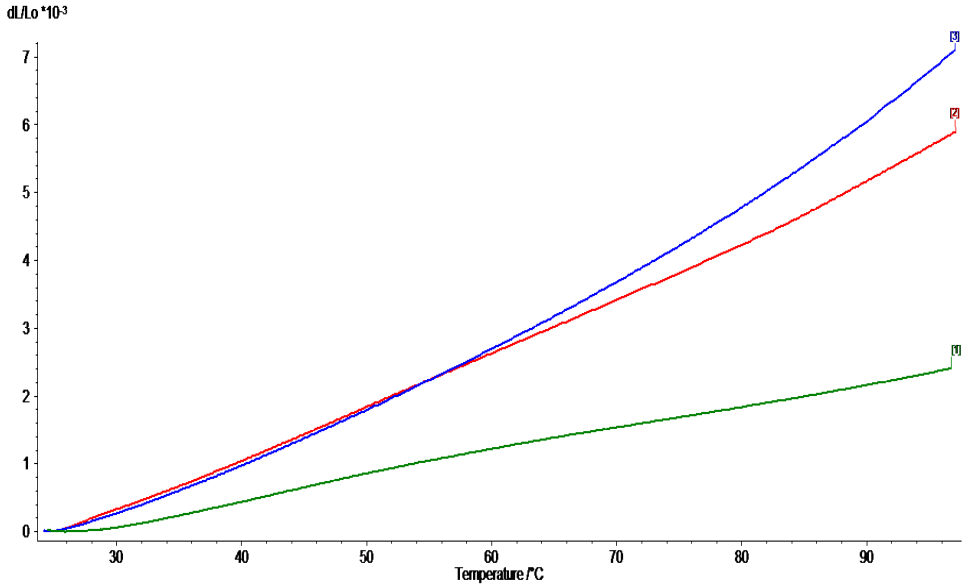

Figure 7.11. TMA graph of HDPE (green line), 20 %wt PPE/HDPE (redline) and PPE (blue line).

7.3 Conclusions

The effect on the positive temperature coefficient (PTC) effect of hybrid polymers filled with silver coated glass flakes has been investigated. The morphological studies revealed a segregated structure with the conductive particles localised in the high density polyethylene (HDPE) phase.

DMA analysis revealed two transitions in the loss modulus corresponding to characteristic relaxation of PPE and HDPE. This indicated the immiscibility of the two polymers and confirmed the phase separation observed in the SEM imaging.

DSC was used to confirm the observations in the DMA. DSC investigations of the hybrid polymer composites only showed the melting temperature of HDPE but the Tg for PPE was also observed. The observation of the characteristic transitions for the polymer blends confirmed the immiscibility of the two polymers. TMA results proved an increase in the linear coefficient of thermal expansion (CTE) when the PPE polymer was added to the HDPE composite. Results from DMA studies confirmed the reduction in stiffness with an increase in PPE content.

The PTC intensity of the composite increased with increasing PPE content but the negative temperature coefficient (NTC) effect was observed in all the composites.

Chapter 8. Conclusions and future work

8.1 Conclusions

This thesis investigated the effect of filler size on the positive temperature coefficient (PTC) effect of conductive polymer composites. In a quest to enhance the electrical properties and the PTC intensity of AgG/HDPE composite, a second filler (AgS_M and AgF_L) and polymer (PPE) was added to the system to form either hybrid filler composite or a hybrid polymer composite.

Silver coated glass particles (spheres and flakes) were used as model conductive fillers to establish for the first time the "true" effect of the filler size and shape on electrical conductivity and PTC intensity.

The electrical conductivity behaviour of the composites increased with increasing filler content. The increase in conductivity with filler content is caused by the increase in conductive networks as the filler content increases. All the composites followed the classical percolation behaviour. The percolation of the composites was dependent on the filler shape and size. An increase in filler size increased the percolation threshold of both filler types. This is linked to the increase in specific surface area as particle size decreases. The percolation thresholds of the AgF/HDPE composites were smaller when compared to that of AgS/HDPE. This is due to the difference in aspect ratio of the particles. An increase in aspect ratio of the fillers decreases the percolation threshold of the composite.

The PTC intensity increases with decreasing filler content and with increasing filler size and this observation was occurred for both spherical and flake-like

conductive filler. This is phenomenologically consistent with the concept of 'robustness' of the conductive filler network. A decrease in filler content results in a reduction in conductive network. The reduction in conductive networks increases the ease of disruption by the polymer matrix hence the increase in PTC intensity. The increase in specific surface area with decrease in filler size increases the interactions between the fillers therefore increasing the difficulty in disturbing the conductive networks. This leads to a reduction in PTC intensity. Flake-like particles formed a more robust network that the spherical particles due to their high aspect ratio.

Two series of mixed filler conductive composites were studied, to explore the possibility to combine low percolation threshold with large PTC intensities. The electrical conductivity of the composites increased with increase in the second filler and this is as a result of the increase in conductive filler content and conductive network.

The study revealed that the PTC intensity of mixed fillers composites is dominated by the filler with the highest aspect ratio, even at very low volume fractions. PTC intensity is dependent on the ease of disturbing the conductive network in a composite and hybrid fillers can have two type conductive networks. The fillers could have formed independent conductive networks or formed a hybrid conductive network with the polymer matrix. Formation of either conductive network requires an increase in energy to disrupt the network.

It was found that the PTC intensity is not only dependent on the conductive particle size but also by its size distribution.

An attempt was made to investigate the effect of difference in linear coefficient of thermal expansion (CTE) of conductive fillers and polymer matrix based on a change in filler core on the electrical and PTC behaviour CPCs. Silver coated PMMA (AgP) beads used in this investigation was damaged during extrusion. Damage to the AgP particles was due to the poor adhesion between the silver coating and the PMMA bead. A higher percolation threshold for the AgP/HDPE compared to the AgS_M/HDPE was observed and this was caused by the damage to the silver coatings on the PMMA beads. The PTC intensity observed for the AgS_M/HDPE composite was higher than that of the AgP/HDPE composite. The conductive network formed by the AgP particles in HDPE due to the damaged AgP particles (Ag shavings) resulted in a small PTC intensity for the AgP/HDPE composite. Two conductive networks could have been formed in the composite with one network involving damage AgP particles and silver shavings while the other network could have been independent conductive networks between just AgP particles and silver shavings.

NTC effect was observed in the AgP/HDPE composite and this might have been caused by the reagglomeration of Ag shavings.

The effect on the positive temperature coefficient (PTC) effect of hybrid polymers filled with silver coated glass flakes was also examined. SEM imaging showed two distinctive phases which indicated that the two polymers are immiscible. DMA investigations of the hybrid polymer composites confirmed the immiscibility of the polymers with the loss modulus against temperature curve showing two transitions for the hybrid polymer. DSC investigation agreed with the findings of the DMA (i.e. proved the immiscibility of the polymers).

The PTC intensity of the composite increased with increasing PPE content but the negative temperature coefficient (NTC) effect was observed in all the composites.

8.2 Future work

In this thesis, two different shaped particles (sphere and flake) have been used to prove that an increase in filler size increases the PTC intensity of conductive polymer composites. Although an attempt was made to extend the size effect to different shaped conductive particles, fibre particles will present an interesting angle to the study. The size effect can be studied by increasing the length (a) of the fibre or decreasing the width (b) of the fibre (fig. 8.1). This change in dimensions of the fibre will affect not only the surface area of the particles but how they pack within the composite. The filler packing factor or density (F) is related to the particle shape with an increase in F resulting in an increase in percolation threshold [34, 137]. This is likely to enhance the understanding of conductive filler size effect on the PTC intensity of CPC.

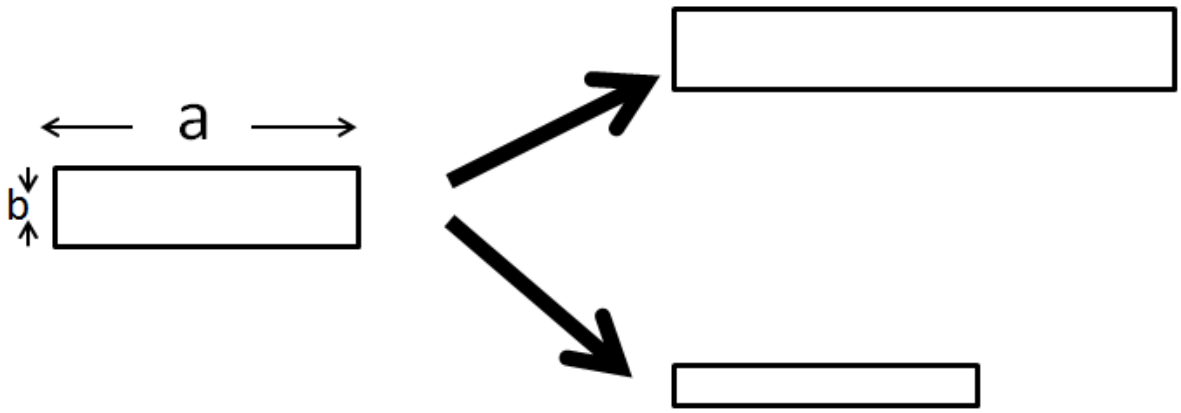

Figure 8.1 Ways to change the filler size of the fibre.

The effect of CTE mismatch between the filler and the polymer matrix was not proven. This study could have shed more light on this effect since most researchers have focused on changing the polymer matrix but studying fillers with the same properties except their thermal behaviour would eliminate the polymer matrix and the filler shape and size effect on PTC. A milder processing route such as solution processing could be used to investigate this effect although dissolving HDPE in xylene with these particles did not work. The particles were damaged as shown in figure 8.2. Better coating of the silver unto the PMMA beads could be explored also.

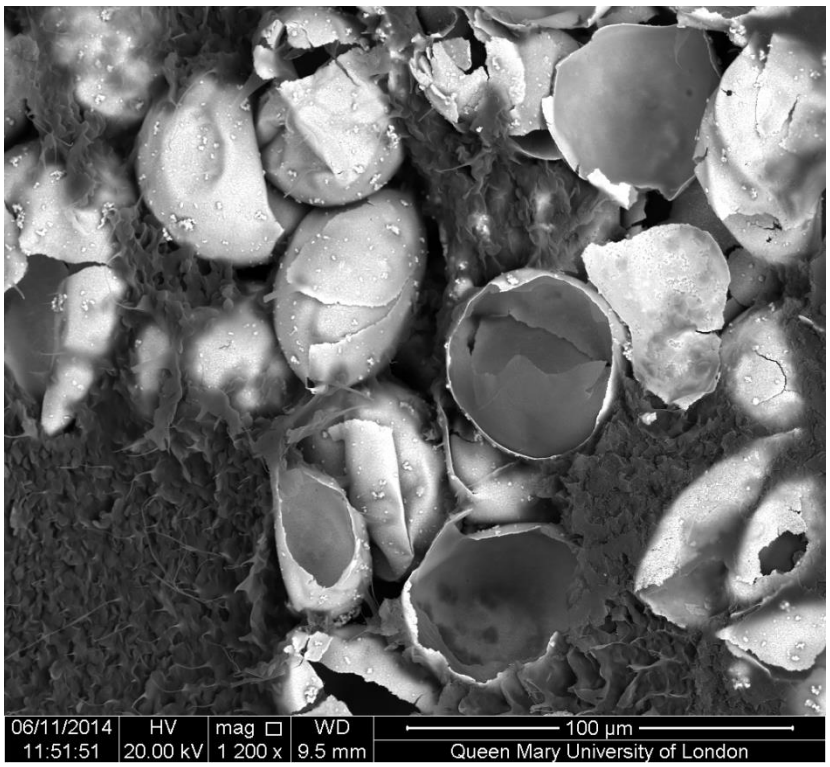

Figure 8.2 SEM image of AgP/HDPE composite prepared via a solution method.

Modelling the PTC behaviour of the particles examined in this thesis will be very interesting and an effort has been made to do that in collaboration with Professor

Paul Schoot of Eindhoven University. In order to model the PTC behaviour of the system, the conductivity behaviour of the system was modelled and the Hamaker constant equation for particles dispersed in another medium used to predict the inter particle distance in the percolated composite. An inter particle distance less than 10 nm will allow electron tunnelling therefore a calculated value equal or less than 10 nm will confirm the suitability of the modelling technique for this study.

$$\varphi_p = \frac{1}{24} \cdot \exp\left(-\frac{\epsilon}{k_B T}\right) \cdot \frac{\sigma}{\delta} \cdot \left(1 + \frac{\delta}{\sigma} + \frac{\delta}{3\sigma}\right)^{-1} \tag{8.1}$$

Here, σ is the diameter of the spheres, δ the connectivity criterion that is equal to the range of the attractive interaction, $\epsilon \geq 0$ is the strength of the attractive potential and $k_B T$ the thermal energy with k_B Boltzmann's constant and T the absolute temperature.

Assuming

$$\delta \ll \sigma$$

because it is of quantal nature. In that limit we retrieve the simplified equation

$$\varphi_p \approx \frac{1}{24} \cdot \exp\left(-\frac{\epsilon}{k_B T}\right) \cdot \frac{\sigma}{\delta} \tag{8.2}$$

The equation can be simplified by introducing the parameter a given as;

$$\exp \frac{\left(-\frac{\epsilon}{k_B T}\right)}{\delta} \tag{8.3}$$

The equation becomes

$$\varphi_p = \frac{1}{24} \cdot a \cdot \sigma \tag{8.4}$$

A graph of the percolation threshold (φ_p) against the filler diameter (σ) will have a gradient of a/24.

The connectivity criterion (δ) can be found by rearranging the equation below

$$\exp \frac{\left(-\frac{\epsilon}{k_B T}\right)}{\delta} \equiv \text{a} \tag{8.5}$$

Taking the natural log (In) of both sides of equation 9.5, the equation becomes

$$\frac{-\epsilon}{\delta} = In\ a\ \times K_B T \tag{8.6}$$

The Hamaker constant (A_{131}) can be used to describe the electronic interactions between the silver particles in the HDPE polymer [138-140]. The equation for finding the Hamaker constant is given as;

$$A_{131} = \left(\sqrt{A_{11}} - \sqrt{A_{33}}\right)^2 \tag{8.7}$$

where A_{11} and A_{33} are the Hamaker constant of silver particles and HDPE polymer matrix acting across vacuum respectively.

Different hamaker constants have been reported for silver from 3.5×10^{-19}J to 5.0×10^{-19}J [138, 141, 142].

A33 can be calculated by using Lifshitz theory [142]:

$$A_{33} = \frac{3}{4} KT \left(\frac{\varepsilon_3 - \varepsilon_{vacuum}}{\varepsilon_3 + \varepsilon_{vacuum}}\right)^2 + \frac{3h\nu_e(n_3^2 - n_{vacuum}^2)^2}{16\sqrt{2}(n_3^2 + n_{vacuum}^2)^{3/2}} \quad (8.8)$$

Where ε is the dielectric constant, *n* is the refractive index, *h* is Planck's constant, *k* is Boltzmann's constant, T is temperature, ν_e is the maximum electronic ultraviolet adsorption frequency typically taken to be $3 \times 10^{15}s^{-1}$ with ε_{vacuum} and n_{vacuum} equal to 1.

The calculated value for A_{33} from equation is 4.79×10^{-22}J. If A_{11} is equal to 3.5×10^{-19}J and 5.0×10^{-19}J then A_{131} yields 3.25×10^{-19}J and 4.69×10^{-19}J respectively.

The interparticle distance can be calculated for the spherical particles used in this experiment by relating the The hamaker constant (A) to the strength of the attractive potential (ϵ) (i.e. A = ϵ).

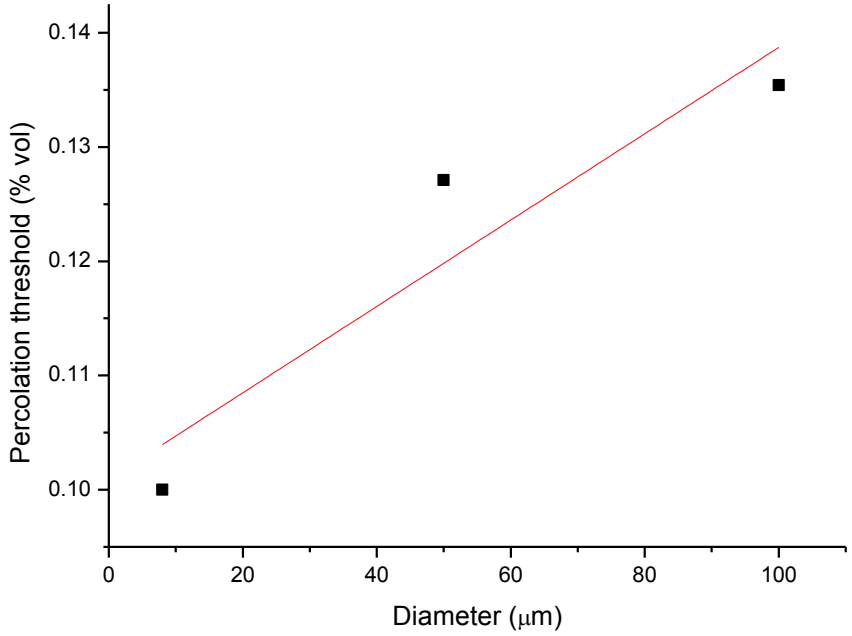

Figure 8.3 Percolation threshold against filler diameter for silver coated glass spheres in HDPE matrix.

From the graph of percolation threshold against filler diameter (fig 8.3.), the gradient

$$\frac{\epsilon}{\delta} = 4.76 \times 10^{-20}$$

If $\epsilon = 3.25 \times 10^{-19}$J then $\delta = 6.32$nm

The maximum distance between silver particles calculated using the highest Hamaker constants (4.69×10^{-19}J) reported for silver was 9.87 nm.

The values calculated for the distance between AgS particles are below the distance required for electron tunnelling to occur. This indicates that the assumptions used in the modelling of the conductivity of the particles are sound.

The second part of the modelling which will focus on the PTC behaviour is currently been worked on. This will shed more light on the effect of filler size and shape on PTC effect of CPCs.

Chapter 9. Reference

1. Bilotti, E., et al., *Fabrication and property prediction of conductive and strain sensing TPU/CNT nanocomposite fibres.* Journal of Materials Chemistry, 2010. **20**(42): p. 9449-9455.
2. Villmow, T., et al., *Polymer/carbon nanotube composites for liquid sensing: Model for electrical response characteristics.* Polymer, 2011. **52**(10): p. 2276-2285.
3. B. Kumar, M.C., J. F. Feller, *Quantum resistive vapour sensors made of polymer coated carbon nanotubes random networks for biomarkers detection.* Chemical Sensors, 2013. **3**: p. 20.
4. Thostenson, E.T. and T.-W. Chou, *Carbon nanotube networks: Sensing of distributed strain and damage for life prediction and self healing.* Advanced Materials, 2006. **18**(21): p. 2837-+.
5. Zhang, H., et al., *Improved fracture toughness and integrated damage sensing capability by spray coated CNTs on carbon fibre prepreg.* Composites Part a-Applied Science and Manufacturing, 2015. **70**: p. 102-110.
6. H. Zhang, E.b., T. Peijs, *The Use of Carbon Nanotubes for Damage Sensing and Structural Health Monitoring in Laminated Composites: A Review.* Nanocomposites, 2015.
7. Mai, F., et al., *Poly(lactic acid)/carbon nanotube nanocomposites with integrated degradation sensing.* Polymer, 2013. **54**(25): p. 6818-6823.
8. Ohe, K. and Y. Naito, *New Resistor Having an Anomalously Large Positive Temperature Coefficient.* Japanese Journal of Applied Physics, 1971. **10**(1): p. 99-&.

9. Rybak, A., et al., *Conductive polymer composites based on metallic nanofiller as smart materials for current limiting devices.* Composites Science and Technology, 2010. **70**(2): p. 410-416.

10. www.te.com.

11. www.thermons.co.uk.

12. Al-Saleh, M.H. and U. Sundararaj, *A review of vapor grown carbon nanofiber/polymer conductive composites.* Carbon, 2009. **47**(1): p. 2-22.

13. Bao, S.P., G.D. Liang, and S.C. Tjong, *Effect of mechanical stretching on electrical conductivity and positive temperature coefficient characteristics of poly(vinylidene fluoride)/carbon nanofiber composites prepared by non-solvent precipitation.* Carbon, 2011. **49**(5): p. 1758-1768.

14. Bao, Y., et al., *Preparation and properties of carbon black/polymer composites with segregated and double-percolated network structures.* Journal of Materials Science, 2013. **48**(14): p. 4892-4898.

15. Bar, H., M. Narkis, and G. Boiteux, *The electrical behavior of thermosetting polymer composites containing metal plated ceramic filler.* Polymer Composites, 2005. **26**(1): p. 12-19.

16. Bin, Y., et al., *Electrical properties of polyethylene and carbon black particle blends prepared by gelation/crystallization from solution.* Carbon, 2002. **40**(2): p. 195-199.

17. Hindermann-Bischoff, M. and F. Ehrburger-Dolle, *Electrical conductivity of carbon black–polyethylene composites: Experimental evidence of the change of cluster connectivity in the PTC effect.* Carbon, 2001. **39**(3): p. 375-382.

18. Lisunova, M.O., et al., *Percolation behaviour of ultrahigh molecular weight polyethylene/multi-walled carbon nanotubes composites.* European Polymer Journal, 2007. **43**(3): p. 949-958.

19. Boiteux, G., et al., *Conductive thermoset composites: PTC effect.* Synthetic Metals, 1999. **102**(1–3): p. 1234-1235.

20. Dang, Z.M., et al., *Complementary percolation characteristics of carbon fillers based electrically percolative thermoplastic elastomer composites.* Composites Science and Technology, 2011. **72**(1): p. 28-35.

21. Feng, J. and C.M. Chan, *Double positive temperature coefficient effects of carbon black-filled polymer blends containing two semicrystalline polymers.* Polymer, 2000. **41**(12): p. 4559-4565.

22. Fournier, J., et al., *Positive temperature coefficient effect in carbon black/epoxy polymer composites.* Journal of Materials Science Letters, 1997. **16**(20): p. 1677-1679.

23. He, X.J., et al., *Positive temperature coefficient effect in multiwalled carbon nanotube/high-density polyethylene composites.* Applied Physics Letters, 2005. **86**(6).

24. Isaji, S., Y. Bin, and M. Matsuo, *Electrical conductivity and self-temperature-control heating properties of carbon nanotubes filled polyethylene films.* Polymer, 2009. **50**(4): p. 1046-1053.

25. Jiang, X. and L.T. Drzal, *Improving electrical conductivity and mechanical properties of high density polyethylene through incorporation of paraffin wax coated exfoliated graphene nanoplatelets and multi-wall carbon nano-tubes.* Composites Part A: Applied Science and Manufacturing, 2011. **42**(11): p. 1840-1849.

26. *Thermon 8-FLX-2 Heat Tracing Cable*. [cited 2016 21/01/2016]; Available from: http://www.heattracing.co.uk/sub-product-details/8-flx-2-thermon-frost-protection-trace-heating-cable.

27. *BriskHeat Heating Cable*. [cited 2016 24/01/2016]; Available from: http://www.briskheat.com/c-70-heating-cable.aspx.

28. *PolySwitch Automotive Devices*. [cited 2016 24/01/2016]; Available from: http://www.te.com/usa-en/products/circuit-protection/overcurrent-devices/polyswitch-resettable-devices/automotive-devices.html?tab=pgp-story.

29. *Over-Current Protectors*. [cited 2016 24/01/2016]; Available from: http://precisionsensors.meas-spec.com/ocp.asp.

30. *Polyswitch Resettable Devices Fundamentals*. [cited 2016 24/01/2016]; Available from: http://www.te.com/content/dam/te-com/documents/circuit-protection/global/CPD-Catalog/S11_PolySwitch-Fundamentals.pdf.

31. Deepa, K.S., et al., *Effect of conductivity of filler on the percolation threshold of composites.* Applied Physics Letters, 2009. **94**(14).

32. Han, Z. and A. Fina, *Thermal conductivity of carbon nanotubes and their polymer nanocomposites: A review.* Progress in Polymer Science, 2011. **36**(7): p. 914-944.

33. Kar, P. and B.B. Khatua, *Highly Reversible and Repeatable PTCR Characteristics of PMMA/Ag-Coated Glass Bead Composites Based on CTE Mismatch Phenomena.* Polymer Engineering and Science, 2011. **51**(9): p. 1780-1790.

34. Mamunya, Y.P., et al., *Electrical and thermal conductivity of polymers filled with metal powders.* European Polymer Journal, 2002. **38**(9): p. 1887-1897.

35. Thommerel, E., et al., *Relations between microstructure, electrical percolation and corrosion in metal-insulator composites.* Materials Science and Engineering a-Structural Materials Properties Microstructure and Processing, 2002. **328**(1-2): p. 67-79.

36. Xu, H.P., et al., *STUDY ON THEORIES AND INFLUENCE FACTORS OF PTC PROPERTY IN POLYMER-BASED CONDUCTIVE COMPOSITES.* Reviews on Advanced Materials Science, 2011. **27**(2): p. 173-183.

37. Sridhar, M.V., et al., *Effect of nanoclay on positive temperature coefficient to resistivity characteristics of high density polyethylene/silver-coated glass bead composites.* Polymer Composites, 2012. **33**(5): p. 819-828.

38. Wong, C.P. and S. Luo, *Conductive Polymer Composites with Large Positive Temperature Coefficients*, in *Encyclopedia of Smart Materials*. 2002, John Wiley & Sons, Inc.

39. stru¨mpler, R. and J. Glatz-Reichenbach, *FEATURE ARTICLE Conducting Polymer Composites.* Journal of Electroceramics, 1999. **3**(4): p. 329-346.

40. Lux, F., *MODELS PROPOSED TO EXPLAIN THE ELECTRICAL-CONDUCTIVITY OF MIXTURES MADE OF CONDUCTIVE AND INSULATING MATERIALS.* Journal of Materials Science, 1993. **28**(2): p. 285-301.

41. Ke, K., et al., *Evolution of agglomerate structure of carbon nanotubes in multi-walled carbon nanotubes/polymer composite melt: A rheo-electrical study.* Composites Part B: Engineering, (0).

42. Shen, L., et al., *The combined effects of carbon black and carbon fiber on the electrical properties of composites based on polyethylene or polyethylene/polypropylene blend.* Polymer Testing, 2011. **30**(4): p. 442-448.

43. Kirkpatr.S, *PERCOLATION AND CONDUCTION.* Reviews of Modern Physics, 1973. **45**(4): p. 574-588.

44. Zallen, R. and H. Scher, *PERCOLATION ON A CONTINUUM AND LOCALIZATION-DELOCALIZATION TRANSITION IN AMORPHOUS SEMICONDUCTORS.* Physical Review B, 1971. **4**(12): p. 4471-&.

45. Zhang, R., et al., *Conductive network formation in the melt of carbon nanotube/thermoplastic polyurethane composite.* Composites Science and Technology, 2009. **69**(10): p. 1499-1504.

46. Liu, F., et al., *Investigation of the electrical conductivity of HDPE composites filled with bundle-like MWNTs.* Composites Part a-Applied Science and Manufacturing, 2009. **40**(11): p. 1717-1721.

47. Bauhofer, W. and J.Z. Kovacs, *A review and analysis of electrical percolation in carbon nanotube polymer composites.* Composites Science and Technology, 2009. **69**(10): p. 1486-1498.

48. Malliari.A and D.T. Turner, *INFLUENCE OF PARTICLE SIZE ON ELECTRICAL RESISTIVITY OF COMPACTED MIXTURES OF POLYMERIC AND METALLIC POWDERS.* Journal of Applied Physics, 1971. **42**(2): p. 614-&.

49. Banerjee, P. and B.M. Mandal, *Blends of HCl-doped polyaniline nanoparticles and poly(vinyl chloride) with extremely low percolation threshold - A morphology study.* Synthetic Metals, 1995. **74**(3): p. 257-261.

50. Karasek, L., et al., *Percolation concept: Polymer-filler gel formation, electrical conductivity and dynamic electrical properties of carbon-black-filled rubbers.* Polymer Journal, 1996. **28**(2): p. 121-126.

51. Ota, T., et al., *Control of percolation curve by filler particle shape in Cu-SBR composites.* Journal of Materials Science Letters, 1997. **16**(14): p. 1182-1183.

52. Jing, X., W. Zhao, and L. Lan, *The effect of particle size on electric conducting percolation threshold in polymer/conducting particle composites.* Journal of Materials Science Letters, 2000. **19**(5): p. 377-379.

53. Luo, S.J. and C.P. Wong, *Study on effect of carbon black on behavior of conductive polymer composites with positive temperature coefficient.* Ieee Transactions on Components and Packaging Technologies, 2000. **23**(1): p. 151-156.

54. Bigg, D.M. and D.E. Stutz, *PLASTIC COMPOSITES FOR ELECTROMAGNETIC-INTERFERENCE SHIELDING APPLICATIONS.* Polymer Composites, 1983. **4**(1): p. 40-46.

55. Bai, J.B. and A. Allaoui, *Effect of the length and the aggregate size of MWNTs on the improvement efficiency of the mechanical and electrical properties of nanocomposites - experimental investigation.* Composites Part a-Applied Science and Manufacturing, 2003. **34**(8): p. 689-694.

56. Martin, C.A., et al., *Formation of percolating networks in multi-wall carbon-nanotube-epoxy composites.* Composites Science and Technology, 2004. **64**(15): p. 2309-2316.

57. Mamunya, Y., et al., *Electrical and thermophysical behaviour of PVC-MWCNT nanocomposites.* Composites Science and Technology, 2008. **68**(9): p. 1981-1988.

58. Ponomarenko, A.T., V.G. Shevchenko, and N.S. Enikolopyan, *FORMATION PROCESSES AND PROPERTIES OF CONDUCTING POLYMER COMPOSITES.* Advances in Polymer Science, 1990. **96**: p. 125-147.

59. Kim, Y.J., et al., *Electrical conductivity of chemically modified multiwalled carbon nanotube/epoxy composites.* Carbon, 2005. **43**(1): p. 23-30.

60. Li, J., et al., *Correlations between percolation threshold, dispersion state, and aspect ratio of carbon nanotubes.* Advanced Functional Materials, 2007. **17**(16): p. 3207-3215.

61. Potschke, P., et al., *Rheological and dielectrical characterization of melt mixed polycarbonate-multiwalled carbon nanotube composites.* Polymer, 2004. **45**(26): p. 8863-8870.

62. Chen, L., X.J. Pang, and Z.L. Yu, *Study on polycarbonate/multi-walled carbon nanotubes composite produced by melt processing.* Materials Science and

Engineering a-Structural Materials Properties Microstructure and Processing, 2007. **457**(1-2): p. 287-291.

63. Saeed, K. and S.Y. Park, *Preparation and properties of multiwalled carbon nanotube/polycaprolactone nanocomposites.* Journal of Applied Polymer Science, 2007. **104**(3): p. 1957-1963.

64. Skakalova, V., U. Dettlaff-Weglikowska, and S. Roth, *Electrical and mechanical properties of nanocomposites of single wall carbon nanotubes with PMMA.* Synthetic Metals, 2005. **152**(1-3): p. 349-352.

65. Tjong, S.C., G.D. Liang, and S.P. Bao, *Electrical behavior of polypropylene/multiwalled carbon nanotube nanocomposites with low percolation threshold.* Scripta Materialia, 2007. **57**(6): p. 461-464.

66. Giuliana, G., et al., *Carbon nanotube induced structural and physical property transitions of syndiotactic polypropylene.* Nanotechnology, 2007. **18**(27): p. 275703.

67. Deng, H., et al., *Effect of melting and crystallization on the conductive network in conductive polymer composites.* Polymer, 2009. **50**(15): p. 3747-3754.

68. Tobias Villmow, P.P.t., Sven Pegel, Liane Ha¨ussler, Bernd Kretzschmar, *Influence of twin-screw extrusion conditions on the dispersion*

of multi-walled carbon nanotubes in a poly(lactic acid) matrix. Polymer, 2008. **49**: p. 3500-3509.

69. Ma, P.C. and J.K. Kim, *Carbon Nanotubes for Polymer Reinforcement*. 2011: CRC Press.

70. Li, M.K., et al., *Electrical conductivity of thermally reduced graphene oxide/polymer composites with a segregated structure.* Carbon, 2013. **65**: p. 371-373.

71. Regev, O., et al., *Preparation of conductive nanotube-polymer composites using latex technology.* Advanced Materials, 2004. **16**(3): p. 248-+.

72. Wu, C., et al., *Highly Conductive Nanocomposites with Three-Dimensional, Compactly Interconnected Graphene Networks via a Self-Assembly Process.* Advanced Functional Materials, 2013. **23**(4): p. 506-513.

73. Levin, Z.S., et al., *Flexible latex-polyaniline segregated network composite coating capable of measuring large strain on epoxy.* Smart Materials and Structures, 2013. **22**(1).

74. Krause, B., P. Pötschke, and L. Häußler, *Influence of small scale melt mixing conditions on electrical resistivity of carbon nanotube-polyamide composites.* Composites Science and Technology, 2009. **69**(10): p. 1505-1515.

75. Potschke, P., S.M. Dudkin, and I. Alig, *Dielectric spectroscopy on melt processed polycarbonate - multiwalled carbon nanotube composites.* Polymer, 2003. **44**(17): p. 5023-5030.

76. Andrews, R., et al., *Fabrication of carbon multiwall nanotube/polymer composites by shear mixing.* Macromolecular Materials and Engineering, 2002. **287**(6): p. 395-403.

77. Yang, Y.L. and M.C. Gupta, *Novel carbon nanotube-polystyrene foam composites for electromagnetic interference shielding.* Nano Letters, 2005. **5**(11): p. 2131-2134.

78. *Global EMI/RFI Shielding Market to Reach $6.6 Billion in 2019*

2014.

79. Kohler, F., 1966: US. p. 3246, 753.

80. Li, Q., et al., *Positive temperature coefficient characteristic and structure of graphite nanofibers reinforced high density polyethylene/carbon black nanocomposites.* Composites Part B: Engineering, 2009. **40**(3): p. 218-224.

81. Pang, H., et al., *Tunable positive temperature coefficient of resistivity in an electrically conducting polymer/graphene composite.* Applied Physics Letters, 2010. **96**(25).

82. Xi, Y., et al., *Positive temperature coefficient effect of LMWPE–UHMWPE blends filled with short carbon fibers.* Carbon, 2004. **42**(8–9): p. 1699-1706.

83. Frydman, E., 1948: UK. p. 604, 695

84. Lee, J.H., S.K. Kim, and N.H. Kim, *Effects of the addition of multi-walled carbon nanotubes on the positive temperature coefficient characteristics of carbon-black-filled high-density polyethylene nanocomposites.* Scripta Materialia, 2006. **55**(12): p. 1119-1122.

85. Luo, Y., et al., *The influence of crystalline and aggregate structure on PTC characteristic of conductive polyethylene/carbon black composite.* European Polymer Journal, 1998. **34**(8): p. 1221-1227.

86. Isaji, S., Y. Bin, and M. Matsuo, *Electrical and self-heating properties of UHMWPE-EMMA-NiCF composite films.* Journal of Polymer Science Part B: Polymer Physics, 2009. **47**(13): p. 1253-1266.

87. Seo, M.-K., K.-Y. Rhee, and S.-J. Park, *Influence of electro-beam irradiation on PTC/NTC behaviors of carbon blacks/HDPE conducting polymer composites.* Current Applied Physics, 2011. **11**(3): p. 428-433.

88. Tsao, K.-Y., C.-S. Tsai, and C.-Y. Huang, *Effect of argon plasma treatment on the PTC and NTC behaviors of HDPE/carbon black/aluminum hydroxide nanocomposites for over-voltage resistance positive temperature coefficient (PTC).* Surface and Coatings Technology, 2010. **205, Supplement 1**(0): p. S279-S285.

89. Meyer, J., *Glass Transition Temperature as a Guide to Selection of Polymers Suitable for Ptc Materials.* Polymer Engineering and Science, 1973. **13**(6): p. 462-468.

90. Kono, A., et al., *Positive-temperature-coefficient effect of electrical resistivity below melting point of poly(vinylidene fluoride) (PVDF) in Ni particle-dispersed PVDF composites.* Polymer, 2012. **53**(8): p. 1760-1764.

91. Xiong, C., et al., *Polyurethane/carbon black composites with high positive temperature coefficient and low critical transformation temperature.* Carbon, 2005. **43**(8): p. 1788-1792.

92. Tang, H., X. Chen, and Y. Luo, *Studies on the PTC/NTC effect of carbon black filled low density polyethylene composites.* European Polymer Journal, 1997. **33**(8): p. 1383-1386.

93. Di, W., et al., *Two-step PTC effect in immiscible polymer blends filled with carbon black.* Journal of Materials Science, 2004. **39**(2): p. 695-697.

94. Feng, J.Y. and C.M. Chan, *Positive and negative temperature coefficient effects of an alternating copolymer of tetrafluoroethylene-ethylene containing carbon black-filled HDPE particles.* Polymer (Guilford), 2000. **41**(19): p. 7279-7282.

95. Xu, H.-P., et al., *Exploration of unusual electrical properties in carbon black/binary-polymer nanocomposites.* Applied Physics Letters, 2007. **90**(15): p. 152912.

96. Zhang, C., et al., *Selective location and double percolation of short carbon fiber filled polymer blends: high-density polyethylene/isotactic polypropylene.* Materials Letters, 1998. **36**(1–4): p. 186-190.

97. Xu, H.-P., et al., *Remarkable selective localization of modified nanoscaled carbon black and positive temperature coefficient effect in binary-polymer matrix composites.* Journal of Materials Chemistry, 2008. **18**(23): p. 2685-2690.

98. Yu, G., et al., *Conductive polymer blends filled with carbon black: Positive temperature coefficient behavior.* Polymer Engineering and Science, 1999. **39**(9): p. 1678-1688.

99. Pang, H., et al., *Temperature resistivity behaviour in carbon nanotube/ultrahigh molecular weight polyethylene composites with segregated and double percolated structure.* Plastics Rubber and Composites, 2013. **42**(2): p. 59-65.

100. Yang, Q.Q. and J.Z. Liang, *Electrical Properties and Morphology of Carbon Black-Filled HDPE/EVA Composites.* Journal of Applied Polymer Science, 2010. **117**(4): p. 1998-2002.

101. Wei, Y., et al., *Temperature-resistivity characteristics of a segregated conductive CB/PP/UHMWPE composite.* Colloid and Polymer Science, 2014. **292**(11): p. 2891-2898.

102. Tan, Y.Q., et al., *Characterization of carbon black-filled immiscible polypropylene/polystyrene blends.* Polymer International, 2011. **60**(5): p. 823-832.

103. Rahaman, M., T.K. Chaki, and D. Khastgir, *Control of the temperature coefficient of the DC resistivity in polymer-based composites.* Journal of Materials Science, 2013. **48**(21): p. 7466-7475.

104. Qu, Y., et al., *Tuning of the PTC and NTC effects of conductive CB/PA6/HDPE composite utilizing an electrically superfine electrospun network.* Materials Letters, 2014. **132**: p. 48-51.

105. Pour, S.A.H., B. Pourabbas, and M.S. Hosseini, *Electrical and rheological properties of PMMA/LDPE blends filled with carbon black.* Materials Chemistry and Physics, 2014. **143**(2): p. 830-837.

106. Pang, H., et al., *Conductive polymer composites with segregated structures.* Progress in Polymer Science, 2014. **39**(11): p. 1908-1933.

107. Kar, P. and B.B. Khatua, *PTCR Characteristics of Polycarbonate/Nickel-Coated Graphite-Based Conducting Polymeric Composites in Presence of Poly(caprolactone).* Polymer Composites, 2011. **32**(5): p. 747-755.

108. El Hasnaoui, M., et al., *Effect of temperature on the electrical properties of copolymer/carbon black mixtures.* Journal of Non-Crystalline Solids, 2010. **356**(31–32): p. 1536-1541.

109. Wu, S.H., *A GENERALIZED CRITERION FOR RUBBER TOUGHENING - THE CRITICAL MATRIX LIGAMENT THICKNESS.* Journal of Applied Polymer Science, 1988. **35**(2): p. 549-561.

110. Nho, P.H.K.a.Y.C., *The Effect of Carbon Black on PTC Characteristics of Conductive Polyethylene/Carbon Black Composite.* J. Ind. Eng. Chem, 2001. **7**(4): p. 199-203.

111. Dang, Z.-M., W.-K. Li, and H.-P. Xu, *Origin of remarkable positive temperature coefficient effect in the modified carbon black and carbon fiber cofillled polymer composites.* Journal of Applied Physics, 2009. **106**(2): p. 024913.

112. Fang, Y., et al., *Improved stability of volume resistivity in carbon black/ethylene-vinyl acetate copolymer composites by employing multi-walled carbon nanotubes as second filler.* Polymer, 2012. **53**(21): p. 4871-4878.

113. Kar, P., et al., *Positive temperature coefficient to resistively characteristics of polystyrene/nickel powder/multiwall carbon nanotubes composites.* Polymer Composites, 2012. **33**(11): p. 1977-1986.

114. Li, Q., et al., *Positive temperature coefficient characteristic and structure of graphite nanofibers reinforced high density polyethylene/carbon black nanocomposites.* Composites Part B-Engineering, 2009. **40**(3): p. 218-224.

115. Liang, G.D., S.P. Bao, and S.C. Tjong, *Microstructure and properties of polypropylene composites filled with silver and carbon nanotube nanoparticles*

prepared by melt-compounding. Materials Science and Engineering B-Solid State Materials for Advanced Technology, 2007. **142**(2-3): p. 55-61.

116. Socher, R., et al., *Electrical and thermal properties of polyamide 12 composites with hybrid fillers systems of multiwalled carbon nanotubes and carbon black.* Composites Science and Technology, 2011. **71**(8): p. 1053-1059.

117. Zha, J.W., et al., *High performance hybrid carbon fillers/binary-polymer nanocomposites with remarkably enhanced positive temperature coefficient effect of resistance.* Journal of Materials Chemistry A, 2013. **1**(3): p. 843-851.

118. Zhang, P., D.L. Cao, and S.N. Cui, *Resistivity-Temperature Behavior and Morphology of Low Density Polyethylene/Graphite Powder/Graphene Composites.* Polymer Composites, 2014. **35**(8): p. 1453-1459.

119. Di, W.H., et al., *Positive-temperature-coefficient/negative-temperature-coefficient effect of low-density polyethylene filled with a mixture of carbon black and carbon fiber.* Journal of Polymer Science Part B-Polymer Physics, 2003. **41**(23): p. 3094-3101.

120. Cui, C.-H., et al., *Percolation and resistivity-temperature behaviours of carbon nanotube-carbon black hybrid loaded ultrahigh molecular weight polyethylene composites with segregated structures.* RSC advances, 2015. **5**(75): p. 61318-61323.

121. Bao, S.P., G.D. Liang, and S.C. Tjong, *Positive Temperature Coefficient Effect of Polypropylene/Carbon Nanotube/Montmorillonite Hybrid Nanocomposites.* IEEE transactions on nanotechnology, 2009. **8**(6): p. 729-736.

122. Zhang, X. and Y. Pan, *A novel polymer composite with double positive-temperature-coefficient transitions: effect of filler–matrix interface on the resistivity–temperature behavior.* Polymer International, 2008. **57**(5): p. 770-777.

123. Jia, W. and X.F. Chen, *Effect of polymer-filler interactions on PTC behaviors of LDPE/EPDM blends filled with carbon blacks.* Journal of Applied Polymer Science, 1997. **66**(10): p. 1885-1890.

124. Yim, M.J., et al., *Oxidation Prevention and Electrical Property Enhancement of Copper-Filled Isotropically Conductive Adhesives.* Journal of electronic materials, 2007. **36**(10): p. 1341-1347.

125. Wang, X., et al., *PTC/NTC Behavior of PVDF Composites Filled with GF and CF.* Chemical research in Chinese universities, 2008. **24**(5): p. 648-652.

126. Kitano, T., T. Kataoka, and Y. Nagatsuka, *Shear flow rheological properties of vinylon- and glass-fiber reinforced polyethylene melts.* Rheologica acta, 1984. **23**(1): p. 20-30.

127. Asare, E., et al., *Effect of Particle Size and Shape on Positive Temperature Coefficient of Conductive Polymer Composites.* Journal of Materials & Design, Submitted.

128. Chu, K., et al., *Smart conducting polymer composites having zero temperature coefficient of resistance.* Nanoscale, 2015. **7**(2): p. 471-478.

129. Kar, P., et al., *PTCR characteristics of poly(styrene-co-acrylonitrile) copolymer/stainless steel powder composites.* Journal of Applied Polymer Science, 2012. **124**(1): p. 607-615.

130. Yi, X.-S., L. Shen, and Y. Pan, *Thermal volume expansion in polymeric PTC composites: a theoretical approach.* Composites Science and Technology, 2001. **61**(7): p. 949-956.

131. Huang, R.Z., et al., *High Density Polyethylene Composites Reinforced with Hybrid Inorganic Fillers: Morphology, Mechanical and Thermal Expansion Performance.* Materials, 2013. **6**(9): p. 4122-4138.

132. Quintens, D., et al., *MECHANICAL-BEHAVIOR RELATED TO THE PHASE MORPHOLOGY OF PC SAN POLYMER BLENDS.* Polymer Engineering and Science, 1990. **30**(22): p. 1474-1483.

133. Komalan, C., et al., *Dynamic mechanical analysis of binary and ternary polymer blends based on nylon copolymer/EPDM rubber and EPM grafted maleic anhydride compatibilizer.* Express Polymer Letters, 2007. **1**(10): p. 641-653.

134. Mohanty, S. and S.K. Nayak, *Interfacial, dynamic mechanical, and thermal fiber reinforced behavior of MAPE treated sisal fiber reinforced HDPE composites.* Journal of Applied Polymer Science, 2006. **102**(4): p. 3306-3315.

135. Dikobe, D.G. and A.S. Luyt, *Comparative study of the morphology and properties of PP/LLDPE/wood powder and MAPP/LLDPE/wood powder polymer blend composites.* Express Polymer Letters, 2010. **4**(11): p. 729-741.

136. Kannan, M., et al., *Thermogravimetric analysis and differential scanning calorimetric studies on nanoclay-filled TPU/PP blends.* Journal of Thermal Analysis and Calorimetry, 2013. **112**(3): p. 1231-1244.

137. Scher, H. and R. Zallen, *Critical Density in Percolation Processes.* The Journal of chemical physics, 1970. **53**(9): p. 3759-&.

138. Sattler, K.D., *Handbook of Nanophysics: Nanoparticles and Quantum Dots*. 2010: CRC Press.

139. Klimov, V.I., *Semiconductor and Metal Nanocrystals: Synthesis and Electronic and Optical Properties*. 2003: Taylor & Francis.

140. Hiemenz, P.C. and R. Rajagopalan, *Principles of Colloid and Surface Chemistry, Third Edition, Revised and Expanded*. 1997: Taylor & Francis.

141. Bargeman, D. and Vanvoors.F, *VAN-DER-WAALS FORCES BETWEEN IMMERSED PARTICLES.* Journal of Electroanalytical Chemistry, 1972. **37**(JUN): p. 45-&.

142. Israelachvili, J.N., *Intermolecular and Surface Forces: Revised Third Edition*. 2011: Elsevier Science.